Studies on AP-1 Sorting Function and Regulation of Membrane Binding

vorgelegt von
Karthikeyan Radhakrishnan
aus Krishnagiri (Indien)

Göttingen 2006

D7
Referent: **Prof. Dr. Dr. h.c. Kurt von Figura**
Koreferent: **Prof. Dr. Hans-Joachim Fritz**

Tag der mündlichen Prüfung: 16 January 2007

To my Parents...

Contents

Abbreviations

ADP	Adenosine diphosphate
AP-1	Adaptor protein-complex-1
APS	Ammonium peroxide sulfate
ARF	ADP-Ribosylation Factor
ATP	Adenosine-5'-triphosphate
BFA	Brefeldin A
BLAST	Basic Local Alignment Search Tool
bp	Base pairs
CCV	Clathrin-Coated Vesicle
COP	Coat Protein
^{o}C	Grade Celsius
cDNA	Complementary DNA
Da	Dalton
ddH2O	double distilled H_2O
DMSO	Dimethylsulfoxide
DNA	Deoxyribonucleic acid
DTT	1,4-Dithiothreitol
dNTPs	2'-Deoxyribonucleoside-5'-phosphate
E.coli	Escherichia coli
EDTA	Ethylendiamine-tetra-acetate
ER	Endoplasmic Reticulum
EST	Expressed sequence tag
et al	et alteri (and others)
GGA	Golgi-localized, γ-ear containing, ARF-binding
GTP	Guanosine triphosphate
IPTG	isopropyl-β-D-galactopyranoside
kDa	kilodalton
l	liter
LAMP-1	Lysosome Associated Membrane Protein-1

LB-medium	Luria-Broth medium
m	meter
MEF	Mouse Embryonic Fibroblast
mM	milliMolar
M	molar
μ	micro, -(x10^{-6})
mA	milliAmpere
min	minute
MgCl$_2$	Magnesium chloride
MPR	mannose-6-phosphate receptor
mRNA	messenger RNA
MVB	Multi Vesicular Body
n	nano, -(x10^{-9})
OD	Optical density
PAGE	Polyacrylamide gel electrophoresis
PBS	Phosphate-buffered saline
PCR	Polymerase chain reaction
PI4P	Phosphotidylinositol 4-phosphate
rpm	Rotation per minute
RT	Room temperature
s	second
SDS	Sodium Dodecyl Sulfate
t	time
Taq	Thermophillus aquaticus
TAE	Tris-acetate-EDTA-buffer
TBS	Tris-buffered solution
TCA	Trichloro-acetic acid
TGN	Trans-Golgi Network
TE	Tris-EDTA
TEMED	N,N,N,N-tetramethylethylenediamine
Tris	Tris-(hydroxymethyl)-aminomethane
UV	Ultraviolet
V	Volt
v/v	Volume per volume
wt	Wild type
w/v	Weight per volume
Y2H	yeast-two-hybrid
Y3H	yeast-three-hybrid

Chapter 1

Introduction

A typical mammalian cell contains up to 10,000 different kinds of proteins; a yeast cell about 5000. For proper organization and functioning of an eukaryotic cell,each of its different kind of proteins should be localized to correct cellular membrane or luminal compartment. This highly regulated and co-ordinated process of directing each newly made polypeptide to its appropriate destination is termed as protein sorting or protein targeting. Along the biosynthetic or the secretory pathway, newly synthesized proteins destined for secretion pass through an array of membrane enclosed organelles including the Endoplasmic Reticulum (ER), the Golgi complex and/or secretory granules before they can be secreted to the extra-cellular space. Proteins bound to reside at other compartments like the Plasma Membrane (PM), endosomes or lysosomes share the routes of the secretory pathway. On the other hand, the proteins that are endocytosed at the PM reach their intracellular destinations through the endocytic pathway along routes that overlap with the secretory pathway.

All protein transport pathways along the biosynthetic pathway are mediated by membrane-bound vesicles. The vesicular transport hypothesis was established based on the seminal work of George Palade and co-workers (Palade, 1975) according to which, membrane-bound vesicles harboring cargoes shuttle between organelles of the secretory pathway. The cargoes to be transported are selectively incorporated into forming vesicles from a donor compartment. The membraneous vesicles with cargoes are then subsequently targeted to a specific acceptor compartment, where the cargoes are unloaded by fusion of their limiting membranes.

Such highly accurate trafficking of vesicles along the cytoskeletal filaments is orchestrated and regulated by motor proteins and by a cross-talk between a variety of cytosolic and vesicle bound proteins.

1.1 Intracellular vesicle transport pathways

A detailed picture of the molecular mechanisms involved in selective cargo transport between organelles have been provided by extensive genetic and biochemical analysis of the secretory pathway. The transport vesicles involved in protein traffic
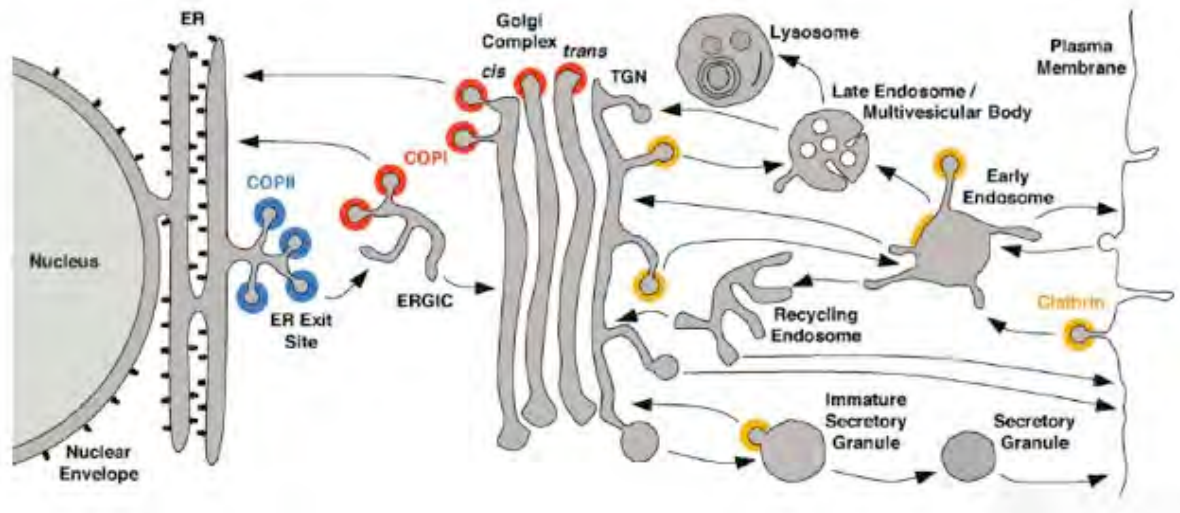
Figure 1.1: Vesicular transport pathways in a mammalian cell. The scheme depicts intracellular protein transport along the secretory, endocytic and lysosomal compartments. Arrows indicate various transport steps. The known or presumed locations of COPI(red), COPII (blue) and clathrin (orange) coats are indicated in colour. Clathrin coats are heterogenous and contain distinct combination of adaptor proteins at different membranes (Bonifacino and Glick, 2004). Additional coats or coat-like components exist but are not depicted in this figure.

in the secretory pathway are equipped with specific protein coats that mediate the budding and selective incorporation of cargo in the forming vesicles (Fig.1.1). Among various types of coats that operate, the most widely studied and known are, the COPI coat and the COPII coatomer complex that function at the early-secretory phase and second, those coats containing clathrin as their main constituent that function exclusively at the post-Golgi sorting events. Apart from the above mentioned pathways, the pathways that are mediated in a, coat-independent mechanism also exist, but are less characterized (Bonifacino and Glick, 2004).

The anterograde and the retrograde transport between ER and Golgi constitute the early-secretory pathway. COPII mediates protein export from ER to Golgi (anterograde) either directly or through a transient intermediate called the ER-Golgi Intermediate Compartment (ERGIC)(Barlowe *et al.*, 1994). Meanwhile COPI coatomer mediates transport from the Golgi to ER (retrograde) and also intra-Golgi transport. COPII coats assemble at specialized ER exit sites (also called transitional

ER sites), which are generally devoid of ribosomes. Coat assembly begins through activation of small G-proteins; Sar1p for COPII and ARF1(ADP-ribosylation factor 1) for COPI and these activated G-proteins recruit the coat proteins. The COPI coatomer complex consists of seven subunits that are organised into one trimeric and two dimeric subcomplexes and the COPII coat has four subunits. Both COPII and COPI coats recognize the sorting signals present in the cytoplasmic tails of membrane cargo proteins.

When a protein to be secreted reaches *trans*-Golgi network (TGN), further transport between the TGN and the plasma membrane(PM) is maintained by clathrin-coated vesicles(CCVs). As shown in Fig. 1.1, TGN acts as a major sorting station and a transport vesicle budding from the TGN can take different routes as dictated by the nature of cargo and the type of clathrin associated adaptor protein (AP) complex. Several different types of adaptor proteins and accessory proteins are found to be associated with clathrin(discussed in detail in the next section). By the constitutive secretory pathway, surface-destined cargo is delivered directly from TGN to the PM by a less understood mechanism and the precise identities of the proteins mediating constitutive secretion at TGN remains to be established. However, recently two proteins called FAPP1 and FAPP2 (four phosphate-adaptor protein 1 and 2) were identified to be components of a phosphotidylinositol-4-phosphate(PtdIns(4)P) and ARF-regulated machinery involved in the generation of constitutive TGN to PM carriers (Godi *et al.*, 2004). In contrast to the constitutive pathway, cargoes in clathrin-coated vesicles can be vectorially delivered to the lysosomes or the PM through the internal endosomal system. The endosomal system acts as a sorting sub-station; anterograde pathways deliver the cargo to the lysosomes and PM and by retrograde pathway deliver back to the TGN. In cells that undergo signal-dependent regulated secretion, proteins are first incorporated into the secretory granules called immature secretory granules and then by a process of maturation get concentrated in so called mature secretory granules, which are then released into the extra-cellular space under appropriate signal stimulation (for review see (Tooze *et al.*, 2001)).

COPI coatomer and clathrin share at least one conserved structural element, implying that they operate by similar principles. But clathrin coats are considerably more complex than COPII and COPI. A variety of clathrin adaptors are recruited from cytosol to membranes and a specific combination of which form a heterogenous membrane-proximal layer onto which clathrin is subsequently deposited. Moreover, when compared to COPI and COPII coat mediated traffic, each and every step in clathrin coated vesicle mediated transport is regulated by an ensemble of kinases, phosphatases and other accessory proteins necessary to maintain the

fidelity and specificity of multiple post-Golgi sorting events mediated by clathrin coats.

1.2 Components of Clathrin-coated vesicle transport machinery

At least ten different transport vesicle coats, and therefore classes of transport vesicle have been identified so far (Robinson and Bonifacino, 2001). One of the major classes of transport vesicles is the clathrin-coated vesicles (CCVs) and their role in internalization of proteins from PM by a process called clathrin mediated endocytosis(CME), is the most extensively studied mechanism of vesicle biogenesis. There are well over 20 proteins implicated in CCV assembly. Many interact with multiple partners creating a complicated network of possible interactions. A CCV is typically spherical and 60-100nm in diameter. CCVs and clathrin-coated pits are considered as having a three-layered structure consisting of an inner layer of embedded transmembrane protein cargo linked to the outer clathrin layer by a middle layer of adaptor molecules. Other components of a CCV or clathrin-coated pits include a large array of proteins with diverse functions, referred to as accessory proteins, which play distinct and dedicated roles in CCV formation, budding and fusion. Over the past decades, biochemical studies dissected most of the components of CCV transport machinery, while recent structural studies on clathrin and clathrin coat components has shed much light on the mechanism of clathrin coat mediated cargo transport at the molecular level.

1.2.1 Clathrin

As a main constituent of CCVs, clathrin polymerizes into polyhedral lattices to form the outer layer of a forming vesicle. It acts as a molecular scaffold to provide stability to the vesicle and also as a platform for the recruitment of a subset of accessory proteins. A Clathrin coat is a three-dimensional array of *triskelia*. Each triskelion unit consists of three (approx.,190-kDa) clathrin heavy chains(CHCs) and three 25-29-kDa clathrin light chains(CLCs). These triskelia polymerize into polyhedral lattices of regular shape, with one unit centered on every edge and its legs lining two sides of a polygon. The N-terminal domains of CHCs are facing inwards to establish contact with adaptor molecules that link clathrin to the membrane and its C-terminal domain accomodates CLCs. For a detailed review on the structural organisation of clathrin and clathrin coats, see (Kirchhausen, 2000; Edeling *et al.*,

2006).

Purified clathrin can spontaneously assemble into cages at slightly acidic pH (Kirchhausen and Harrison, 1981) or , in the presence of adaptor proteins, into coats *in vitro*. Clathrin coats can form different shapes and sizes. But under physiological buffer conditions, in the presence of adaptor molecules, clathrin baskets appear smaller and are of more regular and uniform size (Pearse and Robinson, 1984). Clathrin-coated pits at the PM and TGN are not static, but are dynamic structures. Using fluorescence recovery after photobleaching(FRAP), it was shown that both clathrin and adaptors at coated-pits, rapidly exchange with free proteins in the cytosol and the adaptors were able to exchange independently, even when clathrin exchange was blocked (Wu *et al.*, 2003). In another study (Hinrichsen *et al.*, 2006), it was shown using electron microscopy that at cellular cortices, upon depletion of clathrin, the membrane domains containing only the adaptor molecules lack any curvature suggesting that clathrin is necessary for driving coated-pit invagination and was proposed that clathrin could contribute for vesicle budding by recruiting membrane-bending proteins like epsin. Moreover, apart from playing a major role in vesicular trafficking, a recent study (Royle *et al.*, 2005) demonstrated a novel and an unconventional role for clathrin in mitosis, wherein clathrin binds the mitotic spindle through its heavy-chain and stabilizes it .

1.2.2   Adaptor proteins

Intracellular vesicle transport is mediated by clathrin adaptor molecules which are classified as either multimeric or monomeric adaptors whose function is compartment specific as depicted in Fig. 1.2.

1.2.2.1   Heterotetrameric Adaptor Protein complexes

Two adaptor protein complexes, AP-1 and AP-2, were originally purified from clathrin-coated vesicles (Hirst and Robinson, 1998; Schu, 2001; Robinson and Bonifacino, 2001). According to their ability to promote the assembly of clathrin cages in vitro they were named *assembly polypeptides* or adaptins (Pearse and Robinson, 1984). AP-1 localises to the TGN and to endosomes, whereas AP-2 is exclusively found at the plasma membrane. Database searches have identified two more members of the family, AP-3 and AP-4, which are absent from clathrin-coated vesicle preparations. Although AP-3 was initially assigned to a perinuclear region like the TGN and to endosomal structures, recent studies demonstrate that it is mainly present on endosomal tubules (Dell'Angelica *et al.*, 1997; Simpson *et al.*,
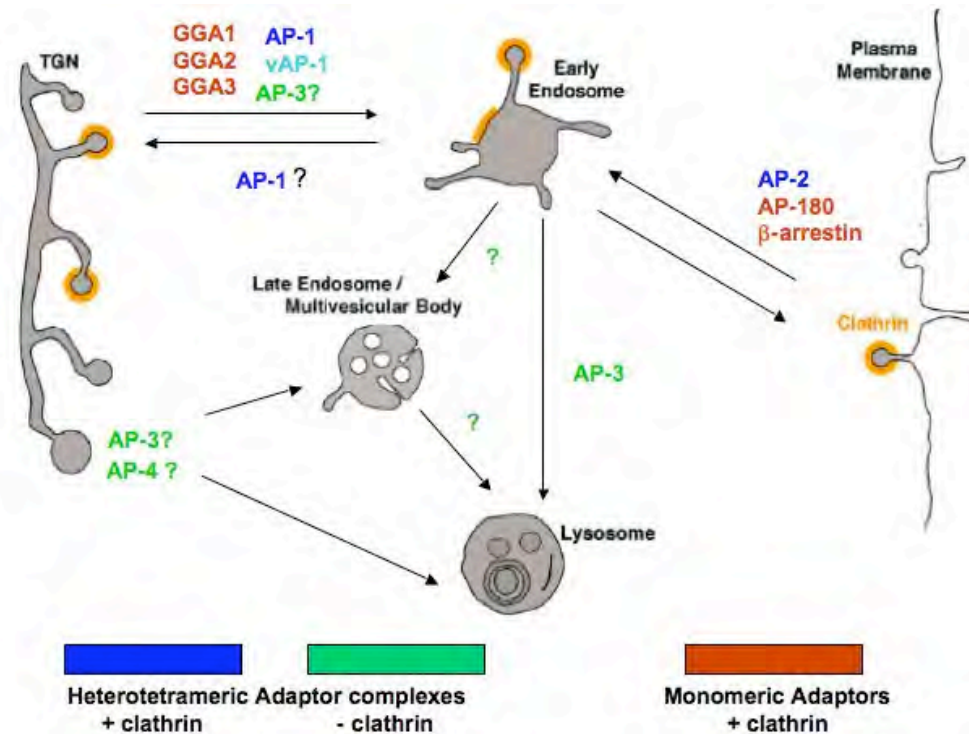
Figure 1.2: **Compartment-specific role of Adaptor proteins.**Different sets of heterotetrameric Adaptor Proteins (AP) operate vesicular transport either in Clathrin dependent (blue) or independent (green) fashion between specific routes. Also Monomeric Adaptors (red) perform overlapping functions along with AP complexes. Ambiguity of the role of adaptors in a certain pathway is indicated by a *question mark*.

1997; Peden *et al.*, 2004). It was shown to interact and colocalise with clathrin, albeit to a lower extent compared to AP-1, suggesting a function as clathrin adaptor of lower affinity or different assembly properties (Dell'Angelica *et al.*, 1998; Peden *et al.*, 2004). In contrast, AP-4, which has been implicated in sorting at the TGN, obviously does not bind to clathrin (Simmen *et al.*, 2002). All the adaptor complexes consist of four adaptin proteins. The two large subunits of about 100 kD, γ/α /δ /ϵ and β 1-4 for AP1-4, respectively, fold into an amino-terminal trunk domain and a carboxyterminal *ear* or appendage domain that are connected by a largely unstructured *hinge*. The trunk domains together with the medium-sized subunits, μ1-4 (about 50 kD), and the small subunits σ1-4 (about 20 kD) form the core complex. Between AP-1 and AP-2, β is the most conserved subunit showing 84% sequence identity. Whereas the μ- and σ-subunits are about 40% identical, only 25% of the amino acids are conserved between γ and α, mostly due to the divergence of the ear domains. Despite the differences in primary sequence, predictions of secondary structure and hydrophilicity profiles indicate that all the four complexes are highly homologous. Comparison of the AP-2 and AP-1 crystal-structures confirms

this prediction. Thus, the crystal structure of AP-2 can serve as a model for the entire family.
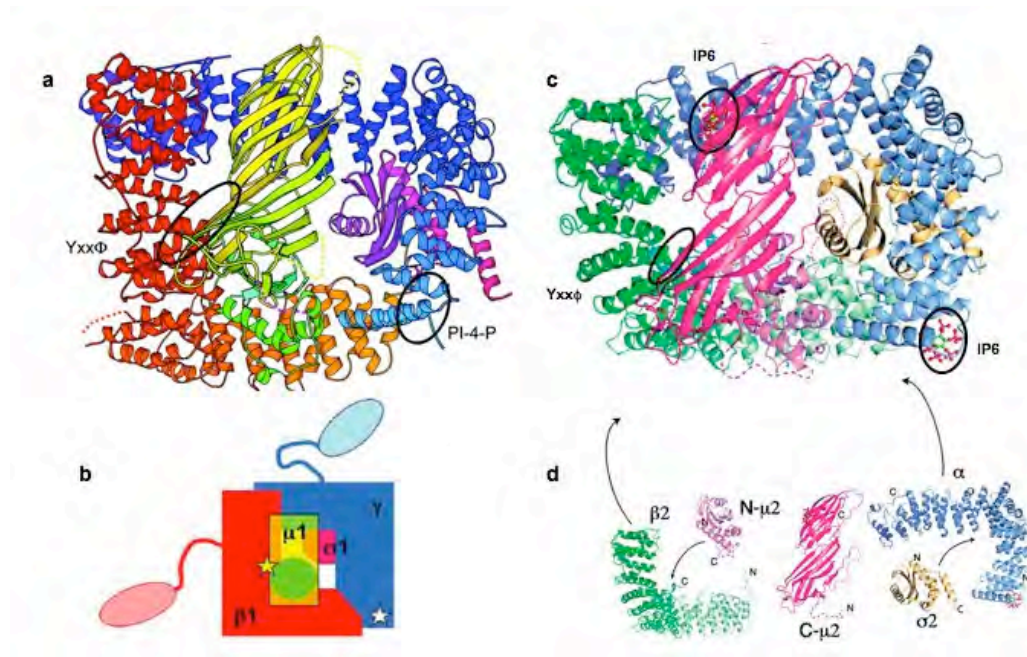
Figure 1.3: Structure and assembly of (a) AP-1 and (c) AP-2 core. Individual subunits are represented by respective colours in (b) and(d). The location of Yxxϕ binding site is indicated by black ellipse. Black circles represent PI-4-P binding site in AP-1 and D-myo-inositol-1,2,3,4,5,6-hexakisphosphate(IP6) in AP-2. Note that AP-1(C-μ1) lacks the phosphoinositide binding site compared to the corresponding site in AP2 (C-μ2). (Heldwein et al., 2004; Collins et al., 2002)

The large subunits α and $\beta2$ form curved arrays of α-helices, which accommodate the globular $\sigma2$ and N-terminal $\mu2$-domains, respectively. $\sigma2$ and N-$\mu2$ both contain a central five-stranded β-sheet surrounded by α-helices. N-$\mu2$ is connected to the all β-sheet by a 23-residue loop. All the subunits contact each other to some extent, but stronger interactions link α to $\sigma2$ as well as $\beta2$ to $\mu2$. In fact, these two dimers show significant similarity on the amino acid level and their folds can be matched onto each other, particularly for the N-terminal domain of $\mu2$ and $\sigma2$ and for the amino-termini of the large subunits. $\sigma2$ is related to the N-terminal domain of $\mu2$ even at the primary sequence level. The AP-2 core complex harbours two phosphoinositide binding sites, one in the C-$\mu2$ domain and one at the N-terminus of α (Fig. 1.3). Sequence alignment of AP-2 and AP-1 counterparts indicates that these binding sites are basically conserved. Recently, the structure of AP-1 core complex was solved by X-ray crystallography (Heldwein *et al.*, 2004) and it turned out to be that the overall structure was similar to AP-2, but significantly the AP-1(C-$\mu1$) lacks the phosphoinositide binding site compared to the corresponding site in

AP2 (C-μ2). The core complex measures about 100 Åx 80 Å, the hinge regions of the two large subunits can probably stretch about 200-300 Åaway from the core, since they have no significant secondary structure. As a consequence, the ear domains can reach long distances facilitating interaction with other proteins.
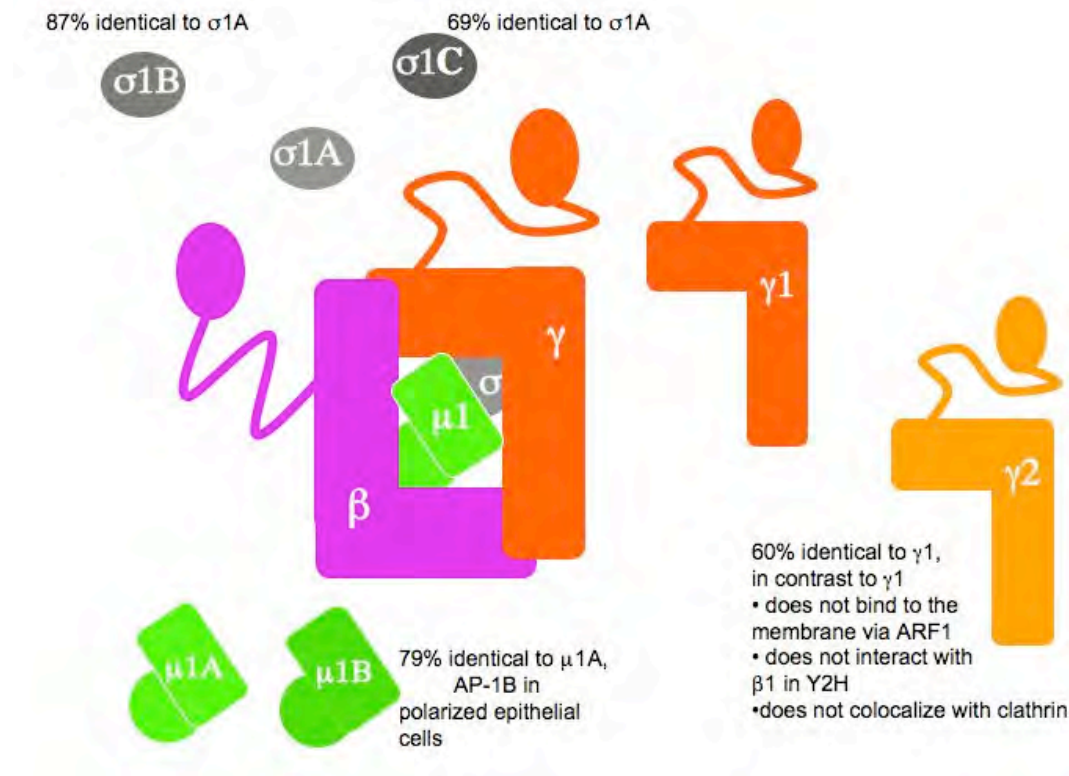
Figure 1.4: Schematic representation of variations in AP-1 subunit Isoforms. See text for details.

For many of the adaptor subunits, several genes are known in mammals. In the case of AP-1 adaptor complex, except for the β1subunit, for all other three subunits at least one isoform is found to be expressed. The variations in the AP-1 subunit isoforms is schematically shown in Fig.1.4. γ2-adaptin is about 60% identical to γ1-adaptin, being shortened in the hinge region. In contrast to γ1, it does not interact with β1 in the yeast two-hybrid system, which indicates that they will not form a complex *in vivo*. Three genes are known for the σ1-subunit, named σ1A, -B and -C that are about 70-80% identical to each other. σ1A and σ1B apparently bind to both γ1 and γ2 *in vitro* (Takatsu *et al.*, 1998, 2001). Moreover, a recent study of our lab, identified different splice variants for the σ1B gene with tissue specific expression pattern which were designated as σ1B2 and σ1B3 and shown to be expressed mainly in the brain and skeletal muscle respectively (Riel, 2004). The significance of this tissue specific expression pattern is presently unknown. In

addition to the ubiquitous subunit μ1A, μ1B is selectively expressed in polarized cells and assembles into the variant complex AP-1B (Ohno *et al.*, 1999; Fölsch *et al.*, 1999; Eskelinen *et al.*, 2002). α-adaptin exists as two different proteins, αA and αC, which are 80% identical (Ball *et al.*, 1995). In addition to a ubiquitous alternative for σ3 (σ3B), neuron-specific variants are known for μ3-adaptin (μ3B) and β3-adaptin (β-NAP) and they have been shown to form a variant neuronal AP-3B complex (Faúndez *et al.*, 1998). No additional genes for AP-4 have been described.

1.2.2.2 Monomeric Adaptor Proteins

In addition to multimeric adaptor complexes, monomeric adaptor proteins were identified to exist, defined by their ability to recruit clathrin and to recognize the cargo for coated vesicle mediated transport. They are generally modular proteins, combining several conserved protein-protein or protein-lipid interaction domains.

The monomeric clathrin adaptors, which are referred to as alternate adaptors, that function at the PM, can be further classified based on their function either as cargo-specific adaptors (such as β-arrestins, ARH, Dab2 or numb) or phospholipid adaptors (proteins that belong to the epsin super family- epsin1, CALM/AP180, HIP1 and Hip1R). β-arrestins-1 and -2 recognize 7-transmembrane helix GPCRs (G-protein coupled receptors) and mediate their rapid internalization and this is mediated by binding of β-arrestins to the PtdIns(4,5)P$_2$ (Gaidarov and Keen, 1999), and the ability to bind physically to both clathrin and AP-2 (Claing *et al.*, 2002; Marchese *et al.*, 2003). ARH (autosomal recessive hypercholesteremia), Dab1/2 (Disabled1/2) and numb are clathrin adaptors involved in the uptake of the members of the LDLR family, by recognizing the sorting motif FxNPxY through their PTB (phospho-tyrosine binding) domain (Garcia *et al.*, 2001; Morris *et al.*, 2002; Santolini *et al.*, 2000). Furthermore, the PTB domain of these proteins can bind to PtdIns(4,5)P$_2$ and similar to β-arrestins, at their COOH-terminus, these proteins contain clathrin and AP-2-appendage binding sequences (Dho *et al.*, 1999; Howell *et al.*, 1999; Mishra *et al.*, 2002a,b). A second group of putative alternate adaptors includes epsin 1, AP180/CALM and HIP1/Hip1R (Wendland, 2002). These proteins contain a structurally related NH$_2$-terminal PtdIns(4,5)P$_2$-binding domain (the ENTH/ANTH domain) (Ford *et al.*, 2001) and all bind to and colocalize with AP-2/clathrin. Epsins contain Ubiquitin interaction motifs (UIMs) and based on the role of yeast epsins, Ent1p and Ent2p which mediate endocytosis of ubiquitinated receptors, in mammals epsins may operate in internalization of ubiquitinated receptors, for example EGFRs. AP180 and HIP1/Hip1R lack these UIMs and in the case of AP180, an interaction with cargo proteins has not been

demonstrated until now, suggesting that it serves mainly to stabilise and shape the coat. It is believed that these endocytic monomeric adaptors would probably function without AP-2 or alone, though not very efficient compared to the concerted activity (Hinrichsen *et al.*, 2003; Motley *et al.*, 2003). For example, AP180 promotes clathrin assembly onto a lipid monolayer *in vitro* and influences the size of coated vesicles *in vivo* (Zhang *et al.*, 1998). However, AP-2 needs to participate to drive bud formation and the combination of AP180 and AP-2 works more efficiently in this respect than AP-2 alone. But a recent study has reported that Dab2 can sort LDLRs into coated-pits independent of AP-2 and ARH (Maurer and Cooper, 2006) which indicates that these monomeric adaptors are not just accessory proteins as previously thought, but can function as bonafide adaptors.
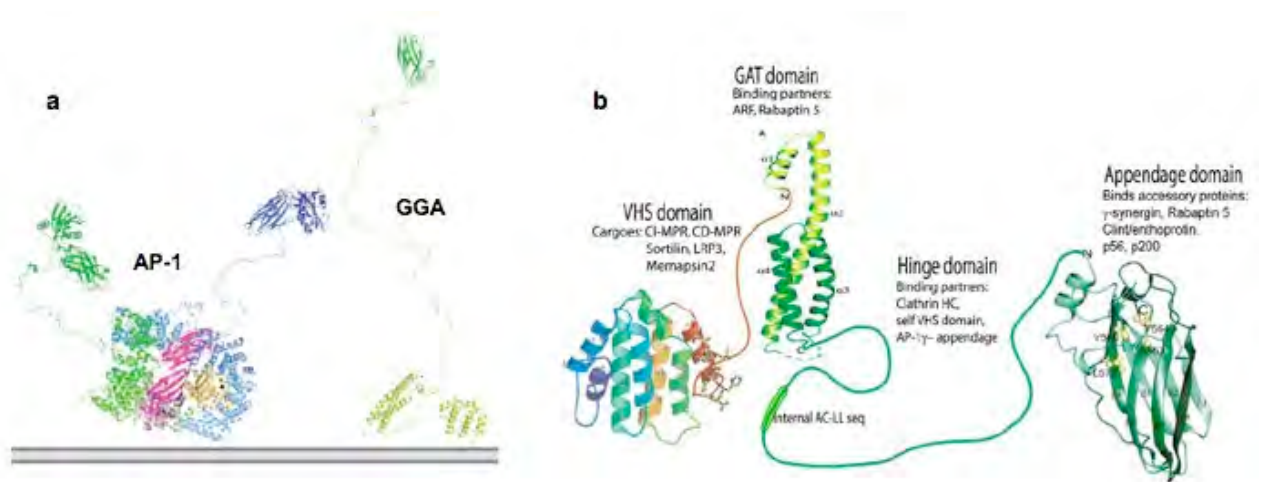
Figure 1.5: GGA1 in comparison to AP-1. (a) Structural models of AP-1 and GGA. (b) Model of the overall structure of GGA1. Different domains and their binding partners are shown. The VHS domain binds to the acidic-dileucine (AC-LL) motif present in the cargoes. Note that the Hinge domain harbors an Internal AC-LL motif which can mask the function of VHS domain by auto-inhibition and hence the sorting function of GGA1 can be regulated (Ghosh and Kornfeld, 2003b). There is no evidence that AP-1 has such a mode of regulation.

The GGA proteins were identified and extensively studied by several groups during the last few years in the context of sorting at the TGN (for rev. see (Bonifacino, 2004)). In addition, they localize to early endosomes. Three genes are known in mammals, encoding for GGA1, GGA2 and GGA3, and the family is conserved among eukaryotes as supported by two homologues in yeast. The GGA proteins consist of several domains that they share with other proteins: At the N-terminus they contain a common interaction module in vesicular traffic, the VHS domain (named after the first family members Vps27p, Hrs and STAM), followed by the GAT domain (which is also present in TOM1=target of Myb1),

a rather unstructured linker and the C-terminal GAE (γ-adaptin-ear-homologous) domain. These domains convey properties which are very similar to AP-1. By means of the GAT domain, GGAs bind to ARF1 and ARF3 which is sufficient for their targeting to the TGN. Sorting signals of the DxxLL type, including a cluster of acidic residues around the essential aspartate and and an upstream serine residue whose phosphorylation enhances sorting efficiency, are recognized by the VHS domain. Clathrin binds to clathrin box motifs in the linker region and to an additional site within GGA1-GAE. In analogy to the adaptins, the GAE domain accounts for recruitment of accessory proteins, displaying preferential affinity to p56, a protein of currently unknown function. Whereas p56 and γ-synergin bind to ear domains of both γ1-adaptin and GGA in vitro, p56 colocalizes with GGA and γ-synergin with AP-1 in vivo and membrane association depends on the presence of GGA or AP-1, respectively (Lui *et al.*, 2003). Rabaptin-5 associates with GGA proteins via the GAT and GAE domains and is involved in their endosomal targeting (Mattera *et al.*, 2003). Despite the similarity of the three GGAs, they are not completely redundant: Crystal structures of the VHS domains revealed that GGA2 differs significantly from GGA1 and GGA3 such that it lacks a critical serine residue that is subject to phosphorylation-induced regulation of function of GGA1 and GGA2. In contrast to GGA2, the two latter proteins are regulated by phosphorylation which induces a conformational change. Phosphorylation of a serine residue adjacent to an internal acidic-cluster-dileucine motif in the linker region enables this motif to occupy the cargo binding site in the VHS domain. Since other interaction sites, namely for ARF and cargo proteins, become buried by this fold, this is considered to be the *closed* cytosolic form of GGA1 and GGA3. Membrane association probably occurs after dephosphorylation by PP2A, whereas phosphorylation can be mediated by CKII, a kinase associated with AP-1 (Doray *et al.*, 2002; Ghosh and Kornfeld, 2003b). It was shown recently that all the GGAs colocalize in coated pits at the TGN and that their membrane-bound pools interact with each other via multiple domains. Depletion of any GGA protein resulted in increased degradation of the other two (Ghosh *et al.*, 2003). Although GGA proteins exhibit the basic properties of adaptors and localize to clathrin-coated pits and/or CCVs by EM (Doray *et al.*, 2002), they have not been detected in purified CCVs until now. They play an essential part during sorting events at the TGN and may cooperate with AP-1, but their function has not been clearly defined. Surprisingly, recent data demonstrate that GGAs bind to ubiquitinated proteins *in vitro* (Puertollano and Bonifacino, 2004). Ubiquitination of endocytosed proteins targets them to lysosomes for degradation. Cargo selection occurs at early endosomes and involves the ESCRT machinery as well as specialised clathrin-coated membrane patches initiated by the monomeric

adaptor Hrs (Raiborg *et al.*, 2001a). In contrast to other coated pits, this region does not generate coated vesicles, but probably clusters the components which should be present in the internal vesicles of a multivesicular body (Sachse *et al.*, 2002). Like the GGA proteins, Hrs contains a VHS domain, followed by a FYVE module, which is a zinc finger fold that binds specifically to PI3P. A ubiquitin-interacting motif (UIM) serves to sequester ubiquitinated proteins destined for degradation in lysosomes. There are further two coiled-coil regions present and a functional clathrin box motif at the C-terminus. The endosomal localization of Hrs depends on a functional FYVE domain together with the coiled-coil domains (Raiborg *et al.*, 2001b). All the GGA proteins were shown to interact with ubiquitin, but GGA3 displayed the highest affinity. Depletion of GGA3 by RNAi significantly delayed the degradation of EGF-receptor (EGFR) in lysosomes in addition to endosomal membrane reorganisation. As GGA3 binds to a subunit of the ESCRT complex as well, a role in ubiquitin sorting seems possible and has to be addressed by further experiments (Puertollano and Bonifacino, 2004)

1.2.3 Accessory Proteins

Apart from the clathrin adaptor molecules, discussed in the previous sections, a number of proteins are increasingly being identified which play necessary roles for clathrin-coated vesicle transport. Structural and biochemical studies have localized the binding sites of a plethora of accessory/regulatory proteins and other proteins called CLASPs (clathrin associated sorting proteins) to the appendage domains of adaptor proteins. These accessory/regulatory proteins act at distinct steps aiding clathrin-coat assembly formation, at downstream steps like inducing membrane curvature by recruiting actin cytoskeleton to membranes, at the step of vesicle scission by recruiting the GTPase-Dynamin and at steps involving the uncoating of CCV to be primed for fusion with the acceptor membrane.

BAR (Bin, amphiphysin, Rvs) and ENTH (Epsin N-terminal Homology) domains are families of α-helical lipid bilayer binding modules found in proteins that function in endocytosis, actin regulation and signaling. Several members of these families not only bind the bilayer, but also participate in the regulation of its curvature. These properties are thought to play physiological roles at sites of membrane budding and at other sites where narrow tubular membranes occur *in vivo*. Studies of BAR and ENTH domains and of their flanking regions have provided new insights into mechanisms of membrane deformation and curvature sensing, and have emphasized the importance of amphipathic helices, thought to intercalate in one of the leaflets of the lipid bilayer, in the generation of membrane curvature (for

review see (Itoh *et al.*, 2001)). One of the widely studied BAR domain containing proteins are amphiphysin 1/2 which contain NH_2-terminal BAR domain followed by an unfolded region and a COOH-terminal SH3 domain. Their SH3 domains bind dynamin and synaptojanin, which are implicated in the fission and uncoating of endocytic vesicles respectively. The central region of the brain isoforms of amphiphysin comprises binding sites for the heavy chain of clathrin and for the clathrin adaptor AP-2 (Slepnev and De Camilli, 2000). Based on these findings, the amphiphysins were proposed to provide a functional link between clathrin-mediated budding, dynamin-dependent fission and the subsequent uncoating.

1.2.3.1 Interaction of AP-1 with accessory Proteins

The γ1-ear domain contains a discontinuous motif of basic amino acids that was shown to interact with several proteins, like γ-synergin, Eps15, EpsinR, Rabaptin-5, Snx9 and ARF1 GAP1 (Page *et al.*, 1999; Kent *et al.*, 2002; Hirst *et al.*, 2003). Their respective binding site to γ1-adaptin was found to conform more or less to the stretch DFxDF (Mills *et al.*, 2003; Duncan *et al.*, 2003). γ-synergin associates with cytosolic and membrane-bound AP-1 and is enriched in CCVs. Both a GTPase and AP-1 are necessary to recruit it onto the membrane. It further contains an 'Eps15-homology' (EH) domain, a common fold among endocytic proteins that binds to the tripeptidyl sequence motif 'NPF', suggesting a function as linker protein (Page *et al.*, 1999; Hirst *et al.*, 2003). Eps15 was mainly characterized in the context of clathrin-mediated endocytosis. Although it shows a BFA-sensitive perinuclear immunostaining, it remains unknown if Eps15 interacts with AP-1 *in vivo* (Kent *et al.*, 2002). EpsinR (synonymous to Enthoprotin / Clint) belongs to a group of proteins that interact with phosphoinositides via their 'epsin N-terminal homology' or ENTH domain, in this case preferentially with PI4P (Mills *et al.*, 2003; Hirst *et al.*, 2003). Surprisingly, the crystal structure of the related epsin1 ENTH domain in the presence of phospholipid molecules visualised an additional amphipathic α -helix compared to the lipid-free structure (Ford *et al.*, 2002). When incubated with liposomes, this ENTH domain generated thin tubules. According to these observations, it was proposed that ENTH proteins can insert an amphipathic helix into the membrane and thereby promote membrane curvature. Even if epsinR seems to bind to lipids with less affinity, the versatile helix region is well conserved. Similar to γ-synergin, epsinR is enriched in CCVs and localizes to the membrane in an ARF-dependent manner, but it does not require AP-1 for membrane binding. Moreover, it directly interacts with clathrin (Mills *et al.*, 2003) and the SNARE protein Vti1b (Chidambaram *et al.*, 2004), supporting a role as tethering and

stabilising factor in coat formation. Rabaptin-5, which binds to the ear domains of $\gamma 1$ and $\gamma 2$ in vitro, functions as a divalent linker between Rab4 and Rab5, GTPases involved in endosomal trafficking (Stenmark *et al.*, 1995). It has been shown to interact with a dimeric $\gamma 1$- $\sigma 1$-adaptin complex on endosomes and to connect it to Rab4 (Deneka *et al.*, 2003). However, it is not known whether this occurs during coat formation or at a later stage of transport. As for ARF1 GAP and the sorting nexin 9 (Snx9), their physiological role as AP-1 binding partners remains to be demonstrated. Recently, a novel protein called γ-BAR ($\gamma 1$-adaptin Brefeldin A Resistance) was found to interact with the $\gamma 1$-ear-domain but not with the highly homologous GAE domain of GGA1 and participate in the regulation of AP-1 membrane binding dynamics (Neubrand *et al.*, 2005). Also, other accessory proteins like aftiphilin and NECAP (adaptin-ear-binding coat-associated protein)1and 2 were shown to bind to both $\gamma 1$-ear-domain and the GAE domain of GGA1 and also α-ear-domain but with different affinities. It is speculated that this difference in affinities could be contributed by acidic residues that lie downstream of the identified interaction motifs WVQF and WGDF of these accessory proteins (Mattera *et al.*, 2004).

1.3   Life-cycle of Clathrin Coated Vesicles(CCVs)

The mechanism of clathrin-coated vesicle formation and the events that follow thereafter have been extensively studied for AP-2 in the synaptic vesicle recycling and endocytic pathway. There is a significant variation in this mechanism at the TGN. It has been shown *in vitro* that adaptors bind to the terminal domain of clathrin and addition of N-terminal fragment of the $\beta 2$-chain, comprising the hinge and the ear domain, will stimulate clathrin assembly (Shih *et al.*, 1995). The entire process of clathrin lattice assembly has been reconstituted in an in vitro assay with fragments of clathrin and adaptors (Greene *et al.*, 2000). The presence of two binding sites in one β-chain suggests that adaptors could potentially crosslink two CHCs to orient them in a conformation favourable for assembly. It has also been shown that phosphorylation of the β-chains plays an important regulatory role in CCV formation (Ghosh and Kornfeld, 2003b; Wilde and Brodsky, 1996). The hinge region of the β-chains is phosphorylated in the cytosol and hence cannot bind clathrin. When membrane-bound, β-chains are dephosphorylated and can interact with clathrin to stimulate assembly. However, the kinetics of phosphorylation-dephosphorylation cycles with respect to the CCV formation is not well understood.

Initiation of the CCV formation occurs by the inward deformation of a flat array

as a result of massive membrane reorganization (see Fig. 1.6, step 1). The factor that determines the location and initiation of coat assembly remains unknown. Adaptors serve to link clathrin to the membrane and to coordinate the structural assembly of the coat with the selection of cargo proteins and lipids. A number of proteins, in addition to the adaptors, contain clathrin-box sequences and any of these in principle could recruit clathrin. In addition to a clathrin scaffold, a membrane, cargo, and cargo adaptors, coated vesicles must include molecules that determine the destination and ultimate fusion of the vesicle. The identities of these targeting and fusion molecules are largely undetermined. They probably include soluble N-ethylmaleimide sensitive factor (NSF) attachment protein receptors (SNAREs) and Rab proteins.
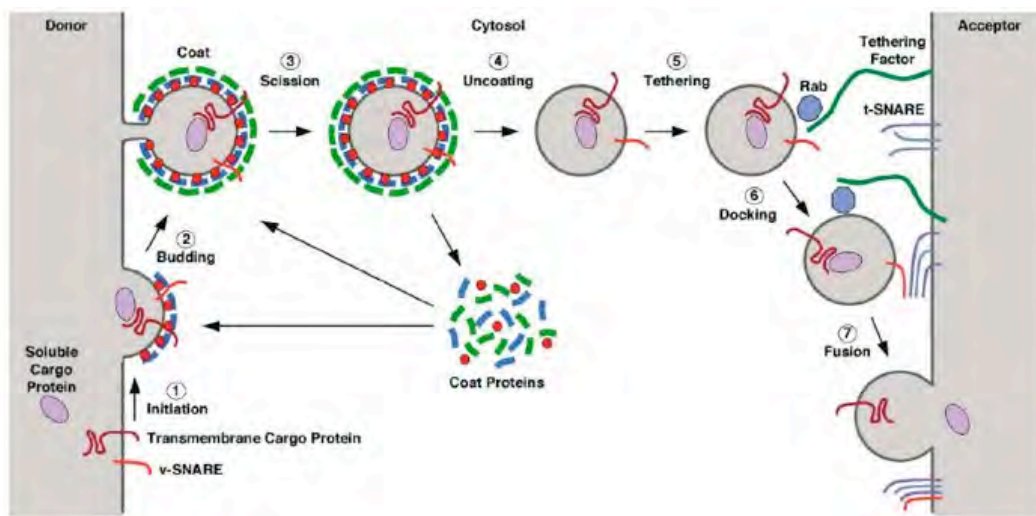
Figure 1.6: Steps in the life cycle of a coated vesicle. This scheme represents the steps involved in the Budding and Fusion of a coated vesicle. Formation of a coated vesicle at the donor membrane initiates by recruitment of membrane-proximal coat components (blue) to a membrane-associated GTPase (red) and/or to a specific phosphoinositide (1). Membrane-distal components (blue) are added and as the membrane curvature increases, the vesicle is severed (2&3). When the coated vesicle reaches the acceptor membrane, coat proteins are shed (4) and the coat proteins are recycled for next rounds of vesicle budding. The naked vesicle then tethers to the acceptor membrane guided by GTP-Rab and tethering factors; primed for fusion aided by v- and t-SNARES complex formation (5&6). Fusion between the vesicle and acceptor membrane bilayer is promoted by this SNARE complex and the cargo transferred to the acceptor compartment (7). (from (Bonifacino and Glick, 2004)).

Once the growing buds (see Fig.1.6, step 2 and 3) at the sites of assembly are completely formed, they need to detach from the donor membrane as a vesicle and travel a certain distance in order to deliver their contents to the target organelle. Detachment of the coated vesicles from the plasma membrane requires the activity of a GTPase, dynamin (Hinshaw and Schmid, 1995). Two of the proteins recruited

to a dynamin proline-rich region through their SH3 domains are amphiphysin and endophilin. Amphiphysin in turn interacts with synaptojanin. Synaptojanin is an inositol 5-phosphatase. Endophilin has lysophosphatidic acid acyltransferase activity (Huttner and Schmidt, 2000). This reaction generates phosphatidic acid potentially causing a change in membrane curvature and contributing to budding and scission. The activity of synaptojanin would favour release of dynamin by dephosphorylation of the head groups that recruit it. This suggests that PIP binding is a critical interaction stabilizing an assembled coat and that a inositide-specific phospholipase may play a role in vesicle uncoating (Cremona *et al.*, 1999). Both isoforms of dynamin (Dynamin 1 and 2) have been shown to be involved in the formation of transport vesicles at the TGN hinting at similarities in the vesicle scission mechanism with plasma membrane CCVs.

The uncoating of the CCVs (fig. 1.6, step 4) is facilitated by the dissociation of the coat proteins from lipid bilayers of the membranes. Hsc70 is an ATP-dependent chaperone, which binds relatively hydrophobic peptides or exposed protein sequences. It is involved in modulating the folding state of intracellular proteins for their translocation across ER, mitochondrial and lysosomal membranes. ATP hydrolysis by hsc70 is required for removing the clathrin triskelion from the vesicle and ADP stabilizes the hsc70- clathrin complex that is released (Prasad *et al.*, 1994). Hsc70 proteins are drawn to specific targets by proteins that contain J domains (named after DnaJ, the partner of the *E.coli* Hsp70, DnaK). The coated vesicle protein Auxilin contains such a J domain. The recently defined role in cellular CCV disassembly for auxilin also strengthens the implication of hsc70 as a regulator of clathrin disassembly (Lemmon, 2001; Ungewickell *et al.*, 1995). The phosphatase activity associated with auxilins could conceivably destabilize coat protein-PIP interaction. The recruitment of hsc70 to CCVs by auxilin followed by ATP binding and hydrolysis by hsc70 may cause a conformational change in assembled clathrin, triggering disassembly. It is not clear how lipid dissociation processes are coupled to disassembly of the clathrin lattice. Hsc70 releases clathrin, but not adaptors, from the isolated coated vesicles, which hinted that clathrin and adaptor dissociation are separate events. It was indeed shown that clathrin and adaptors dissociate from CCVs in separate steps (Hannan *et al.*, 1998), but very little is known about how adaptors are released from the membranes. The regulatory events involved in sensing the completion of formation of the vesicle and initiating the uncoating reaction still remain a puzzle. Earlier studies had reported the requirement of a cytosolic factor in the uncoating process at the TGN which was also shown to require ATP and Hsc70 (Hannan *et al.*, 1998). Recently it was shown that protein phosphatase 2A (PP2A) treatment of phosphorylated AP-1 from

CCVs abolished binding to the tail peptides and released adaptors from CCVs to the cytosol. Hence PP2A was shown to be the cytosolic co-factor required in adaptor uncoating of CCVs at the TGN (Ghosh and Kornfeld, 2003a).

Some of the proteins, that can classify as cargo proteins during vesicle formation, belong to the transport machinery themselves. Rab proteins, another family of small GTPases, link the vesicles to the cytoskeleton or manage their correct docking at the target membrane. SNARE proteins mediate membrane fusion in the last step of transport (for rev. see (Jahn *et al.*, 2003)). As assumed for all membrane fusion events, SNARE proteins reside on both the vesicle and the target membrane. Specific docking of the vesicle depends on the formation of the correct SNARE complex, which also approaches the two membrane surfaces to prepare for membrane fusion.

1.4   Sorting signals

The adaptor molecules bind to at least two different types of sorting signals in the tail of cargo. At least three types of sorting signals have been characterized in the context of AP mediated trafficking (for a detailed review, see (Bonifacino and Traub, 2003)).

1.4.1   Tyrosine-based motifs

Tyr-based motifs of the consensus Yxxϕ (x for any amino acid and ϕ for a bulky hydrophobic residue) are selectively recognized by the medium subunits. Co-crystallisation of the μ-adaptin C-terminal domain with peptides containing a Tyr-motif identified the precise interaction site (Owen and Evans, 1998). Yxxϕ motifs function in various transport pathways including endocytosis, lysosomal targeting or sorting to the basolateral plasma membrane (Marks *et al.*, 1996; Bonifacino and Traub, 2003). Consistently, all the four μ-adaptins bind to Yxxϕ sequences in vitro with distinct preferences for specific motifs (Ohno *et al.*, 1998). The surrounding residues obviously contribute to this specificity as well as the exact spacing of the motif within the cytoplasmic domain of the protein. The motifs that were identified so far to be necessary for endocytosis are found in the middle of the cytoplasmic domain far from the transmembrane domain, but not at the C-terminus of the protein. In contrast, motifs for lysosomal targeting are often located close to the C-terminus. As shown for the lysosomal protein Lamp-1, changing the distance of the GYQTI signal from the membrane interfered with sorting to lysosomes, but not with internalization from the plasma membrane (Rohrer *et al.*, 1996). Another Tyr-based motif with the consensus FxNPxY functions exclusively

in clathrin- mediated endocytosis. Peptides comprising this signal can interact with the N-terminal domain of clathrin heavy chain as well as with purified AP-2 *in vitro*, but it is still unclear if these mediate the sorting *in vivo*. Moreover, monomeric proteins like ARH, Dab2 and numb, which were initially termed accessory proteins and were initially known for recognition of phosphotyrosine residues and implicated in downstream signalling of tyrosine-kinase receptors, show a remarkable affinity for unphosphorylated FxNPxY and are localized in coated-pits through interactions with AP-2, phospholipids and clathrin.

1.4.2   Leu-based motifs

Leu-based motifs were identified as sorting determinants from the plasma membrane and from the TGN to endosomes and lysosomes. Apparently, there are two different classes. (D,E)xxxL(L,I) signals, like Yxxϕ , bind to adaptor complexes with preference for specific complexes and are found close to transmembrane domain as well as to the C-terminus. The acidic residue at the first position is not strictly required although favoured. Competition experiments with Tyr- and Leu-based motifs demonstrated that they are recognized by independent binding sites (Marks *et al.*, 1996). Until now, several subunits have been proposed to contain this site, namely μ, as inferred from several *in vitro* studies, and β, which was crosslinked to peptides (Rapoport *et al.*, 1998; Hofmann *et al.*, 1999). Recently, Y3H experiments reported an interaction between (D,E)xxxL(L,I) signals and a γ1-σ1- or δ-σ3-dimer, whereas none of the AP-1 or AP-3 subunits alone bound the motif (Janvier *et al.*, 2003). The other class of Leu-based signals, DxxLL seems to be required for transport between TGN and endosomes. Because the leucines are generally preceeded by several acidic residues, these motifs are also named acidic-cluster di-leucine motifs. In this case, the D residue cannot be replaced. In contrast to (D,E)xxxL(L,I) signals, DxxLL does not bind to AP complexes in vitro, but to the monomeric adaptor group of GGA proteins (Zhu *et al.*, 2001; Puertollano *et al.*, 2001). Another family of sorting motifs consists of a stretch of acidic amino acids containing one to three phosphorylation sites for casein kinase II (CKII). This motif is present in a number of transmembrane proteins that cycle between the TGN and endosomes, and phosphorylation of the CKII sites is particularly required for retrieval from endosomes to TGN. A protein called PACS-1 (phosphofurin acidic cluster sorting protein 1) was shown to bind to phosphorylated acidic clusters, as well as to the adaptor complexes AP-1 and AP-3. Remarkably, the binding interface to AP-1 was mapped to μ1 and σ1 (Wan *et al.*, 1998; Crump *et al.*, 2001).

1.5   Protein sorting at the TGN and endosomes

A number of cargo proteins have been shown to interact with AP-1 at the TGN and are transported from the TGN to the endosomes by AP-1-mediated clathrin coated vesicle assembly. Most prominent among them are the MPRs (Hille Rehfeld, 1995), lysosomal membrane glycoproteins (LGP85 or LIMPII), invariant chain of MHC class II complexes (Rodionov and Bakke, 1998), furin (Molloy *et al.*, 1999), gp48 (Reusch *et al.*, 1999), HIV-1 Nef (Erdtmann *et al.*, 2000). MPRs are the best known example of the transmembrane proteins sorted into the clathrin coats found on the TGN. They are selectively sorted at the TGN and exit this compartment in AP-1 containing clathrin-coated vesicles. MPRs are significantly enriched in purified clathrin-coated vesicle preparations (Borgne and Hoflack, 1997). Electron microscopic analysis have shown that both the MPRs and AP-1 or clathrin colocalize on budding profiles at the TGN (Klumperman *et al.*, 1993, 1998). There is a direct interaction between the sorting signals in cytosolic domain of the MPR300 and AP-1 (Höning *et al.*, 1997). AP-1-mediated sorting ensures that newly synthesized lysosomal hydrolases, bound to MPRs, are segregated from the molecules destined for constitutive transport to the plasma membrane and are delivered efficiently to the lysosomes via an intracellular route. However, since the GGA-proteins appear to have the same properties, the different functions of these two adaptor proteins in TGN-to-endosome sorting is not clear.

1.5.1   AP-1 Versus GGA adaptors at the TGN sorting station

For a long time, AP-1-containing-clathrin-coated vesicles were thought to form at the TGN and transport mannose-6- phosphate receptors (MPRs), the sorting receptors for lysosomal hydrolases that contain mannose-6-phosphate residues (Hille Rehfeld, 1995), to endosomes. The trafficking of MPRs in the μ1A 'knockout mice' (Meyer *et al.*, 2000) provided the first evidence for a role of AP-1 in the retrograde transport from endosomes to the TGN. If AP-1 mediates anterograde transport from the TGN to endosomes, one would expect that in AP-1 deficient cells, the MPRs would get stuck in the TGN. But surprisingly, the MPRs exit the Golgi, get transported to the plasma membrane and are re-endocytosed, finally accumulating in an early endosomal compartment that contains the early endosome marker EEA1. This indicated that AP-1 might mediate not anterograde, but retrograde, transport between endosomes and TGN. The observation that Shiga toxin co-localizes with AP-1 on early/recycling endosomes during a 20 ^{o}C block of retrograde transport and that toxin transport is inhibited by BFA supports this idea (Mallard *et al.*, 1998).

This model gained further support when it was shown that the recently discovered GGA proteins mediate anterograde transport of MPRs and other transmembrane proteins that have acidic di-leucine motifs (Puertollano *et al.*, 2001). However other studies showed by fluorescent tagged AP-1 that vesicular or tubular structures containing AP-1 leave the TGN and reach peripheral structures (Huang *et al.*, 2001; Waguri *et al.*, 2003), supports the idea that AP-1 is indeed involved in anterograde transport too.

When the N-terminal portion of a GGA protein that has the VHS and GAT domains, but lacks the clathrin-binding hinge domain and the GAE domain is expressed in mammalian cells, both MPRs accumulate in the TGN and clathrin is no longer detected on TGN membranes (Puertollano *et al.*, 2001). AP- 1 localization is unaltered if the expression of the GGA N-terminus is kept at moderate levels. These data suggest that GGA proteins mediate clathrin-dependent anterograde transport of MPRs from the TGN to endosomes, a function long attributed to AP-1. So far, however, in mammalian cells there is no evidence that GGA proteins are a stable component of clathrin-coated vesicles; instead they redistribute very quickly to the cytoplasm under conditions where AP-1 stays on the membrane (Hirst *et al.*, 2001). Subsequently, another study showed that the GGA hinge region binds to the γ-ear of AP- 1. This indicates that AP-1 and GGA proteins might interact and cooperate in the same sorting step (Doray *et al.*, 2002). In immunoelectron microscopic studies using cells stably transfected with tagged GGA2, the authors demonstrate colocalization of GGA2 and AP-1 on coated buds of the TGN. Moreover, mutant MPR that does not bind GGA proteins fails to enter AP-1-coated vesicles.This let to the idea that GGA proteins are not necessarily packaged into vesicles but rather help recruit coat components and cargo into a budding vesicle. Further, the finding that the GGAs 1 and 3 are regulated by phosphorylation leading to an auto-inhibited state led to a hypothesis (Fig. 1.7) where GGAs were shown as adaptors that help to recruit cargo molecules into AP-1 conataining clathrin-coated vesicles. However, this model does not apply to GGA2, as it lacks the critical serine residue which was shown to be subjected to phosphorylation and dephosphorylation cycles. Altogether, the precise role of AP-1 and the GGAs is still not clear.
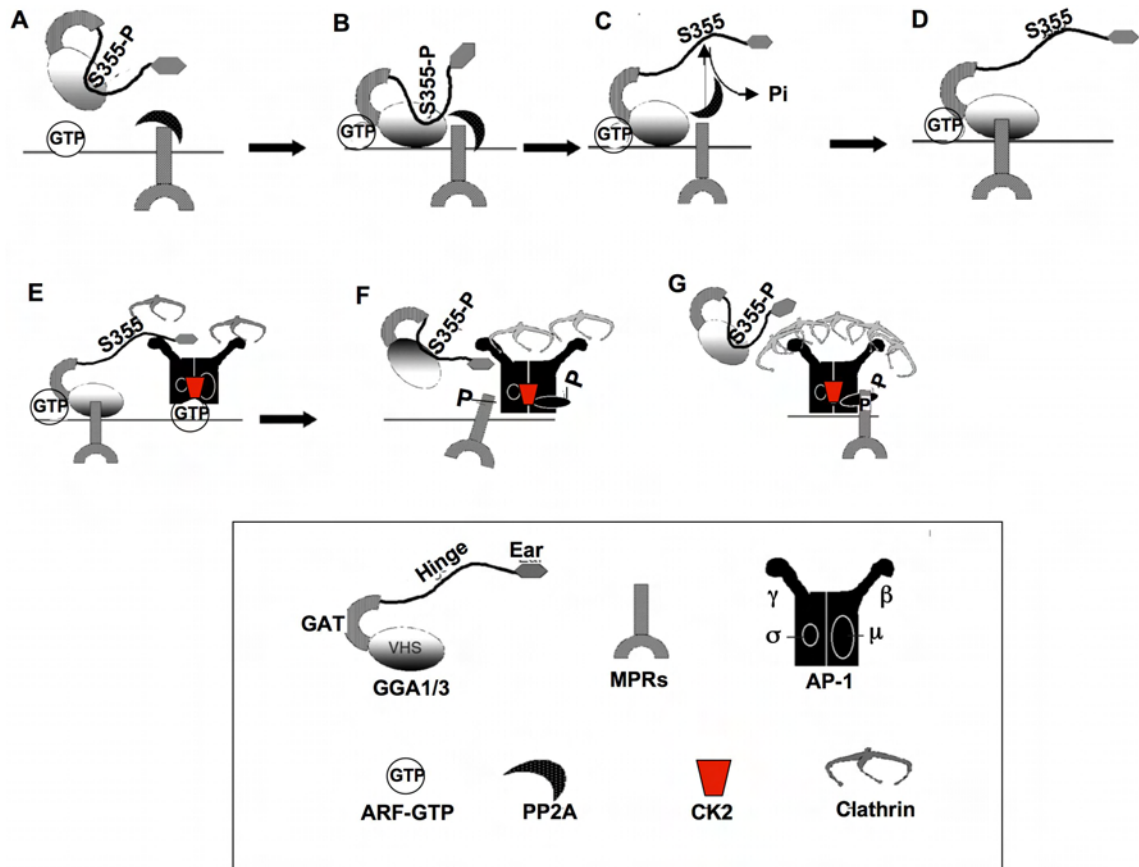
Figure 1.7: A model for Phosphoregulation of GGAs 1 and 3. (A) Cytosolic GGA in phosphorylation induced auto-inhibited state. (B) GGAs bind to membrane through ARF-GTP. (C) PP2A dephosphorylates GGA and relieves it from auto-inhibition. (D) The open form is now capable of binding to the cytoplasmic tail AC-LL motif of MPR. (E) GGAs can interact with γ-appendage domain of AP-1 on membranes via its hinge domain. (F) AP-1 associated CK2 phosphorylates GGAs and restores the auto-inhibited state. CK2 also phosphorylates the MPR tail. The phosphroylation of AP-1 μ1A at some point on membrane recruitment induces a open conformation of μ1A, exposing ligand binding sites. This phosphorylation of MPR and of μ1A generates high avidity binding of MPR tails to AP-1, thereby ensuring directed transfer of cargo from GGAs 1 and 3 to membrane associated AP-1. (G) Thus MPR cargo molecules are trapped by AP-1 and as the clathrin coat assembly proceeds the auto-inhibited GGAs dissociate from AP-1 and are released to cytosol. (from (Ghosh and Kornfeld, 2003b))

1.6 Aim of the study

In the course of her Ph.D project in our group, C.Riel analyzed the expression pattern of σ1-adaptin isoforms A,B and C in mouse tissues, each of which is encoded by an individual gene. In addition, she identified tissue specific variants of σ1B-adaptin (C.Riel and P.Schu, unpublished). μ1 adaptins and γ1-σ1 hemicomplex are able to bind to different sorting motifs in the cytoplasmic tails of cargo proteins. Sortilin receptor belongs to the family of Vps10p-domain receptors and it has been shown that it is sorted similar to the well studied mannose-6-phosphate receptors. Sortilin has been shown to be able to mediate lysosomal sorting, however it has also essential functions at the plasma membrane and internal organelles via heterodimerization. It has been reported that sortilin is sorted by GGA2, however nothing is known about AP-1-dependence of sortilin trafficking.

In a second project, the mechanism of AP-1 membrane binding should be studied. To identify possible function(s) of different domains of μ1A-adaptin, a μ2/μ1 chimera was constructed which was shown to assemble into a functional chimeric AP-1 complex, designated as AP-1*. But this AP-1* complex, was unable to restore the phenotype of μ1A-deficient cells. During his Ph.D thesis project, Medigeshi R. Guruprasad discovered that the N-terminal seventy amino acids of μ1A are required for proper membrane-cytoplasm recycling of AP-1 and that impairing recycling causes mis-sorting of MPRs as indicated by secretion of their ligand cathepsin D into the culture medium (Guruprasad Medigeshi and P. Schu, unpublished). Therefore membrane binding of AP-1* should be analyzed in more detail. In addition, proteins binding to the N-terminal seventy amino acids of μ1A were to be identified.

Chapter 2

Materials and Methods

2.1 Materials

2.1.1 Laboratory equipment

Analytic balances type 1602 MP and 1265 MP	Sartorius, Goettingen
Intelligent Dark Box II, Las-1000+	Fuji, Japan
Ice machine	Ziegra, Isernhagen
Centrifuges:	
Eppendorf centrifuge Type 5415C and 5402	Eppendorf, Hamburg
Table ultracentrifuge TL-100	Beckmann, München
Ulracentrifuge L8-70M	Beckmann, München
Cold Centrifuge J-21C and J2-MC	Beckmann, München
Labofuge GL	Heraeus Sepatech
Rotors:	
JA10, JA 20	Beckmann, München
Ti 45, Ti 60, Ti 70	Beckmann, München
TLA 45,	Beckmann, München
TLA-100.3	Beckmann, München
Electrophoresis chambers for agarose gels	Workshop of the Institute
Electrophoresis chambers for polyacrilamide gels	Workshop of the Institute
Gel dryer	Bio-Rad, Hilden
Magnetic mixer	IKA, Works, INC.
Microwave oven	Siemens, München
pH-Meter	Beckmann, München
Photometer, UV 160 A	Shimadzu, Kioto/Japan
UV-hand lamp (365/254nm), Type 5415 and 5402	Eppendorf, Hamburg

Vacuum concentrator model 100H	Bachhofer, Reutlingen
Vortex-Genie	Scientific Industries, USA.
DNA-Sequencer Type 310	ABI, PE Biosystems
Electroporator 1000 (used for bacteria)	Stratagene, USA
Confocal Laser Scanning Microscope	Leica, Bensheim
Leica TCS SP2 AOBS	
(Ar: 488, 514 nm; He/Ne: 543 nm; 63x Oil Objective)	
Incubators Innova 4230 and 4330	New Brunswick Scintific
Phosphoimager Fujix BAS1000	Fuji, Japan
Ultra turrax T8	IKA Labortechnik, Staufenv
Supersignal Chemiluminiscent Substrate	Pierce, Illinois
Thermocycler GeneAmp PCR system 9600	Perkin-Elmer Cetus

2.1.2 Chemicals, plasticware and membranes

Chemicals	Boehringer/Roche, Mannheim,
	Merck, Darmstadt,
	Roth, Karlsruhe,
	Serva, Heidelberg,
	Sigma, Deisenhofen
Cell culture plasticware	Greiner, Frickenhausen
	Nalge Nunc International, Denmark
Nitrocellulose membrane	Schleich and Schüll, Dassel
PVDF membrane, 0.2μM	Schleich and Schüll, Dassel
Hybond-N Nylon membrane	Amersham Biosciences, UK
Whatman GB002 paper	Schleich and Schüll, Dassel
Whatman GB003 paper extra thick	Schleich and Schüll, Dassel

2.1.3 Kits, spin columns and reagents

2.1.3.1 DNA, RNA

HiSpeed Plasmid Midi kit	Qiagen
Omniscript Reverse Transcription kit	Qiagen
PCR purification kit	Qiagen
QIAprep Spin Miniprep kit	Qiagen
QIAquick Gel Extraction kit	Qiagen
Rapid-hyb hybridisation buffer	Amersham Pharmacia Biotech

rediprimeTMII labeling system	Amersham Pharmacia Biotech
RNAlater RNA Stabilisation Reagent	Qiagen
RNase inhibitor RNase Out	Invitrogen
RNeasy Mini and Midi Kit	Qiagen
TA Cloning Kit	Invitrogen
Effectene Transfection kit	Qiagen
Fugene Transfection reagent	Roche
Lipofectamine 2000	Invitrogen
MATra transfection reagent	IBA,Goettingen

2.1.3.2 Protein

Bio-Rad Protein Assay	Bio-Rad
DAKO fluorescent mounting medium	DakoCytomation, USA
ECL Plus	Amersham Biosciences
ConcanavalinA-Sepharose 4B	Amersham Biosciences
Protease Inhibitor Cocktail	Sigma
PD-10 Sephadex G-25 M column	Amersham Pharmacia Biotech
Supersignal Chemiluminescence Kit	Pierce, USA
Roti-blue Colloidal Coomassie Brilliant Blue	Roth
Bovine Serum Albimin (BSA)	Serva
Iodoacetamide, Iodoacetic acid	Sigma
PANSORBIN cells	Calbiochem
Protein A sepharose	Sigma
Protein G agarose	Sigma
Prestained Marker	Biorad

2.1.4 Strains and Cell lines

2.1.4.1 Bacterial strains

Strain	Genotype	Reference
XL1-Blue	*recA1,endA1,gyrA96,th-1,hsdR17, supE44,relA1,lac[F,proAB,laclqZΔM15, Tn10(Tetr)]c*	Stratagene
BL21(DE3)	*F$^-$ompT,dcm$^+$,hsdS$_B$($r_B{}^-$ $m_B{}^-$), Tet^r,galλ(DE3),endA,Hte[pT-Trx Cam^r]*	(Yasukawa *et al.*, 1995)

2.1.4.2 Yeast strains

Strain	Genotype	Reference
AH109	*MATa, trp1-901, leu2-3, 112, ura3-52, his3-200, gal4Δ, gal80Δ, LYS2 : : GAL1$_{UAS}$-GAL1$_{TATA}$-HIS3, GAL2$_{UAS}$-GAL2$_{TATA}$-ADE2, URA3 : : MEL1$_{UAS}$-MEL1$_{TATA}$-lacZ*	CLONTECH
CG1945	*MATa, ura3-52, his3-200, ade2-101, lys2-801, trp1-901, leu2-3, 112, gal4-542, gal80-538, cyh^{r}2, LYS2 : : GAL1$_{UAS}$-GAL1$_{TATA}$-HIS3, URA3 : : GAL4$_{17-mers(x3)}$-CYC1$_{TATA}$-lacZ*	CLONTECH

2.1.4.3 Mouse cell lines

Cell line	Source	Reference
E14-1 ES cells	established from blastocysts of mouse 129/Ola strain	(Hooper *et al.*, 1987)
neomycin resistant **MEF**	established from a neomycin-resistant mouse strain in this institute	(Müller *et al.*, 1991)
μ**1A-/- MEF**	established from the μ1A-/- mouse strain (mixed C57 BL/6J : 129/Ola background)	(Meyer *et al.*, 2000)
σ**1B-/- MEF**	established from the σ1B-/- mouse strain (mixed C57 BL/6J : 129/Ola background)	(Riel, 2004)

2.1.4.4 Mouse Strains

C57 BL/6J	Inbred strain,black colour	BRL,Switzerland
129SV/J	Inbred strain,agouti colour	BRL,Switzerland

2.1.5 Vectors

2.1.5.1 Mammalian System:

pGK Hygro	Invitrogen life technologies
pUB/Bsd	Invitrogen life technologies
pcDNA3.1	Invitrogen

2.1.5.2   yeast System

pGBT9	BDBiosciences Clontech
pGBKT7	BDBiosciences Clontech
pGADT7	BDBiosciences Clontech
pBRIDGE	BDBiosciences Clontech

2.1.5.3   Bacterial System

pGEX2T	Amersham Biosciences
pCR2.1	Invitrogen

2.1.6   Antibiotics and drugs

Ampicillin	Serva
Blasticidin-S Hydrochloride	Invitrogen life technologies
Hygromycin	Calbiochem
Neomycin (Gentamycin sulfate or G418)	Gibco
Penicillin/Streptomycin	Gibco
(100 x =10,000 U/ml)	

2.1.7   Enzymes and Standards

Restriction endonucleases	New England Biolabs
Klenow DNA polymerase	New England Biolabs
DNA ligase	New England Biolabs
Taq DNA polymerase	Amersham Pharmacia Biotech
Alkaline phosphatase	Boehringer
Ultrapure dNTP Set	Amersham Pharmacia Biotech
Adenosine 5'-triphosphate (ATP)	Sigma
1-kb DNA ladder	Gibco BRL

2.1.8 Primary antibodies

Antigen(epitope)	Type	WB	IF	Reference
HA tag	mouse mAb	1:2000	1:100	Covance Inc.
HA tag	Rat mAb	1:2000	1:100	Covance Inc.
γ1-adaptin 100.3, (mouse γ1-adaptin hinge)	mouse mAb, purified	1:5000	1:100	Transduction Laboratories
μ1A-adaptin 144, (mouse μ1A residues 295-310)	rabbit pAb	1:1000	-	(Meyer *et al.*, 2000)
α-adaptin, (mouse α-adaptin residues 38-215)	mouse mAb, purified	1:5000	1:100	Transduction Laboratories
MPR46-MSC I, (cytoplasmic tail of MPR46)	rabbit pAb	-	1:50	(Klumperman *et al.*, 1993)
MPR300-**I**5, (rat MPR300)	rabbit pAb	-	1:50	(Claussen *et al.*, 1995)
LAMP-1(1D4B)	rat mAb	-	1:100	Hybridoma Bank (USA)
sortilin	mouse mAb	-	1:200	C.M.Petersen (Denmark)
IL2R	mouse mAb	-	1:200	C.M.Petersen (Denmark)
sortilin	rabbit pAb	1:200	-	Abcam (UK)

2.1.9 Secondary antibodies

Goat anti-rabbit Horseradish peroxidase conjugate (WB,1:10,000)
Goat anti-mouse Horseradish peroxidase conjugate (WB,1:10,000)
Goat anti-rat Horseradish peroxidase conjugate (WB,1:10,000)
Goat anti-rabbit Alexa633 conjugate (IF,1:400)
Goat anti-mouse Alexa488 conjugate (IF,1:400)
Goat anti-rat Cy3 conjugate (IF,1:400)
All secondary antibodies were purchased from Dianova, Hamburg.

2.1.10 Stock solutions and buffers

1 M Sodiumphosphate buffer
1 M solution of sodium di-hydrogen phosphate was slowly added to 1 M di-sodium hydrogenphosphate solution with constant mixing on a magnetic stirrer till the pH came down to 7.4.

10 x PBS
100 mM sodium phosphate pH 7.4
9 % sodium chloride
Dissolved in 800 ml water and pH was adjusted to 7.4 with HCl, volume was made up to 1000 ml and autoclaved. Stored at room temperature.

1 x TBS
10 mM Tris/ HCl pH 7.4
150 mM Sodium chloride
1 x TAE 0.04 M Tris-acetate
1mM EDTA (pH 8.0)

50x TAE
242 g Tris base
57.1 g glacial acetic acid
100 ml of 0.5 M EDTA (pH 8.0)
Dissolved in water and the final volume was made upto one litre.

TE Buffer
10 mM Tris/ HCl pH 7.5
1 mM EDTA

2.2 Methods

2.2.1 Molecular biology

2.2.1.1 Cultivation of E.coli

Luria Bertani (LB) medium
10 g Bacto-Tryptone
5 g Bacto-yeast extract
5 g NaCl
Dissolved in 900 ml distilled water, pH adjusted to 7.0 with 10 N NaOH, made up the volume to one liter, sterilized by autoclaving and stored at room temperature.
LB-Ampicillin Agar Plates

1.5% of Agar was added to the LB medium and autoclaved. After autoclaving, the medium was let to cool down to 55 ^{o}C and ampicillin was added to a final concentration of 100 μg/ml. This medium was poured into 10 cm petriplates in the hood and left undisturbed for about 30 min to solidify. LB-Agar plates were stored in the cold room.

2.2.1.2   Preparation of electrocompetent Bacterial cells

10% (v/v) Glycerol : 1 ml (1.26 g) of glycerol in 10 ml sterile water
A single E. coli colony was inoculated into 10 ml of LB media and allowed to grow overnight at 37 ^{o}C, 250rpm in a shaker incubator. This pre-culture was diluted 1:100 into fresh LB media and allowed to grow to an OD_{600} of 0.3-0.35 at 37 ^{o}C. The culture was pre-chilled on ice for 15 min and centrifuged at 5000 rpm for 15 min at 4 ^{o}C in a JA-10 rotor. The pellet was resuspended in 500 ml of ice cold water and centrifuged as described above. This washing was repeated once again with 250 ml ice cold water. The resulting pellet was resuspended in 20 ml of filter sterile ice-cold 10% glycerol and centrifuged at 4 ^{o}C for 15 min in a JA-20 rotor.The pellet was resuspended in 2 ml of ice-cold 10% glycerol. Aliquots of 40 μl were quick frozen in dry-ice and stored at -80 ^{o}C.

2.2.1.3   Transformation of plasmid DNA by Electroporation

SOC medium
0.5% Yeast extract
2% Bacto-tryptone
10 mM Sodium chloride
2,5 mM Potassium chloride
10 mM Magnesium sulfate
10 mM Magnesium chloride
20 mM Glucose
For each electroporation, a 40 μl aliquot of the electrocompetent cells was thawed on ice and 1-5 μl of the DNA sample was added and mixed.The resulting mixture was transferred into a sterile, pre-chilled electroporation cuvette and subjected to a 1800 V pulse in the electroporator. Immediately after the pulse, the cells were diluted in 500μl of ice-cold SOC medium and transferred to a sterile e-cup and incubated at 37 ^{o}C with mild shaking for 30-40 min. After the recovery period, the cells were plated onto LB plates supplemented with the appropriate antibiotic and allowed to grow over night at 37 ^{o}C .

2.2.1.4 Preparation of Glycerol stocks for bacterial strains

Bacterial cultures were grown to log phase at 37 ^{o}C, 250rpm in a shaker-incubator. 0.7 ml of this logarithmic culture was mixed with 0.3 ml of sterile 100% glycerol. The contents were gently mixed, shock frozen on dry ice and stored at -80 ^{o}C.

2.2.1.5 Plasmid DNA preparation and cloning protocols

All required instructions from the manufacturer were followed for the isolation of plasmid DNA (Qiaprep Kit), for the digestion or modificaion of DNA by enzymes, for the analysis of DNA by agarose gel electrophoresis in TAE buffer and for the purification of DNA fragments from sliced agarose gels (Qiaspin Gel Extraction Kit).

2.2.1.6 Determining the concentration of DNA

DNA concentration was determined using a spectrophotometer. DNA was diluted in water and the absorbance was measured at 260 nm. Absorbance or optical density (OD) of 1 at 260 nm corresponds to $\sim$50μg/ml of double stranded DNA or $\sim$40μg/ml of single stranded DNA and RNA or $\sim$20μg/ml of oligonucleotides. The ratio between the readings at 260 nm and 280 nm (OD260/ OD280) provides an estimate of the purity of the nucleic acid. Pure preparations of DNA and RNA have OD-260/OD-280 values of 1.8 and 2.0, respectively. Any contamination with proteins or phenol would yield values less than mentioned above.

2.2.1.7 Restriction endonuclease digestion of DNA

The activity of restriction enzymes is measured in terms of 'Units' (U).
One unit of restriction enzyme is the amount of enzyme required to completely digest 1 μg substrate DNA in 1 hr.

Plasmid DNA	0.5 - 1 μg
10 x buffer	2 μl
Restriction enzyme	1-2 U
BSA	1 μg/μl (added where essential)

Water was added to a final volume of 20 μl. Reaction mix was incubated at 37 ^{o}C* for 2 hours.
*Incubation temperatures were set as recommended by the manufacturer (New England Bio Labs Beverly U.S.A.) which varies from enzyme to enzyme. Reaction mix was analyzed on agarose gel (0.8 to 2% depending on the size of the DNA of

interest) The buffers and enzymes used were all from New England Biolabs. The composition of the buffers is as follows:

NEB 1: 10 mM Bis Tris Propane-HCl (pH 7.0), 10 mM $MgCl_2$, 1 mM DTT

NEB 2: 10 mM Tris-HCl (pH 7.9), 10 mM $MgCl_2$, 50 mM NaCl, 1 mM DTT

NEB 3: 50 mM Tris-HCl (pH 7.9), 10 mM $MgCl_2$, 100 mM NaCl, 1 mM DTT

NEB 4: 20 mM Tris-acetate (pH 7.9), 10 mM Magnesium acetate, 1 mM DTT, 50 mM Potassium acetate

2.2.1.8 Agarose gel electrophoresis of DNA

The size and purity of DNA is analyzed by agarose gel electrophoresis. Concentration of agarose used for analysis is inversely proportional to the size of the DNA of interest, that is, the larger the DNA the lower the concentration of agarose.

Agarose concentration (%)	DNA size (kb)
0.7	20 - 1
0.9	7 - 0.5
1.2	6 - 0.4
1.5	4 - 0.2
2.0	3 - 0.1

Gel loading buffer (10x)

0.25% (w/v) Bromophenol blue

40% Saccharose in 1x TAE

Agarose was weighed and dissolved in 1 x TAE by boiling in microwave oven. The agarose solution was cooled to 60 ^{o}C and ethidium bromide was added to a final concentration of 0.5 μg/ml. This was poured into the agarose gel cassette and allowed to polymerize completely. The sample DNA was mixed with gel loading buffer and loaded onto the gel. The gel electrophoresis was carried out at 100 V. Ethidium bromide is a fluorescent dye which contains a planar group that intercalates between the stacked bases of the DNA. The fixed position of this group and its close proximity to the bases cause the dye to bind DNA. It results in an increased fluorescent yield compared to that of the dye in free solution. Ultraviolet radiation at 254 nm is absorbed by the DNA and transmitted to the dye; radiation at 302 nm and 366 nm is absorbed by the bound dye itself. In both cases, the energy is re-emitted at 590 nm in the red orange region of the visible spectrum. Hence DNA can be visualized under a UV transilluminator. The gel can be photographed using a gel documentation system.

2.2.1.9   Isolation of RNA from mouse cells or mouse tissue

All the preparations were done according to the RNeasy protocol (Qiagen) with the following details: For isolation of total RNA from cells, they were grown to confluency on a 10 cm culture dish and lysed directly on the plate. The lysate was eventually stored at -80 ^{o}C. For isolation of total RNA from tissue, the organs were excised from a mouse and immediately either frozen in liquid nitrogen for storage at -80 ^{o}C or immersed in RNAlater reagent (10 ml/g tissue) for storage at 4 ^{o}C or at lower temperature. An appropriate amount of tissue was cut into mm-sized pieces and homogenised with an ultra-turrax. For tissues with a low yield of RNA such as brain, heart etc., about twice the recommended tissue weight could be successfully loaded onto one column, if the volume of lysis buffer and subsequent buffers was doubled as well.

2.2.1.10   Polymerase chain reaction (PCR)

PCR is a rapid and versatile *in vitro* method for amplifying defined target DNA fragments by DNA polymerase which occurs naturally in living organisms, where it duplicates DNA when cells divide. It is used to amplify a short, well-defined part of a DNA strand. *Taq* polymerase is widely used but the disadvantage is that it lacks 3'→5' proof reading exonuclease activity, leading to mutations in the sequence. For amplification of DNA fragments of size above 1 kb, Expand high fidelity Taq polymerase (Roche) was used.

Condition	Temperature	Time
Denaturation	95 ^{o}C	2 min
Amplification	95 ^{o}C	40 sec
	55 ^{o}C	40 sec
	72 ^{o}C	1min for upto 1.5-2 kb
Extention	72 ^{o}C	10 min
End	4 ^{o}C	∞

PCR Mix

Components	Volume
10X *Taq* buffer (100 mM Tris/HCl pH 9.0; 500 mM KCl)	10 μl
2.5 mM dNTPs (Amersham, Stock 100 mM)	10 μl
25 mM MgCl$_2$	5 μl
5-primer (Stock 100 pmol/μl)	2 μl
3-primer (Stock 100 pmol/μl)	2 μl
Template DNA (40 ng/μl)	1μl
Taq polymerase + 1/10 *Pfu*-Polymerase	1 μl
Final volume made upto 100 μl with HPLC water	

2.2.1.11   Ligation

Joining linear DNA fragments together by a phosphodiester bond between the 3'
hydroxyl of one nucleotide and the 5' phosphate of another is called ligation. T4
DNA ligase is used for this purpose, it ligates the cohesive ends of the fragments.
There are two types of ligation viz., cohesive end or sticky end ligation and blunt
end ligation, depending on the restriction digestion of the DNA. For the blunt
end ligation and also if digestion was with single sticky end enzyme, the vector
should be dephosphorylated by alkaline phosphatase, and the ligation mix should
be incubated for overnight.
For example:

x μl	linearised vector DNA
y μl	Insert DNA [1(vector DNA):10 (insert DNA)]
1.5 μl	10x Ligase buffer
1.0 μl	T4-DNA-Ligase (400 U/μl)

Made upto 10 μl with ddH$_2$O, incubated overnight at 16 ^{o}C or 1 hr at RT and
transformed into *E.coli* competent cells.

2.2.1.12   Sequencing PCR

DNA sequencing was done by Sanger's method using a DNA sequencer. The plasmid
DNA to be sequenced was supplied with a mixture of all four nucleotides plus four
ddNTPs, each labeled with a tag that fluoresces different color. For sequencing
reaction, clean DNA should be used (prepared by QIAprep-Spin-Miniprep-Kit).

For example:

x μl	Plasmid-DNA (0.2 - 0.5 μg)
3.2 μl	Forward primer or reverse primer (1 pmol/μl)
2.0 μl	ABI PRISM Dye Terminator Cycle Sequencing Ready Reaction Premix
x μl	HPLC-H$_2$O (Make it upto 10 μl)

Condition	Temperature	Time
Denaturation	96 ^{o}C	10 sec
Amplification	96 ^{o}C	10 sec
	50 ^{o}C	5 sec
	60 ^{o}C	4 min
25 cycles		
End	4 ^{o}C	∞

The PCR product for sequencing should be cleaned thoroughly to remove fluorescently labeled free ddNTPs to avoid background. To the PCR product 2 μl of 3 M Sodium acetate (pH 5.2) and 50 μl 95 % ethanol (room temperature) was added, incubated at RT for 10 min and centrifuged for 20 min at 13000 rpm. The pellet was washed with 250 μl of 70% ethanol for 10 min at 13000 rpm, dried and resuspended in 25 μl of HPLC water and given for sequencing.

2.2.2 Yeast Genetics

2.2.2.1 Lithium acetate mediated yeast transformation

Stock solutions

50% PEG (3350)	Sterilize with 0.22 μm cellulose-acetate membrane filter
10X LiAc (1M)	Adjust pH to 7.5 with Glacial acetic acid.
	Filter sterilize as above
10X TE	100 mM Tris-HCl pH 8.0
	10 mM EDTA pH 8.0
	Sterilize by autoclaving

This method is extremely efficient to transform PCR products, plasmids and libraries. The yeast cells are made competent freshly before the transformation. All materials used for this procedure should be sterilized well. Preparation of competent cells.

Inoculate a single colony of yeast into 5ml YAPD medium and grow overnight. Inoculate 250 ml of YAPD medium with 5 ml of pre-inoculum and grow for 4- 5 hr (OD600 0.6 - 0.8) at 30 ^{o}C and 225 rpm. Pellet the cells at 5,000 rpm for 15 min at 4 ^{o}C in JA-20 rotor. Washed the pellet twice with ice cold sterile water. Resuspended the pellet in 3 ml 1X LiAc/TE sterile.

Incubate yeast competent cells for about 30 min at 30 ^{o}C and aliquot 100μl for transformation by making a cocktail as follows.

Ingredients	Volume or Amount
Yeast cells in LiAc/TE	100 μl
PEG/LiAc (sterile)	700 μl
SSDNA (Salmon/Herring sperm DNA)	5 μl
pDNA (in less than 5 μl)	0.1 μg

Incubate the cells at 30 ^{o}C for 30 to 60 min. After the incubation time, the mixture heat shock to the cells at 42 ^{o}C for 15 min. Spin the cells for 1 min at 2000 rpm, 4 ^{o}C in a tabletop centrifuge. Discard the supernatant. Wash the cells at least once with 1 ml of water at room temperature so that PEG is completely washed out (PEG can induce fusion of cells). Resuspend the pellet in 200 μl of sterile water and plate on appropriate plate lacking the auxotrophic marker. Incubate the cells at 30 ^{o}C for 3 to 5 days until colonies appear.

2.2.2.2 Yeast cell plasmid rescue

Reagents
Appropriate SC medium
TE pH-7.5
3% SDS
0.2N NaOH
3M CH$_3$COONa
pH-5.3
Phenol Chloroform Absolute alcohol and 70% ethanol

Yeast cells with the pDNA were grown ($\sim$24-32 hr) in selective medium. Pelleted the cells 1.5 ml of well grown cell culture of yeast and resuspended in 100 μl of lysis buffer (TE pH-7.5, 3% SDS and 0.2 N NaOH) and incubated at room temperature for 30 min. To the above lysate 600 μl of TE pH-7.5 was added, followed by the

addition of 70 μl of 3 M sodium acetate pH-5.3. Vortex and extract sequentially with phenol/chloroform (1:1) and chloroform. Precipitated the plasmid pDNA in the aqueous supernatant with two volumes of ethanol. Incubate at -20 ^{o}C for an hour. Pelleted the pDNA at 12,000 rpm for 10 min at 4 ^{o}C. Rinse the pellet with 70% ethanol and resuspended the pDNA in 20 μl of TE or sterile water. 2 μl of this is used to transform in E.coli cells by electroporation. The transformants were selected on LB plates containing appropriate antibiotic marker.

2.2.2.3 Testing interaction by growth

The growth patterns of different yeast transformants were compared on selection plates by growth test either by dropping nearly equal number of cells or by streaking. For drop out the transformant were inoculated in 8 ml of YEPD or SD-medium and grown overnight at 24°C till OD$_{600}$ 0.2-1.0. The selection plates SD/-Leu/-Trp, SD/-His/-Leu/-Trp, SD/-Ade/-Leu/-Trp and SD/-Ade/-His/-Leu/-Trp plates were pre-warmed at 30°C. For each strain, two dilutions were prepared in sterile water viz., 0.01 OD/ml and 0.05 OD/ml. 10 μl from each dilution is spotted onto the pre-warmed plates using a pattern. The spots were allowed to dry and the plates were incubated at 30 ^{o}C. The growth was scored after 24 hr and the strength of interaction was assessed based on the growth of yeast; faster growth implicates strong interaction.

Other approach for growth test was by streaking the transormants on the selection plates SD/-Leu/-Trp, SD/-His/-Leu/-Trp, SD/-Ade/-Leu/-Trp and SD/-Ade/-His/-Leu/-Trp plates were pre-warmed at 30 ^{o}C. Monitored the growth after 36-48 hrs.

2.2.2.4 Filter lift assay - *lacZ* reporter gene

Reagents

Components	Amount (g)
NaH$_2$PO$_4$.H$_2$O	13.79
KCl	0.75
MgSO$_4$.7H$_2$O	0.246

X-Gal(5-bromo-4-chloro-3-indolyl-β-d-galactopyranoside):(20 mg/ml)
Disslove one gram of X-Gal in 50 ml of N,N-dimethylformamide. Store at -20°C.

Z buffer/β-mercaptoethanol

This should be made fresh by adding 270 μl of -mercaptoethanol to 100 ml of Z buffer.

Z buffer/β-mercaptoethanol/X-Gal

This should be made fresh by adding 270 μl of β-mercaptoethanol and 1.67 ml of X-Gal solution (20 mg/ml) to 100 ml of Z buffer.

Yeast transformants to be checked for the β-galactosidase (*lacZ* reporter gene) were streaked on SD/-Leu/-Trp plates and grown for 36-48 hr. Carefully placed a sterile 75 mm circle of Whatmann No.1 filter paper on top of the colonies or patches growing on selective medium. Ensured that filter paper makes good contact with the colonies. Mark the orientation of the filter paper relative to the plate using an 18-guage needle to punch through the filter in an asymmetric pattern. Remove the filter paper from the plate with a clean forceps after it has become fully absorbed to the colonies and immerse in liquid nitrogen for 10-15 sec. Filter paper was removed from the the liquid nitrogen and thawed by placing on a piece of plastic wrap with colony side up. Repeat freeze and thaw cycle twice. Placed another 75 mm sterile Whatman No. 1 filter into an empty petri plate and dispense 1.25 ml of Z buffer/β-mercaptoethanol/X-Gal onto the filter, on top of this placed the filter with colony side up. Wrap it with aluminium foil and incubate at 37 ^{o}C for 24 hr.

2.2.2.5   X-α-Gal assay

Mel1 is an endogenous gene found in several yeast strains because α-galactosidase is a secreted enzyme, it can be assayed directly on X-α-Gal (No.8061-1, BD Bioscience) indicator plates, which employs blue/white screening. Yeast transformants to be checked for the α-galactosidase (*Mel1* reporter gene) were streaked on SD/-Leu/-Trp or SD/-Ade/-His/-Leu/-Trp plates containing X-α-Gal and grown for 36-48 hr and monitored for the color development.

2.2.3 Cell culture and transfections

2.2.3.1 Basics

Normal growth medium:	DMEM, 10% fetal calf serum, Pen-Strep
Trypsin-EDTA solution:	0.5 g/l Trypsin, 0.2 g/l EDTA
phosphate-buffered saline (PBS):	150 mM NaCl, 120 mM KCl,
	10 mM Na_2HPO_2/KH_2PO_2 pH 7.4
Freezing medium:	10% DMSO in normal growth medium

All cell lines were grown in Dulbecco's modified Eagle's medium (DMEM) supplemented with 10% fetal calf serum (FCS) and 1% penicillin/streptomycin (Invitrogen) under 5% CO_2 at 37 ^{o}C.

2.2.3.2 Passaging by trypsinisation

Cell line was passaged every 2-7 days depending on the growth rate. After two washes with PBS, 0.5 ml trypsin solution per 25 cm^2 was added to the cell layer. The cells were incubated at 37 ^{o}C for 5 min, then singled by tapping to the dish and resuspended in medium. To concentrate, wash or harvest cells, centrifugation was always done at 500xg for 5 min.

2.2.3.3 Freezing cells for stock maintenance

Usually, cells from a confluent 35 cm^2 flask were frozen as 2-4 vials. Cells were pelleted after trypsinisation, resuspended in 1 ml freezing medium per vial, immediately placed on ice and stored at -80 ^{o}C overnight. The vials were transferred to the liquid nitrogen container the following day.

2.2.3.4 Thawing cells

The frozen vial was taken out of liquid nitrogen, the cap was carefully loosened to release pressure and the vial was thawed in 70% ethanol at 37 ^{o}C, until the suspension had almost completely melted. Under the hood, the cells were then transferred to a tube containing 5 ml chilled cell culture medium. The cells were pelleted, resuspended in prewarmed culture medium and transferred to a culture flask. Medium was replaced on the next day.

2.2.3.5   Transient transfection

Transient transfection was performed with Lipofectamine 2000 (Invitrogen) or magnetic bead assisted transfection(MaTra)(IBA, Goettingen) and followed the recommended protocol. Typically, 1 μg of plasmid DNA/well were used for transfection in a 24 well plate. Approximately 18 hours after transfection, the cells were processed for subsequent analysis.

2.2.4   Biochemical Methods

2.2.4.1   Protein estimation by BIORAD reagent

Bovine Serum Albumin (BSA) stock solution 1 mg/ml
Concentration range : 2 -16 μg/μl
A standard curve was made using BSA in the range of 2 -16 μg. 10μl of the sample was used for the protein estimation. The sample volume was made up to 800μl with water. 200μl of the BIORAD reagent was added to each samples, votexed and incubated for 3 - 5 min at room temperature, 200μl from each tube was pipetted into ELISA strips and optical density was measured at 595 nm in the ELISA reader.

2.2.4.2   Solubilization of proteins

2 x Laemmli buffer
125 mM Tris-Cl, pH 6.8
4% SDS
0.004%Bromophenol blue
20% (w/v) Glycerol
10% β-mercaptoethanol
Protein samples dried by speed vac were resuspended in 1x Laemmli buffer. The resuspended proteins were boiled at 95 ^{o}C for 5 min, cooled on ice for 1 min, centrifuged at 13,000 rpm for 2 min and resolved by SDS-PAGE.

2.2.4.3   SDS-Polyacrylamide Gel Electrophoresis

The elecrophoretic separation of the proteins was performed through high-tris discontinuous SDS polyacrylamide gel electrophoresis. A system with vertical oriented glass plates (16 x 16 cm; 1 mm spacer) was used. The gels were prepared as follows: first the resolving gel (12.5-17.5% acrylamide) was put between glass plates and covered with a layer of butanol. After polymerisation of the gel was completed, butanol was removed and the space between glass plates was dried with Whatmann

paper. Then the concentrating gel was put on top of the polymerised resolving gel and the sample combs were introduced immediately. After polymerization was complete, the combs were removed. The glass plates with the gel between them were fixed inside the electrophoresis chamber and covered with electrophoresis buffer. Protein samples were mixed with Laemmli loading buffer 1:1, denatured by 95 ^{o}C and centrifuged at 14000 rpm in a table-top centrifuge at room temperature. The supernatant was introduced into the stacking gel pockets. Electrophoresis was performed for 2-3 hours with the constant current of 35 mA.

Electrophoresis buffer:

SDS (w/v) – 10g/10 litre

Glycine (w/v)– 144,27g/10 litre

Tris (w/v) – 60,53g/10 litre

20% Ammoniumperoxiddisulfate (APS) in ddH2O

2.2.4.4 Stacking gel(1X)

Ingredients	5%
30% Acrylamide solution: (ml)	0.4
1% bisacrylamide solution (ml)	0.275
ddH2O (ml)	1.175
0,5 M Tris-HCl, pH 6.8 (ml)	0.625
(10%) SDS (μl)	25
TEMED (μl)	2.5
(20%) APS (μl)	10

2.2.4.5 Separating gel (1X)

Ingredients	15%
30% Acrylamide solution: (ml)	8.75
1% bisacrylamide solution (ml)	2.74
ddH2O (ml)	1.4
1.5 M Tris-HCl, pH 8.8 (ml)	4.3
(10%) SDS (μl)	175
TEMED (μl)	14.58
(20%) APS (μl)	58.33

2.2.4.6   Staining with Roti-Blue Colloidal Coomassie

Colloidal Coomassie staining is one of the most sensitive staining protocols. Due to the colloidal properties of the dye, it binds with high specificity to proteins and only minimal to the gel matrix. This allows visualisation of proteins separated by SDS-PAGE with sensitivity as high as 30ng of protein. Roti-Blue collodial Coomassie was purchased from Roth and staining was performed according to the protocol as follows. Immediately after completion of electrophoresis, gels were incubated in the fixing solution for 60 min, shaking. The staining solution was applied on to the gels for 60 min. In special cases the gels were stained for several days, which improved the sensitivity of the staining. After staining, gels were incubated in the washing solution for 5-10 min and then kept in the stabilising solution or prepared for drying in the drying solution.

Fixing solution:	20% (v/v) methanol
	8.5% (v/v) o-phosphoric acid
Staining solution:	20% (v/v) methanol
	20% (v/v) 5x concentrate Roti-Blue colloidal Coomassie
Washing solution:	25% (v/v) methanol
Stabilising solution:	20% (w/v) ammonium sulphate
Drying solution:	10% (v/v) glycerol
	20% (v/v) ethanol

2.2.4.7   Western blot (semi-dry)

Cathode buffer	40 mM -aminocaproic acid, 20 mM Tris-Cl, 20% (v/v) methanol, pH 9.0 (pH was adjusted with free Tris base before addition of methanol)
Anode buffer	75 mM Tris-Cl, 20% (v/v) methanol, pH 7.4
Phosphate-buffered saline (PBS)	140 mM NaCl, 2.7 mM KCl, 10mM-Na$_2$HPO4, 1.8 mM KH$_2$PO$_2$, pH 7.3
TBST	0.1% (v/v) Tween-20 in TBS
Blocking buffer	5% milk powder in TBST
stripping solution	0.2 M NaOH
SDS stripping solution	16 mM Tris-Cl pH 6.8, 2% SDS, 0.1 M -mercaptoethanol

Six pieces of 3 mm Whatman paper and one piece of nitrocellulose membrane were cut to the size of the SDS gel. Gel and membrane were equilibrated for 5-15 min

in cathode buffer. The blot was assembled without air bubbles according to the following scheme:

cathode (-)
3x paper in cathode buffer
gel
membrane
3x paper in anode buffer
anode (+)

For transfer, the current was set to 1 mA/cm^2 gel size for 45-60 min. The membrane was then briefly washed with PBST and incubated in blocking buffer for one hour at room temperature. Decoration with the primary antibody diluted in blocking buffer was performed by incubating overnight at 4 ^{o}C. After three 30-45 min washes with TBST, the membrane was incubated with horse radish peroxidase (HRP)-coupled secondary antibody, diluted 1:10,000 in blocking buffer, for one hour at room temperature. The blot was washed three times 30-45 min with PBST and incubated with chemiluminescence substrate solution. Intelligent Dark Box II Camera was used for signal detection.

2.2.4.8   Stripping of nitrocellulose membranes

Removal of antibodies from a blot was done under mild conditions, if it should serve to reduce the background for incubation with another primary antibody, either from a different species or for a protein of clearly distinct size than in the first decoration. After washing the membrane in TBST, it was incubated 5-10 min in 0.2 M NaOH stripping solution. Washed the membrane in distilled water for 10 min. For stringent stripping, the blot was incubated in SDS stripping solution for 30 min, tightly closed, on a wheel at 50 ^{o}C, followed by several washes in TBST. Decoration of the membrane was done as described above, starting from the blocking step again.

2.2.4.9 Preparation of cytosol fraction for pull-down assay

Buffer-A
PBS containing protease inhibitors
1 mM EDTA
1 mM PMSF
5 mM IAA (iodo-acetamide)
0.1% Triton X-100
Cells were grown to confluency in a 10 cm dish till near-confluency in DMEM medium. They were washed twice with cold PBS and scraped in lysis buffer A, sonicated 3 x 10s and centrifuged at 3,000 rpm, 5 min. The pellet was discarded and the supernatant was centrifuged at 100,000g (45,000 rpm; TLA-45 rotor), 1 hr, 4 ^{o}C. Supernatant was the cytosol and the pellet was the membrane fraction. The cytosol fraction was preserved and the protein concentration determined. The cytosol containing equal amount of total protein was used for incubation with GST-fusion protein bound to GSH-Sepharose beads.

2.2.4.10 purification of GST-fusion proteins

buffer A: PBS, protease inhibitors with 0.1%Triton X-100
buffer B: 50 mM Tris-Cl pH 8.0, 10 mM reduced glutathione, adjusted to pH 8-8.5 with NaOH (prepared freshly)
A bacterial clone expressing the GST-fusion protein under the control of an inducible promoter was grown in a 10ml LB preculture overnight. The culture was diluted 1:20 in fresh LB medium and grown for 3 h up to an optical density of 0.3-0.5 (600 nm). Protein expression was induced by adding 0.15 mM IPTG to the culture, which was further grown for 3-5 hr at 30 ^{o}C. The cells were harvested at (6,000 rpm in a JA 10 rotor) and washed once with cold PBS. All the following steps were performed on ice. The pellet was resuspended in 4 ml buffer A, and lysed in french press with maximum 1000psi. The insoluble fraction was pelleted by centrifugation at 11,000xg (12,000 rpm in a JA 20 rotor) and the supernatant transferred to a new tube. 50-100 μl of glutathione-coupled sepharose beads (75% suspension), corresponding to a bead volume of 100-125 μl, were centrifuged at 1000 rpm for 5 min in a tabletop centrifuge and washed twice with 0.5 ml of buffer A. The beads were incubated with the soluble lysate fraction on a wheel at room temperature for 1 hr. After the incubation period, the sepharose was washed 5 times with buffer A. GST-fusion protein was eluted from the beads by adding 250 μl of buffer D and incubating the sample for 15 min at room temperature. Elution was repeated at least 2 times. The eluted GST-fusion protein/GST alone was coupled to the beads

and used to pull-down assay.

2.2.4.11 Indirect immunofluorescence

Cells were seeded on round coverslips in a 24-well plate 1-2 days in advance and grown to 50-70% confluency. All the incubation steps given were performed by filling the wells with 0.2 ml of the respective solution unless indicated otherwise. Solutions were changed carefully, for the cells should neither be washed away nor become dry. The lid of the cell culture plate was closed during prolonged incubations and upon application of the secondary, fluorescent antibody the samples were protected from light.

Fixation with para-formaldehyde:

PFA reacts with nitrogen-containing groups and in effect crosslinks the proteins in a cell.

3% para-formaldehyde (PFA):
The required amount of PFA was suspended in 1/5 of the final volume, mixed with 50 μl of 1 M NaOH per g PFA and dissolved by incubation at 60 ^{o}C for about 1 hr with intermittent mixing. The solution was always freshly prepared but can be stored for 1-2 weeks at 4 ^{o}C.

0.5% saponin-PBS:
Prepared fresh from a 10% stock solution stored at -20 ^{o}C

Protocol

Cells were washed twice with PBS and fixed with 3% PFA for 20 min at room temperature. After two washes with PBS, aldehyde groups were blocked by 50 mM NH_4Cl for 10 min at room temperature. The cells were washed twice with PBS and permeabilised for 3x5 min at room temperature with 0.5% saponin in PBS. After permeabilization, cells were wased once with PBS/saponin and incubated with primary antibody for 45 min-1 hr at 37 ^{o}C. Then cells were washed twice with PBS/saponin and incubated with 10% goat serum in PBS. After incubation, cells were washed once with PBS/saponin and incubated with secondary antibody coupled with flurochrome for 40 min at 37 ^{o}C. Then cells were washed twice with PBS and twice with water. The coverslips were carefully taken out with forceps, dried excess water and mounted upside-down over a drop of DAKO mounting medium on a glass slide. The slides were protected from light to dry overnight

and sealed with nail-polish the next day. Confocal images were taken on Leica TCS SP2 AOBS laser scanning microscope.

2.2.4.12   Trypsin sensitivity assay

preparation of adaptors from CCVs

Cells were plated on 15 cm dishes to 80% confluency. Washed the cells twice with 20 ml of ice-cold PBS. The cells were scrapped with a rubber police man in 1 ml of MES buffer (0.1 M MES pH 6.6, 1mM EGTA, 0.5mM $MgCl_2$, 0.02% sodium nitrite). The cell suspension was frozen for minimum 20 min at -80 ^{o}C. The cells were thawed on ice and and lysed by gently passing through 22G needle for 10 times. Centrifuged the lysate at 1000xg (3000 rpm in Heraeus centrifuge) at 4 ^{o}C. The pellet containing unlysed cells and the nuclear fraction was discarded and the post-nuclear supernatant (PNS) was centrifuged at 7000xg (9000 rpm) for 40 min at 4 ^{o}C. The resulting supernatant was subjected to centrifugation at 100,000g (45000 rpm) in an ultracentrifuge using TLA45 rotor at 4 ^{o}C. The resulting pellet containing CCVs, was resuspended in 100 μl of 1 M Tris (pH 8.0) and incubated for 20 min at room temperature, to strip the membrane bound proteins. Then, centrifuged the fraction at 100,000g for 45 min at 4 ^{o}C. The resulting supernatant was saved and its pH was adjusted to 7.0 and diluted such that the final concentration of Tris is 0.2 M. The concentration of protein was estimated by Biorad method.

Partial Trypsin digestion

Trypsin stock solution: 1mg/ml in millipore grade water
working concentration of trypsin: 0.01 μg/μl
Trypsin inhibitor stock solution: 1mg/ml
Equal amount of total protein from CCVs were subjected to digestion with increasing concentrations of trypsin (0; 0.25; 0.5; 0.75; 1.5 μg/ml) by incubating the mixture at room temperature for 15 minutes. Immediately and quickly, trypsinisation was stopped, by adding trypsin-inhibitor to a final concentration of 20 μg/ml and placing the tubes in ice. The samples were boiled at 95 ^{o}C in 1X laemlli buffer containing 50mM DTT and placed on ice for 5 minutes and centrifuged for 5 minutes at 13000 rpm and subjected to 10% SDS-PAGE, blotted onto nitro-cellulose membrane and probed with anti-γ-1 and anti-μ-1 antibody. The signals were quantified by 2D densitometry.

2.2.4.13 Fluorescence recovery after photobleaching (FRAP)

Cells were grown to 80% confluency and transfected using FuGENE 6 (Roche Diagnostics, Penzberg, Germany). After 12 h cells received 5 mM sodium butyrate for 18 h. Cultures were confluent at the time of the experiment excluding differences due to cell cycle transissions. Hypertonic treatment was performed by incubating the cells in 0.2 M sucrose for 30 min at 37 ^{o}C. FRAP experiments were performed with a laser scanning confocal microscope (Leica TCS SP2, Heidelberg, Germany) using a 63x, 1.2 N.A. plan apochromat water objective. The EGFP-γ1-adaptin construct was excited with the 488 nm line of an Argon ion laser. Fluorescence was detected between 500 and 600 nm. A single photobleaching run consisted of 10 prebleach and 150 postbleach frames. A defined region at the TGN was scanned for photobleaching once at 2 mW laser power (at back pupil of objective) for 1.3 s to reduce the fluorescence intensity to background level. The recovery of fluorescence was monitored by scanning the whole cell every 1.5 s at 0.15 mW laser power. All FRAP experiments were performed at 28 ^{o}C with opened pinhole for high signal-to-noise ratio. Images were analysed using Metamorph software (Universal Imaging, Philadelphia, USA). Fluorescence signals in the photobleached region were corrected for background. For reconstructing the recovery time series fluorescence in the bleached region of the TGN was normalized with respect to the fluorescence of a nearby unbleached region at each time point. This way we corrected for the loss of total fluorescence due to the bleaching in the TGN subregion as well as for the slight photobleaching during the collection of the recovery time series. Fluorescence recovery data are normalized with the measured prebleach intensity, I$_{pre}$, and the intensity measured directly after photobleaching, I$_0$, according to I$_n$(t)=(I(t)-I$_0$)/(I$_{pre}$-I$_0$).

2.2.4.14 Immunoelectron microscopy

Ultrathin cryosections were prepared as described. Cells were fixed with 2% para-formaldehyde and 0.1% glutaraldehyde in 0.1 M sodium phosphate buffer (pH 7.4) for 30 min at RT directly on cell culture dishes. Cells were postfixed with 4% para-formaldehyde and 0.1% glutaraldehyde for 2 hr on ice and removed from the dishes with a cell scraper. After washing twice with PBS/0.02 M glycine, cells were embedded in 10% gelatin, cooled on ice and cut into small blocks. Blocks were infused with 2.3 M sucrose overnight, mounted on small metal pins, frozen and stored in liquid nitrogen. Ultrathin sections were cut at -110 ^{o}C using a diamond knife (Diatome) in an ultracryomicrotome (Leica, Bensheim, Ger), collected using a 1:1 mixture of 1.8% methyl-cellulose and 2.3 M sucrose (Liou *et al.*, 1996), and

deposited on formvar- and carbon-coated grids. For immunolabelling, sections were incubated with antibodies against clathrin heavy-chain, γ1-adaptin or LAMP-1 (additional bridging antibody rabbit anti-rat IgG) for 30 min followed by a 20 min incubation with protein A-gold (5 and 10 nm). For double labelling experiments, sections were fixed for 5 min with 1% glutaraldehyde after incubations with the first antibody and protein A-gold. After quenching with glycine (0.02 M) and blocking with BSA, sections were incubated with the second antibody and protein A-gold. BSA-gold endocytosis was done by incubating the cells in DMEM, 0.5% BSA and 5.0 OD BSA-gold (G. Posthuma, University Utrecht, NL). Sections were contrasted with uranyl acetate/methyl-cellulose (Tokuyasu, 1978) for 10 min on ice, embedded in the same solution and examined with a Philips CM120 electron microscope (Philips, Berlin, Ger). Images were processed for presentation using Adobe Photoshop versions 5 and 7.

2.2.4.15 Preparation of whole cell lysate from isolated adipocytes

Krebs-Ringer bicarbonate buffer(KRB)
12.5 mM HEPES-NaOH (pH 7.4), 120 mM NaCl, 6 mM KCl, 1.2 mM MgSO$_4$, 1 mM CaCl$_2$, 1 mM Na$_2$HPO$_4$, 10 mM NaHCO$_3$, 10 mM Glucose.
Homogenization buffer
20 mM Tris-HCl (pH 7.4), 1 mM EDTA, 255 mM sucrose.

For isolation of adipocytes, the epidydmal fat pads were excised from a mouse and used fresh. The tissue was carefully cut into mm-sized pieces with a scalpel. The minced tissue was incubated at 37 ^{o}C with gentle shaking for not more than 30-40 min in 2 ml of KRB containing 10 mg/ml untreated bovine serum albumin and 10 mg crude collagenase -Type II (sigma). The digested tissue was washed five times with 2 ml of KRB by centrifugation at 600 x g$_{max}$ over 1 min. During each wash step, the supernatant and pellet containing connective tissues were carefully removed by aspiration and care was taken not to aspirate the isolated adipocytes that float on top of the supernatant. The isolated adipocytes were washed twice with homogenization buffer at approx. 20 ^{o}C by centrifugation as before. After washes, the cells were resuspended in 1 ml of homogenization buffer and homogenizaion was done with 10 strokes in a teflon pestle homogenizer. The homogenate was centrifuged at 16,000 x g$_{max}$ at 4 ^{o}C for 15 min in a cooling table-top centrifuge. the solidified fat cake was carefully removed and the supernatant was saved for further analysis. The total protein concentration was estimated by Bio-Rad assay and 100 μg of total protein were seperated in a SDS-PAGE, blotted onto membranes and

decorated with appropriate antibodies and signals quantified using 2D densitometry.

Chapter 3

Results

3.1 Role of AP-1 in intracellular sorting of sortilin

3.1.1 Analysis of the intracellular distribution of sortilin in AP-1 deficient cells

Sortilin is a member of a growing family of Vps10p-domain containing, multi-ligand type I receptors involved in intracellular sorting of various ligands. A recent study identified, that the cytoplasmic tail of sortilin contained bonafide intracellular sorting signals (Nielsen *et al.*, 2001). The primary sequence of the cytoplasmic domain of sortilin is closely related to the cytoplasmic domain of cation-independent mannose-6-phosphate receptor (MPR300), with a conserved tyrosine-based endocytic motif and a di-leucine based Golgi to endosome transport motif. Sortilin was shown to be predominantly localized at the TGN and vesicles with an extensive co-localization with MPR300 (Petersen *et al.*, 2001). Moreover, it was shown that the MPR300-sortilin tail chimeras were as effective as wildtype MPR300 in restoring intracellular transport of β-hexosaminidase in mpr$^-$ cells, indicating that sortilin cytoplasmic domain can substitute for the cytoplasmic domain of MPR300 in lysosomal sorting. The authors also reported that the sortilin cytoplasmic domain interacted with GGA2, a member of the GGA family of monomeric adaptors that are involved in the transport of cargo from the TGN to the endosome, thereby concluding that the transport of sortilin from the TGN to endosomes is mediated by GGA2 (Nielsen *et al.*, 2001). Previous studies from our group, based on AP-1-deficient mice (μ1A-adaptin 'knock-out') has demonstrated the involvement of AP-1 in the transport of MPR300. Since sortilin exhibits similar sorting characteristics as of MPR300, we were interested to know the fate of sortilin in AP-1-deficient cells.

As a first step, we analyzed the intracellular distribution of sortilin in AP-1-

deficient MEFs (mouse embryonic fibroblasts) by indirect-immunofluorescence microscopy. μ1A -/- fibroblasts and control(ct) fibroblasts (μ1A -/- fibroblasts ectopically expressing μ1A), shown to rescue the μ1A deficient phenotype (Meyer *et al.*, 2000) were used. The cells were plated on coverslips and after recovery, transiently transfected with sortilin(human full length construct in pcDNA3.1). The cells were fixed and permeabilized, 18 hours post-transfection, using the PFA fixation method and stained with either mouse anti-γ1 adaptin; mouse anti-sortilin antibody and rabbit anti-MPR300 antibody(Fig. 3.1) or rat anti-LAMP1 antibody (Fig. 3.2).

As previously shown, in μ1A -/- cells, γ1 adaptin staining is lost or very weak at the TGN (Fig. 3.1 D) with more peripheral distribution of MPR300 (Fig. 3.1 E) compared to ct cells, where both show overlapping staining at the TGN (Fig. 3.1 C). The distribution of sortilin(Fig. 3.1 G) and MPR300 (Fig. 3.1 H) in ct cells was mainly peri-nuclear and overlapped extensively (Fig. 3.1 I). But in μ1A -/- cells, there was a remarkable distribution of sortilin mainly to peripheral structures(Fig. 3.1 J) with dispersed staining, overlapping extensively with re-distributed MPR300 (Fig. 3.1 L). Since MPR300 is known to re-distribute to early endosomal structures in AP-1-deficient cells, this co-localization implies that sortilin is also re-distributed to early-endosomes in a similar way as MPR300.

Since sortilin staining appeared even more widely dispersed compared to MPR300 positive endosomes in μ1A -/- cells, we co-stained sortilin also with LAMP1, a marker for late endosomes and lysosomes (Fig. 3.2). In ct cells, γ1 adaptin (Fig. 3.2 A) and LAMP1(Fig. 3.2 B) are completely segregated in distinct structures (Fig. 3.2 C) serving as marker for the TGN and late endosomes/lysosomes respectively. In μ1A -/- cells, as shown in Fig. 3.2(D,E and F), sortilin is found in dispersed structures, which were LAMP1 negative implying that sortilin is not missorted to lysosomes. To validate whether AP-3 is involved in the sorting events of sortilin, we analyzed the steady-state distribution of sortilin in AP3-/- (mocha) cells which are deficient for δ-3 adaptin. AP-3-/- cells transiently expressing sortilin were fixed as mentioned above and stained with mouse anti-sortilin antibody and rat anti-LAMP1 antibody. Sortilin stained predominantly in the peri-nuclear area(Fig. 3.2 G) and was completely segregated from LAMP1 positive structures(Fig. 3.2 I) implying that its steady-state distribution is unaltered in the absence of AP-3.

Endocytosed sortilin was shown to travel to the TGN showing little or no recycling (Nielsen *et al.*, 2001). In μ1A -/- cells it has been shown previously that the endosome-TGN transport of the MPRs is blocked leading to the accumulation of the MPRs in early-endosomes (Meyer *et al.*, 2000). Since the steady-state localization of sortilin was redistributed to MPR300 positive early-endosomes in μ1A -/- cells, we were interested to know whether the endosome-TGN transport of sortilin is affected
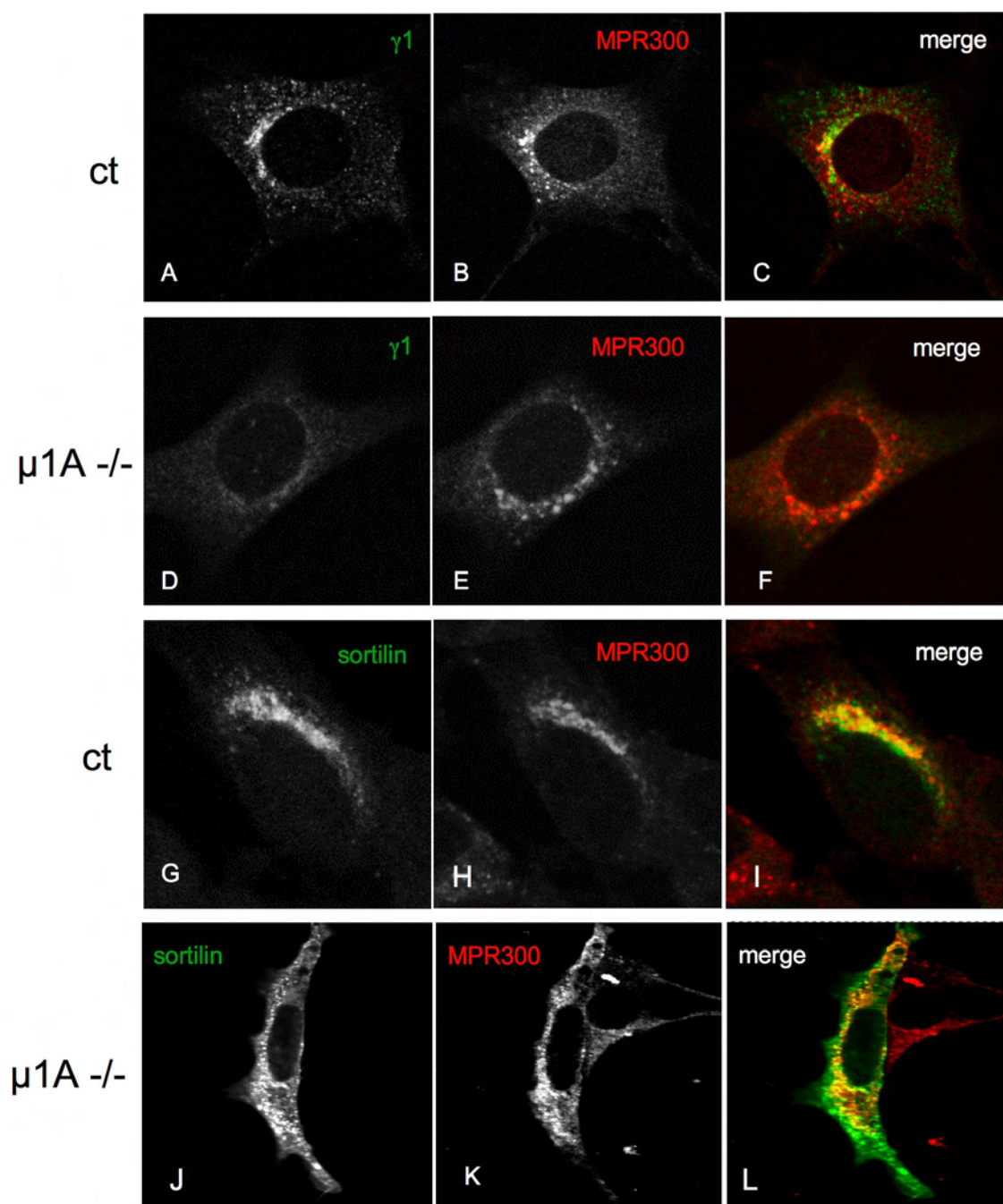
Figure 3.1: Intracellular localization of sortilin in AP-1(μ1A)deficient cells. Sortilin was transiently transfected in control(ct) and μ1A 'knockout' (μ1A-/-) cells and fixed using 3% PFA, 18 hours post-transfection. Fixed cells were permeabilized with 0.5% saponin in PBS and incubated with antibodies against either γ1adaptin (anti-mouse IgG-Alexa 488 (green);A,D) and MPR300 (anti-rabbit IgG-Texas Red (red); B,E); merge (C and F) respectively or sortilin (anti-mouse IgG-Alexa 488 (green); G,J) and MPR300 (red;H,K); merge (I and L) respectively.
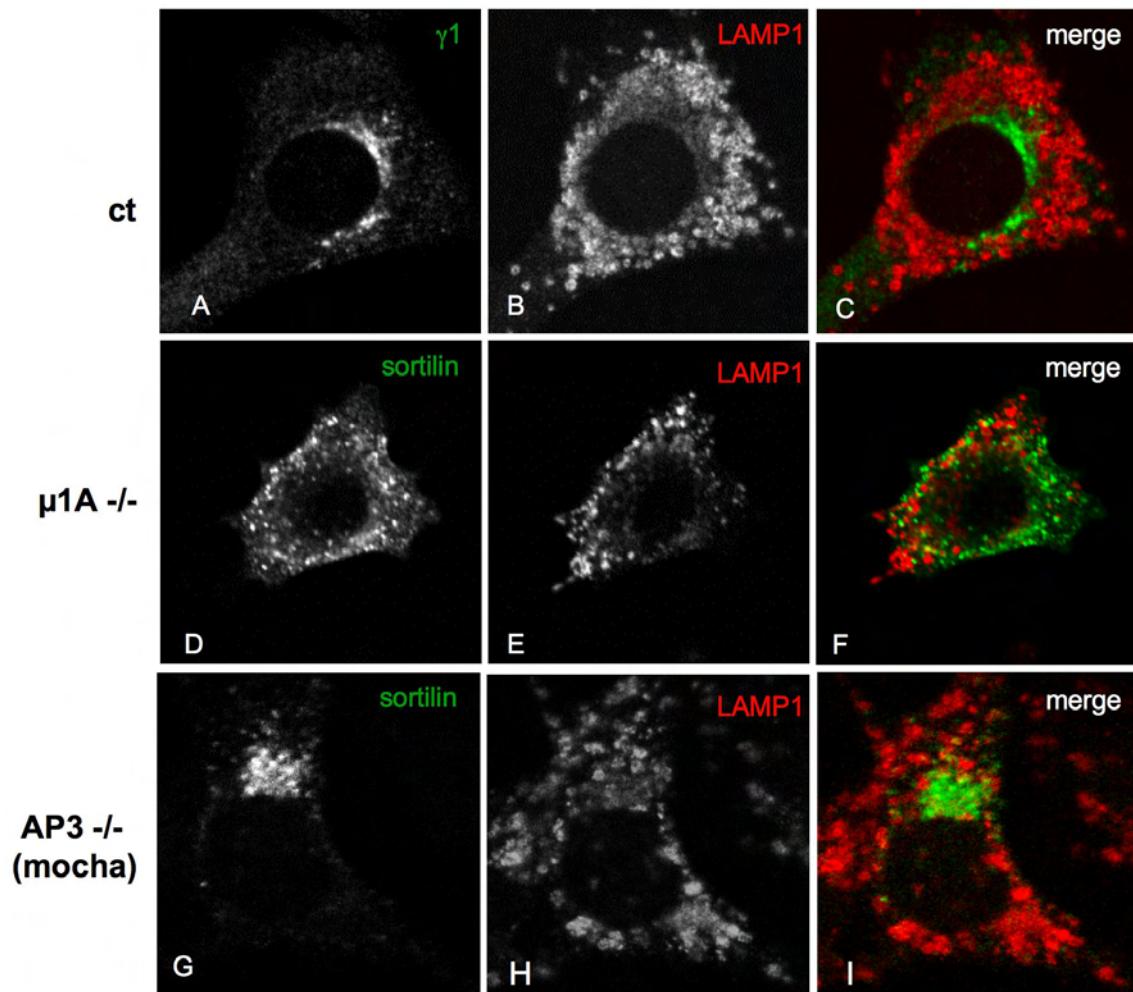
Figure 3.2: Intracellular localization of sortilin in AP-1-deficient and AP-3-deficient cells. Fixed cells were stained with antibodies against γ-1adaptin (green;A), sortilin (green;D and G) and LAMP1 (red;B,E and H). Merge represent the overlay of respective images (A,B:C; D,E:F; G,H:I).

in a similar way. For this purpose, we performed sortilin antibody endocytosis assay in control(ct) as well as in μ1A -/- cells and analyzed the intracellular distribution of sortilin by indirect-immunofluorescence microscopy. Control(ct) and μ1A 'knockout' (μ1A-/-) cells were grown on coverslips and were transiently transfected with sortilin. At 18 hours post-transfection, the cells were allowed to endocytose sortilin antibody for 30 min at 37 ^{0}C. Endocytosis was stopped immediately after 30 min by incubating the cells in ice and washing with ice-cold PBS to remove unbound antibodies. The cells were fixed and permeabilized and incubated with Alexa 488-conjugated secondary antibody.

In control cells, endocytosed sortilin localized in the peri-nuclear region in a similar way as observed in steady-state (Fig. 3.3 A,B). This indicates, that

endocytosed sortilin reaches the TGN. But in μ1A-/-cells, endocytosed sortilin did not display a peri-nuclear concentration, but was seen redistributed to peripheral structures as observed at steady-state (Fig. 3.3 C,D), indicating that the endosome to TGN transport is blocked upon AP-1 deficiency (μ1A 'knock-out'), in a similar way, as shown for the MPRs (Meyer *et al.*, 2000).
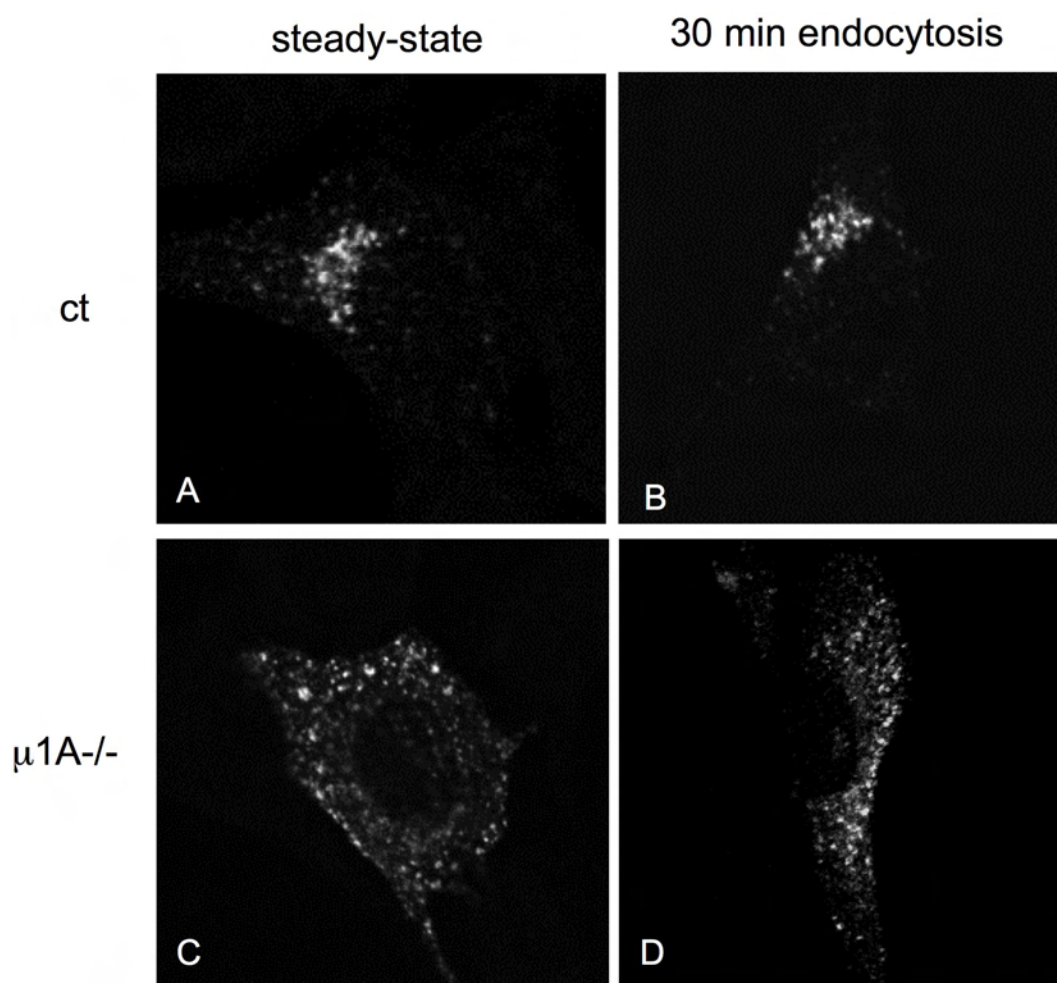
Figure 3.3: Sortilin antibody endocytosis in AP-1-deficient (μ1A -/-) cells. Control(ct) and μ1A 'knockout' (μ1A-/-) cells grown on coverslips were transiently transfected with sortilin and 18 hours post-transfection allowed to endocytose sortilin antibody for 30 min at 37^0C. Immediately after 30 min, cells were incubated on ice to stop endocytosis, washed with ice-cold PBS, fixed with 3% PFA, permeabilized with saponin and incubated with anti-mouse IgG-Alexa 488. For steady-state analysis, fixed cells were permeabilized and incubated with sortilin antibody and anti-mouse IgG-Alexa 488.

3.1.2 Analysis of interaction between sortilin and AP-1

3.1.2.1 Y2H analysis of sortilin-tail interaction with μ1A

The observed difference in the steady-state localization of sortilin in μ1A-/- cells prompted us to check whether the sortilin tail could to μ1A. We adopted the Y2H method to check for possible interaction, as this system has proven to be successful in identifying even weak interactions. Two different constructs of sortilin cytoplasmic domain(CD) were used in this analysis, because the sortilin CD contains two sorting motifs: a tyrosine-based motif and a di-leucine motif (Fig. 3.4). Both motifs are able to mediate binding to AP-1 and AP-2 complexes as it has been shown for MPR300 and many other proteins (Bonifacino and Traub, 2003).
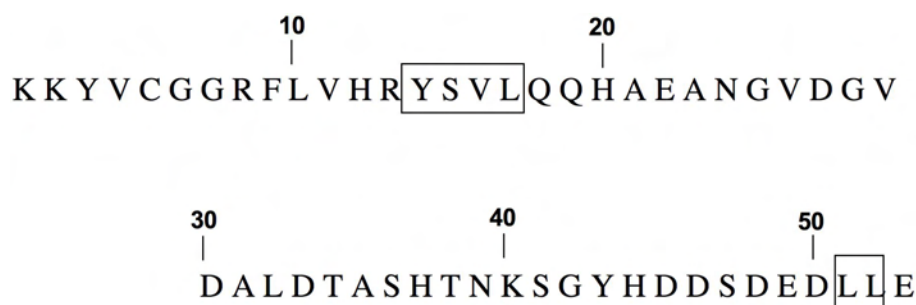
Figure 3.4: Primary structure of sortilin cytoplasmic domain(CD). The tyrosine-based and di-leucine based sorting motifs are highlighted by boxes and the acidic motif is underlined.

To this end, the cDNAs encoding the full length CD (sortilin CD) and a truncated form lacking the tyrosine-based motif, but containing the di-leucine motif (sortilin CD(Δ1-30)), were cloned into the bait vector (pGBT9) as a fusion to the Gal4 DNA-binding domain. As prey, the cDNA encoding the C-terminal domain (150-450 aa) of μ1A (μ1A CT) that contains the sorting motif binding site, was cloned into the prey vector (pGADT7) as a fusion to the Gal4 activation domain. Since sortilin CD contains sorting motifs related to MPR300 and MPR46, cDNAs encoding the CDs of both the MPRs were also cloned into bait vectors and included in this analysis. Both the bait and the prey vectors were co-transformed into the yeast strain AH109 using the standard lithium-acetate transformation method. The co-transformants were allowed to grow in liquid medium and equal amount of exponentially growing cells were dotted in respective selection plates in the fashion as shown (Fig. 3.5) and incubated at 30 ^{0}C for a minimum of 3 to 5 days. The growth in the selection plates is a direct measure of activation of reporter genes and thereby is a measure of the strength of interaction. To test for the possibility of auto-activation of the reporter genes, the baits were co-transformed with empty prey vector and vice versa.

As shown in Fig. 3.5, after 3 days of incubation, the observed growth of yeast clones corresponding to MPR300 CD and μ1A CT, but not in the respective control spot indicates a positive and strong interaction between MPR300 CD and μ1A CT.
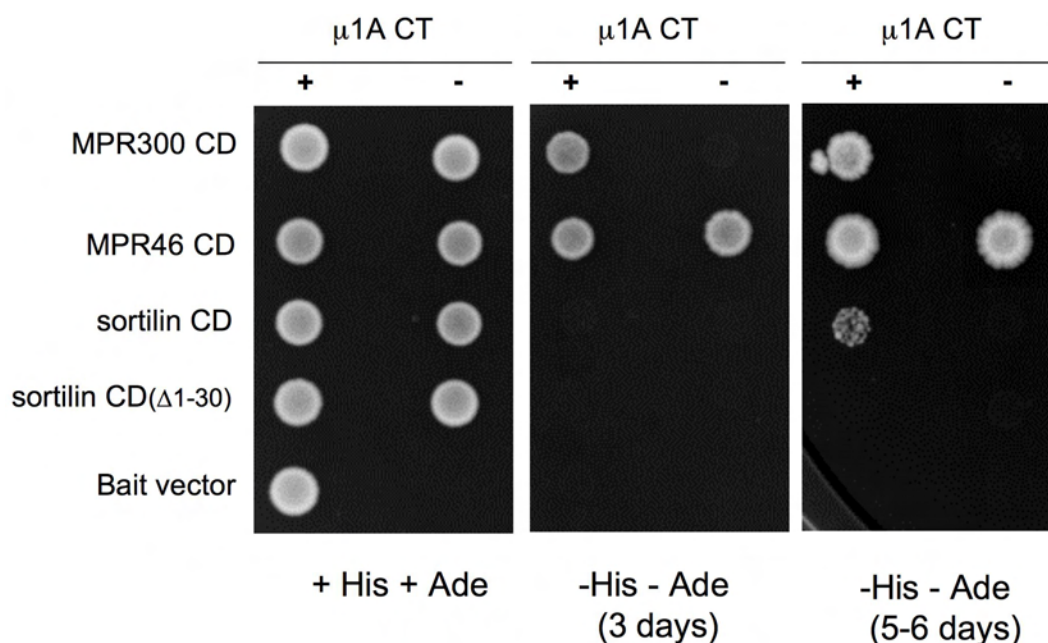
Figure 3.5: Y2H analysis of Interaction between sortilin CD and μ1A. cDNAs encoding cytoplasmic domains(CD) of MPR300,MPR46 or sortilin (full length or truncated) were cloned into bait vector pGBT9 and cDNA encoding C-terminal domain(150-450 aa) of μ1A was cloned into prey vector pGADT7 to be expressed as a fusion with Gal4-DNA Binding domain and Gal4 Activation domain respectively. The bait and prey constructs were co-transformed into yeast strain AH109 in a combination as depicted in the figure and co-transformants were grown in liquid medium. Exponentially growing cells were diluted 1 to 10 and 5μl were dotted on selection plates (-Histidine-Adenine; -His-Ade) to test for activation of reporter genes and recorded after incubation for either 3 or 6 days. Growth in reporter selection plates indicates interaction. (+) and (-) indicate the presence or absence of the prey μ1A.

However, MPR46 CD exhibited auto-activation and so its interaction could not be validated. In the case of sortilin CD and μ1A CT, growth was observed only after 5 to 6 days of incubation, implying a weak interaction. No interaction was observed between sortilin CD(Δ1-30) and μ1A CT. The above results indicate that sortilin CD interacts directly with μ1A CT albeit weakly and this interaction is most likely, solely mediated by the tyrosine-based motif, as the sortilin CD lacking this motif failed to show even weak interaction.

3.1.2.2 In vitro analysis of sortilin and AP-1 interaction

To confirm the interaction between sortilin CD and μ1A as observed by Y2H interaction study, sortilin CD-μ1A interaction was tested in a GST-pull down assay using GST-sortilin CD fusion proteins and cytosol preparations from control and μ1A -/- cells. Sortilin CD and sortilin CD(Δ1-30) cDNAs were cloned into the vector pGEX2T through BamHI and EcoRI sites to express N-terminally fused GST fusion proteins in *E.coli* BL21(DE3).

Purification of the fusion proteins from bacterial lysate were done by binding the fusion proteins or GST alone to glutathione sepharose 4B and subsequent elution with reduced glutathione. The purity of the GST-fusion proteins were checked by loading 25 μg of the purified proteins on a 15% SDS-PAGE and visualizing after coomassie staining. As shown, the purified fusion proteins were pure enough to be used for further pulldown assays (Fig. 3.6).
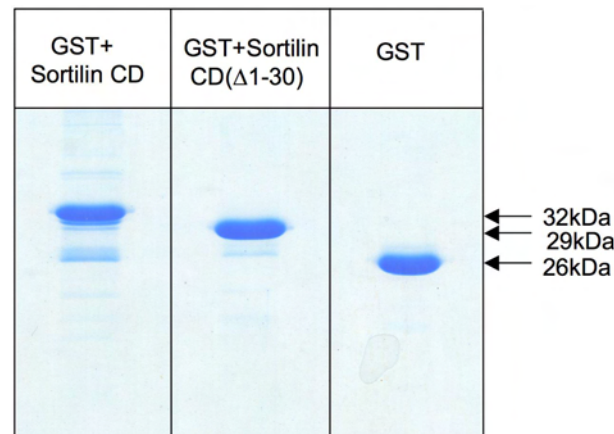
Figure 3.6: Purification of GST-Sortilin fusion proteins for pull down assay. GST-sortilin fusion proteins or GST alone from bacterial lysate were bound to Glutathione sepharose 4B, washed and eluted with elution buffer containing 10 mM reduced glutathione. 25 μg from each purified fraction were loaded on a 15% SDS-PAGE and stained with coomassie-blue. Their respective molecular sizes are indicated.

For preparation of cytosol fractions from control and μ1A -/- cells, the cells were plated in 10 cm plates and when sub-confluent, harvested by scrapping in ice-cold lysis buffer that contains 0.5% (v/v) Triton X-100. The cells were then lysed by sonication and the cytosol was prepared using the protocol as described in the materials and methods. Cytosol at a total protein concentration of 1.5 mg/ml in lysis buffer was added to 150 μg of GST-fusion proteins or GST alone pre-bound to 100 μl of glutathione sepharose beads and incubated overnight at 4 ^{0}C with end-over-end rotation. After the incubation period, the flow-through(FT) was collected, beads were washed five times with 100 μl of lysis buffer and then eluted with 10

mM reduced glutathione and pooled the eluate fractions(E). 5% of FT and 35% of Eluate(E) fractions were seperated on a 7.5% SDS-PAGE and blotted on PVDF membranes and tested for γ1adaptin (Fig. 3.7). It has been demonstrated that upon μ1A-deficiency, protein levels of γ1 and σ1 adaptins are decreased (Meyer *et al.*, 2000). Therefore the signal for γ1 adaptin in the SM fraction from μ1A -/- cytosol is reduced to 70%.

GST-Sortilin CD efficiently pulled down AP-1 from the control(ct) cytosol compared to GST-Sortilin CD(Δ1-30) that lacks the tyrosine-based motif (Fig. 3.7). Yet a weak signal for γ1 was observed in the pull-down fraction of GST-Sortilin CD(Δ1-30) which means that the interaction is not completely lost. This result together with the Y2H results, indicates that the interaction between GST-Sortilin CD and AP-1 is mediated by the tyrosine-based motif that binds to the μ1A subunit.
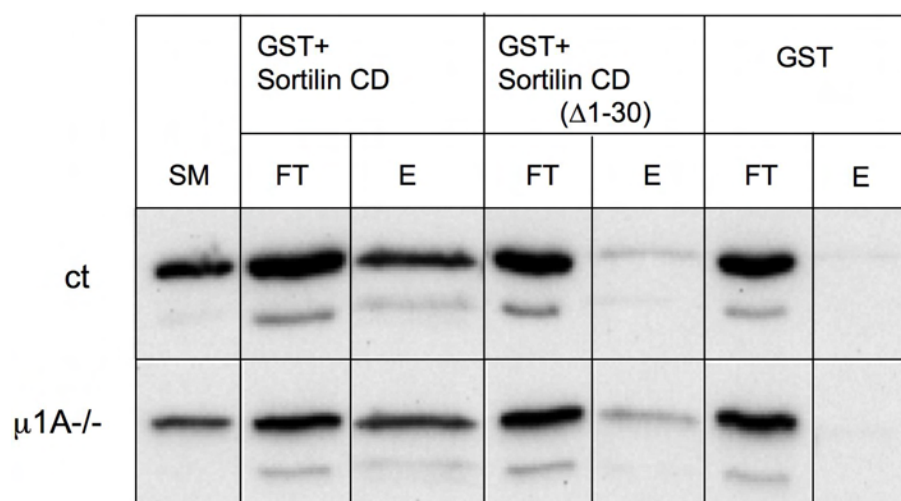
Figure 3.7: *In vitro* **interaction of sortilin and AP1.** Cytosol from ct or μ1A -/- cells at a total protein concentration of 1.5mg/ml were added to 150μg each of GST-Sortilin CD, GST-Sortilin CD(Δ1-30) or GST alone bound to 100μl of GSH-sepharose beads. After over night incubation, the flow-through(FT) was collected, beads washed 5 imes with lysis buffer and the bound fractions were eluted with 10mM reduced glutathione and the eluate(E) fractions pooled. 1% of starting material(SM), 5% of FT and 35% of E fractions were loaded on a 7.5% SDS-PAGE and blot was decorated with anti- γ-1adaptin antibody (representative of two experiments).

Surprisingly, similar results were observed when cytosol from μ1A -/- cells was used for pull-down assays (Fig. 3.7). Apparently GST-Sortilin CD was able to pull down γ1-adaptin indicating that sortilin could bind to γ1, or most likely to a γ1-σ1 hemi-complex, independent of μ1A. It has been shown that a trimeric complex consisting of a γ1- σ1-β1 adaptin still exists in μ1A-/- fibroblasts (Meyer *et al.*, 2000). However, this trimeric complex is non-functional in protein sorting, because it does not bind to membranes *in vivo*, leading to a loss of γ1 adaptin staining

in the peri-nuclear area, but with a weak cytoplasmic staining, as also shown in (Fig. 3.1 E). So, it is possible that sortilin CD interacts with the cytosolic $\gamma1$-$\sigma1$-$\beta1$ complex present in $\mu1A$-/- cells. Recent studies have shown that $\gamma1$-$\sigma1$ hemi-complex interacts with acidic di-leucine motif present in the cytosolic tails of HIV-Nef and LIMP-II (Janvier *et al.*, 2003) and so one can expect that the interaction between sortilin and the $\gamma1$-$\sigma1$ hemi-complex could be mediated by the acidic di-leucine motif present in sortilin CD, although only a weak signal for $\gamma1$ was observed in the pull-down fraction of GST-Sortilin CD($\Delta1$-30). One possible explanation to this discrepancy could be that the acidic di-leucine motif in GST- Sortilin CD($\Delta1$-30) was not completely accessible for interaction due to steric hinderance or due to the requirement of a post-translational modification. It is also possible that binding of the di-leucine motif is mediated by the $\beta1$-adaptin core domain. The interaction observed between sortilin and AP-1 was authentic since no interaction was observed when GST alone was used for the pulldown with control(ct) or $\mu1A$ -/- cytosol (Fig. 3.7).

3.1.2.3 Analysis of Interaction between sortilin and $\gamma1$-$\sigma1$ hemi-complex

3.1.2.4 Yeast-3-Hybrid analysis

To elaborate on the *In vitro* interaction studies, we decided to verify a direct interaction between sortilin and the $\gamma1$-$\sigma1$ hemi-complex using the Yeast-3-Hybrid(Y3H) method. Y3H is a valuable tool to check the interaction between three proteins, wherein the interaction between two chimeric proteins requires the presence of a third protein.

The cDNAs encoding the full length sortilin CD or sortilin CD ($\Delta1$-30) were cloned into one of the two cloning sites of the bait vector pBridge to be expressed as a fusion with the Gal4-DNA binding domain. Full length cDNAs encoding different isoforms of $\sigma1$ adaptin, $\sigma1A$, $\sigma1B1$- its splice variants $\sigma1B2$, $\sigma1B3$ and $\sigma1C$ were cloned into the second cloning site of pBridge vector to be expressed under the control of *MET25* promoter. $\sigma1$-adaptins are therefore only expressed, if the yeast is grown in medium lacking methionine and are repressed in the presence of 1mM methionine. The cDNA encoding $\gamma1$ adaptin was cloned into the prey vector to be expressed as a fusion with the Gal4-activation domain. Bait and prey constructs were co-transformed into yeast strain CG1945 using lithium acetate transformation protocol. The co-transformants were grown in liquid medium containing 1 mM methionine, then equal amount of cells from exponentially growing cultures were dotted onto medium lacking histidine and methionine (-His,-Met), incubated for 3 to 5 days and results were recorded. As shown in Fig. 3.8 A, sortilin CD and
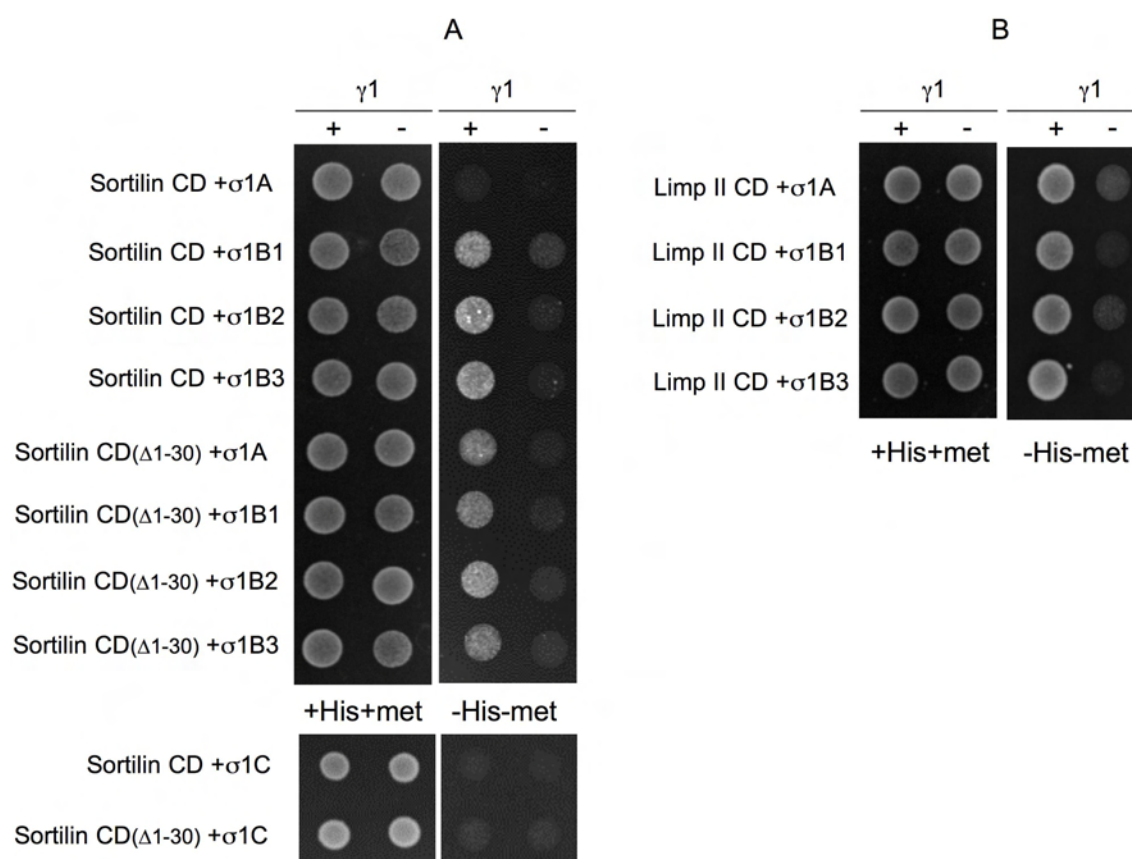
Figure 3.8: Y3H analysis of the interaction between sortilin and $\gamma1$-$\sigma1$ hemi-complex.(A) sortilin CD/sortilin CD(Δ1-30) or (B) LIMP II cytosolic tail as a fusion of Gal4-DNA binding domain and different isoforms of $\sigma1$ adaptin viz., $\sigma1$A,$\sigma1$B1 and its splice variants $\sigma1$B2,$\sigma1$B3 and $\sigma1$, were expressed from the bait vector pBridge. The $\sigma1$ adaptins were under the control of MET25 promoter;expressed when the yeast is grown in medium lacking methionine and repressed in the presence of 1mM methionine. $\gamma1$ adaptin was expressed as a fusion of Gal4-activation domain from the prey vector pGADT7. Both the bait and prey constructs were co-transformed into yeast strain CG1945. The co-transformants were grown in liquid medium containing 1mM methionine and equal OD of cells from exponentially growing culture were dotted onto medium lacking histidine and methionine (-His,-Met); incubated for 3 to 5 days and interaction was evaluated according to the growth of yeast in the selection medium.

sortilin CD(Δ1-30) interacted with the $\gamma1$-$\sigma1$ hemi-complexes. Since, the truncated sortilin CD(Δ1-30), lacking the tyrosine-based motif, but containing the di-leucine motif was sufficient for the interaction, it can be concluded that the interaction between sortilin and the $\gamma1$-$\sigma1$ hemi-complex is mediated by the di-leucine motif. Surprisingly, this interaction was restricted only to the hemi-complex containing the $\sigma1$B isoform and its splice variants $\sigma1$B2 and $\sigma1$B3, but little to $\sigma1$A and no interaction with and $\sigma1$C containing hemi-complexes was detected. Interestingly no interaction was detectable with sortilin CD $\gamma1$-$\sigma1$A, however sortilin CD(Δ1-

30) containing only the di-leucine motif did show a weak γ1-σ1A binding. This indicates that aa 1-30 of sortilin CD prevent binding of the membrane distal di-leucine motif with a γ1-σ1A hemi-complex, presumably by adopting a secondary structure preventing di-leucine motif binding to the hemi-complex. For example, the acidic residues preceding the di-leucine motif could bind to membrane proximal basic residues. This also indicates that the affinities of sortilin to γ1-σ1B hemi-complexes are higher than the γ1-σ1A binding affinities, because they are able to bind to the full-length tail.

Further, it was interesting to note different affinities to the σ1B splice variants. σ1B1 containing hemi-complex showed strong interaction with sortilin CD and σ1B2 containing hemi-complex showed strong interaction with sortilin CD(Δ1-30) as assessed from the difference in growth rate of the yeast in corresponding spots (Fig. 3.8 A). Absence of growth in yeast containing the baits and empty prey vector or vice versa served as controls for auto-activation. In a seperate experiment, we checked for interaction between sortilin and γ1 subunit alone, but no interaction was observed. The interaction observed only with the hemi-complex implies that both subunits are necessary for interaction with sortilin. The low affinities of the interactions observed are also demonstrated by the absence of detectable β-galactosidase activities in a colony filter-lift assay and by complete inhibition of growth in the presence of 0.5 mM 3-AT, an inhibitor of the *HIS3* gene product.

Since it was reported in a study (Janvier *et al.*, 2003), that the acidic di-leucine motif of the type D/EXXXL(L/I) present in the cytoplasmic tails of HIV-Nef and LIMP-II mediated their interaction with the γ1-σ1A hemi-complex, we were interested to know whether the differential interaction, observed in our interaction studies with the sortilin tail (Fig. 3.8 A), is maintained with other di-leucine motif containing proteins. For this purpose we chose to test for the interaction of LIMP-II cytosolic tail with γ1-σ1 hemi-complexes. All four different γ1-σ1 hemi-complexes interacted with the LIMP-II cytosolic tail (Fig. 3.8 B) with no apparent difference in specificity or affinity. However, the affinities appear to be higher than those of sortilin, indicating that only low-affinity binding allows to discriminate between the family of γ1-σ1 hemi-complexes.

3.1.2.5   *In vitro* interaction of sortilin with AP-1 from σ1B-/- cells

After observing an interaction between sortilin and the γ1-σ1B hemi-complex at the Y3H level, we performed GST pull-down assay to see whether we can observe the interaction *in vitro*. The σ1B-deficient mouse embryonic fibroblasts were obtained from a σ1B 'knock-out' mouse generated in our lab (Riel, 2004). GST-Sortilin CD,
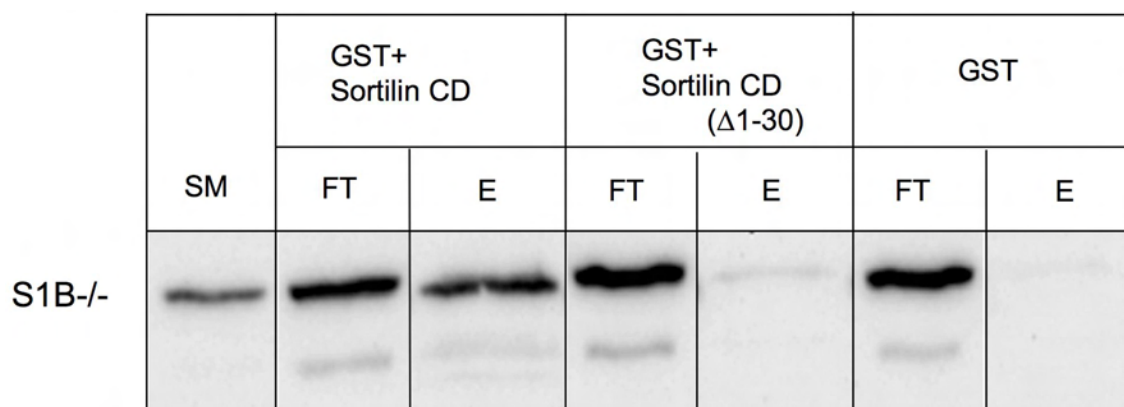
Figure 3.9: *In vitro* **interaction of sortilin and AP-1 in** σ1B-/- **cells.** GST-Sortilin or GST alone bound to beads were incubated with cytosol prepared from σ1B-/- MEFs. The flow-through(FT) was collected before washing the beads 5 times with lysis buffer and finally eluted with reduced Glutathione, pH(8.0). 1% of the starting material(SM), 5% of flowthrough(FT) and 35% of the Eluate(E) were loaded on a 7.5% SDS-PAGE and the blot was probed with antibody against γ1 adaptin (representative of two experiments).

GST-Sortilin CD(Δ1-30) or GST alone bound to GSH-sepharose beads and cytosol prepared from σ1B-/- fibroblasts were incubated overnight at 4 ^{0}C and the pulldown assay was performed essentially in the same way as described in the previous section (3.1.2.2).

GST-Sortilin CD was able to pull-down AP-1 from the σ1B-/- cytosol, but no interaction with either GST-Sortilin CD(Δ1-30) or GST alone (Fig. 3.9), was detected. This was not surprising, because sortilin CD is able to bind to μ1A CT through the tyrosine-based motif (Fig. 3.5). Thus this interaction appears to be responsible for the pull-down of AP-1 by sortilin CD. In all pull-down experiments, the contribution of the di-leucine motif is barely detectable, confirming the low-affinity interaction observed in the Y3H assay. This observation substantiates the idea that sortilin CD interacts with AP-1 via both the tyrosine-based and acidic di-leucine motif independent of each other.

3.1.2.6   Analysis of steady-state distribution of Sortilin in σ1B-/- cells

Having observed from previous experiments that sortilin could interact with γ1-σ1B hemi-complex, we were interested to check for the steady-state distribution of sortilin in σ1B-/- fibroblasts by indirect immunofluorescence microscopy. Wild-type (WT) and σ1B-/- MEFs transiently expressing sortilin were fixed, permabilized according to the PFA fixation method and incubated with mouse anti-sortilin and rabbit anti-MPR300/rat anti-LAMP1. The secondary antibodies conjugated with
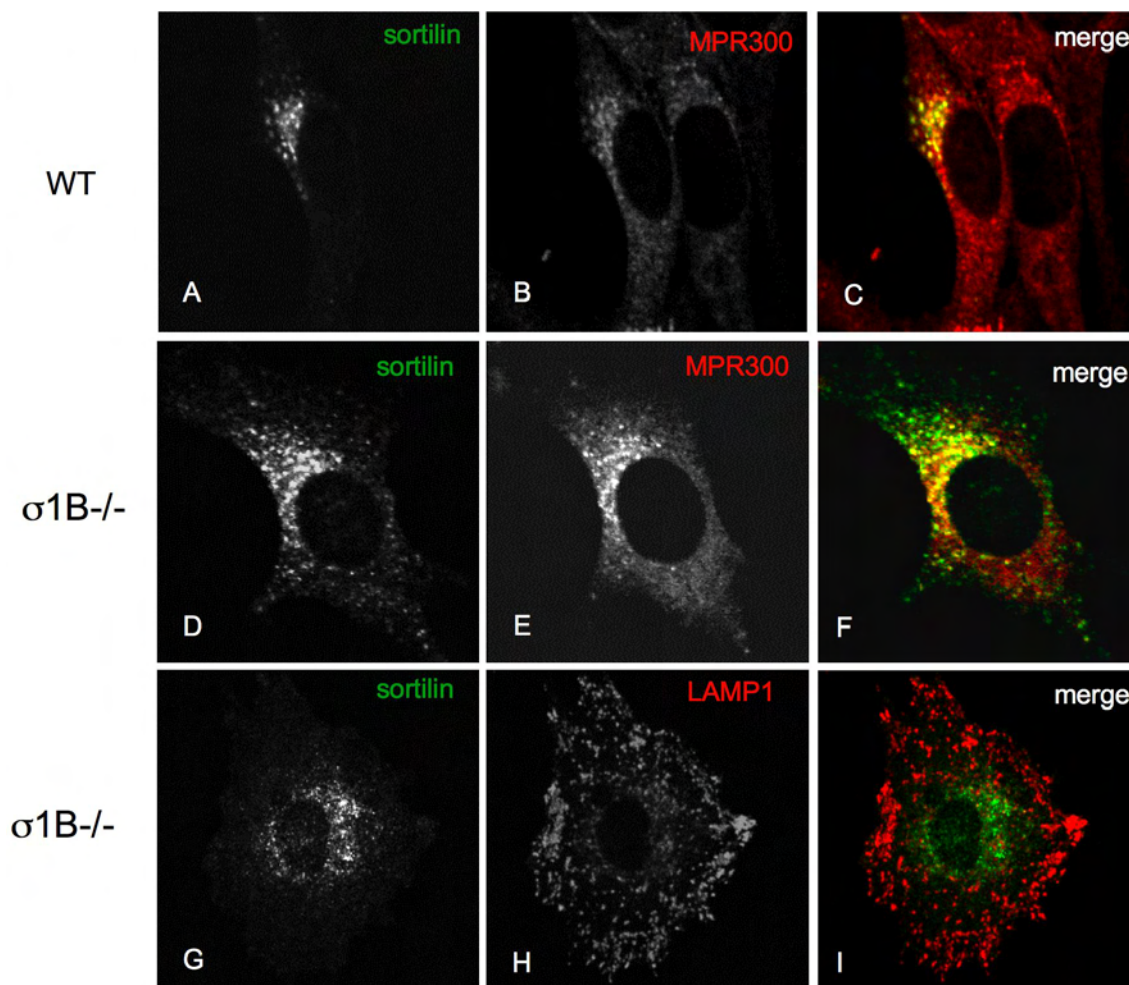
Figure 3.10: Steady state distribution of sortilin in σ1B-/- MEFs . Cells transiently expressing sortilin were fixed using 3% PFA and permeabilized by 0.5% saponin in PBS, pH(7.4) and incubated with antibodies against sortilin (green; A,D,G), MPR300 (red;B,E) and LAMP1(red,H). Merge C, F and I represent the overlay of images A&B, D&E and G&H respectively.

fluorescent probes used were goat anti-mouse Alexa 488 for sortilin, goat anti-rabbit Texas Red and goat anti-rat Cy3 for LAMP1.

In σ1B-/- cells, sortilin was found to be predominantly localized in the perinuclear region and showed high overlap with the distribution of MPR300 (Fig. 3.10 D,E and F) as observed in wild-type cells (Fig. 3.10 A,B and C). This indicates, that the steady state distribution of sortilin was unaltered upon σ1B deficiency. When costained along with LAMP1 a marker for late endosomes/Lysosomes, sortilin staining was completely segregated from LAMP1 staining (Fig. 3.10 G,H and I).

3.1.3 Analysis of intracellular distribution of Sortilin sorting-motif mutants

To further delineate the interactions observed between sortilin and AP-1 and to characterize the sorting motifs that mediate this interaction, we looked for the intracellular distribution of sortilin CD mutants in control (ct) and σ1B-/- MEFs by indirect immunofluorescence microscopy. For this purpose, Interleukin-2 Receptor-α(IL2Rα)-sortilin CD mutant chimeras were used, which were obtained from Prof. C.M.Petersen's lab (Denmark) as part of a collaboration. Sortilin CD mutants were created by either deleting certain selected potential residues or exchanging them by alanine, or by aspartate in the case of S47. These sortilin CD mutants were combined with the extracellular and transmembrane segments of IL2Rα to create IL2R-Sor CD mutants (Nielsen *et al.*, 2001). The interleukin-receptor luminal domain allowed immunofluorescence microscopy analysis with a commercially available interleukin-receptor antibody. In our study, these IL2R-Sor CD mutants were transiently transfected into either Control(ct) or σ1B-/- MEFs. The cells were fixed after 18 hours of transfection using PFA fixation method and incubated with mouse anti-IL2R. The bound primary antibody was then decorated with anti-mouse IgG-Alexa488.

In control cells and in σ1B-/- cells, IL2R-sortilin CD-wt was predominantly localized in the peri-nuclear compartments in agreement with the published study (Nielsen *et al.*, 2001)(not shown). As shown, IL2R-sortilin CD mutants expressed in control cells and in σ1B-/- cells (Fig. 3.11 and Fig. 3.12, respectively), exhibited a similar pattern of steady-state distribution. Both IL2R-sortilin CD-Y14A and IL2R-sortilin CD-Y14A/L17A were re-distributed to peripheral structures, a pattern similar to that observed in μ1A-/- cells. This indicates that the tyrosine residue is most important for μ1A-dependent transport between the endosomes and the Golgi. In contrast, IL2R-sortilin CD-ΔLL exhibited an absolute localization at the peri-nuclear compartment with little or no distribution in vesicular structures in contrast to sortilin-wt in control cells (fig. 3.1 G). This could indicate a possible blockade in the exit of IL2R-Sortilin CD-ΔLL receptor at the TGN, implicating the significance of di-leucine in transport of the receptor from the TGN. The mutant sortilin CD-Y14A/L17A+ΔLL exhibited a mixed pattern with prominent localization at the plasma membrane and also with considerable peri-nuclear and vesicular staining. All other sortilin mutants: sortilin CD-S47D, -S47A, -G42A/Y43A, -D45A/D46A and -D48A/E49A/D50A showed a predominant localization at the peri-nuclear compartment, a pattern as exhibited by sortilin-wt in control cells, indicating that they are dispensable for the intracellular sorting of sortilin.

Figure 3.11: Steady state distribution of IL2R-Sor CD mutants in Control cells. IL2R-Sor CD mutants indicated in their respective images were transiently expressed in control cells and the cells were fixed, permeabilized and incubated with primary antibodies against IL2R and then decorated with secondary antibodies conjugated with Alexa488.

These results indicate that the phenotype observed in μ1A-/- cells is attributable to the tyrosine-based sorting motif as supported by sortilin and AP-1 interaction studies presented in this study. Analysis of the steady-state distributions of these mutants in MEF lacking the σ1B-adaptin did not reveal differences to wt cells. Thus, the tyrosine-based motif apparently required for endosome to TGN transport, can mediate sortilin sorting by AP-1/σ1A as well as AP-1/σ1B complexes.
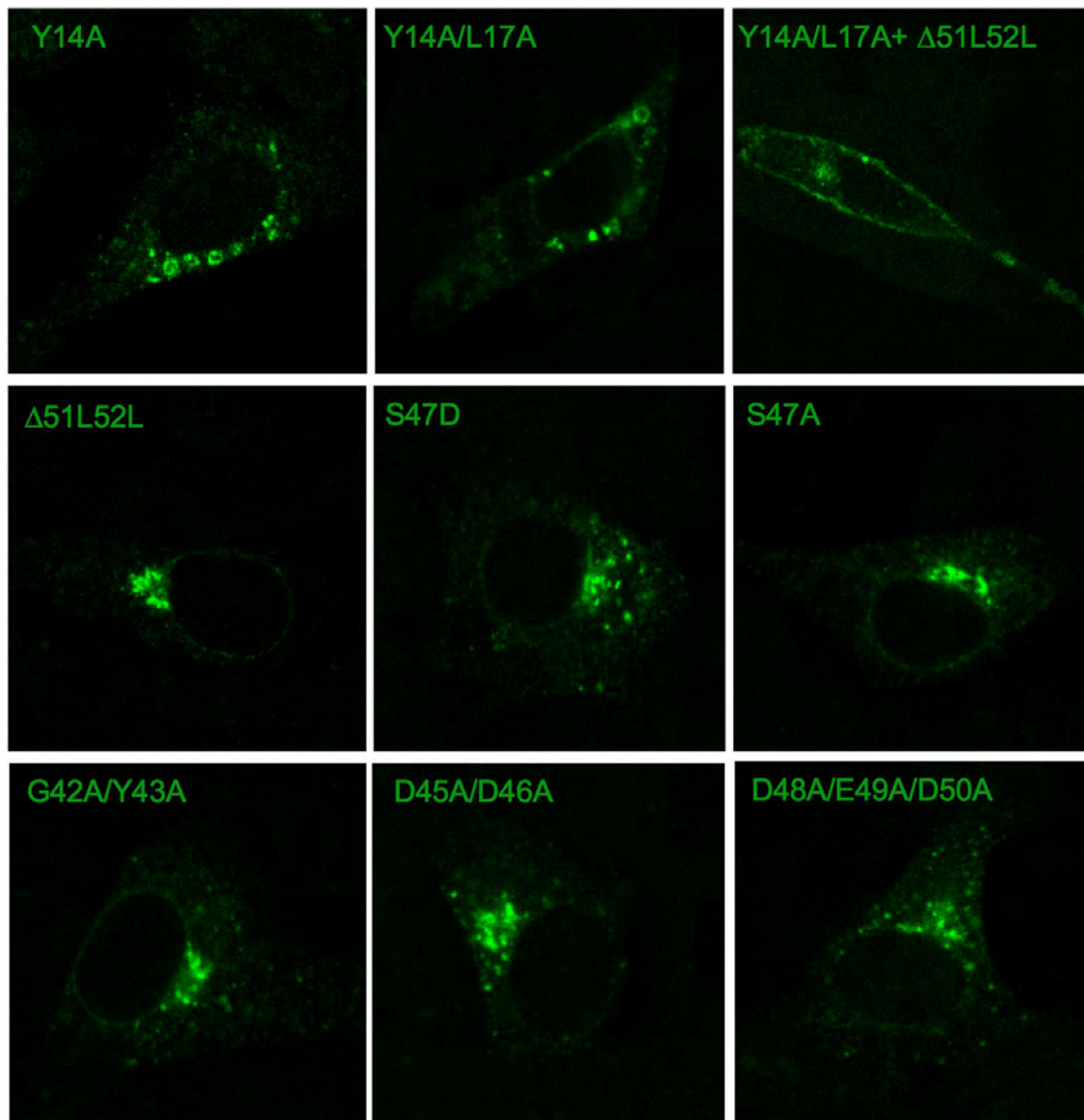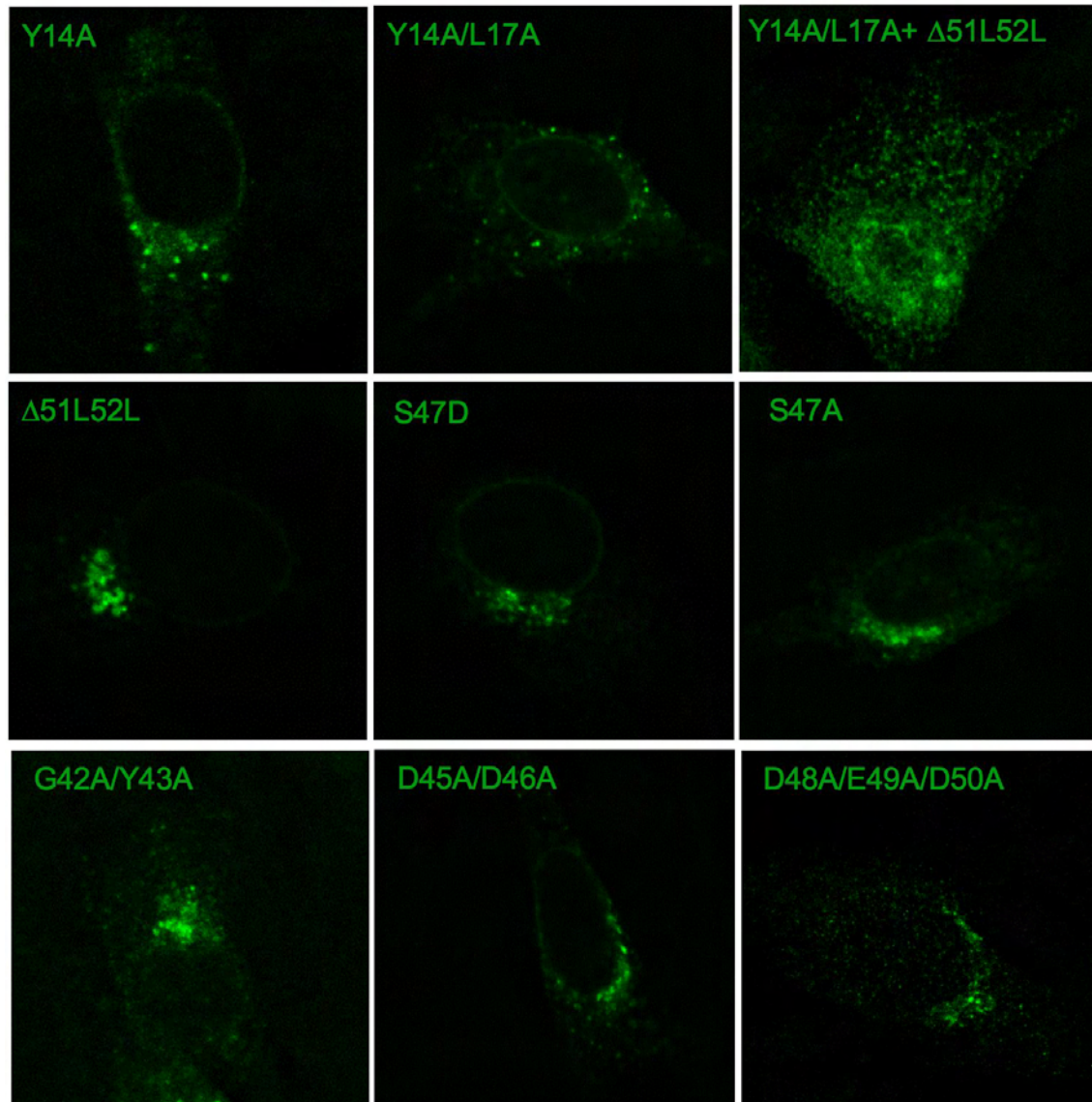
Figure 3.12: Steady state distribution of IL2R-Sor CD mutants in σ1B-/- cells. IL2R-Sor CD mutants indicated in their respective images were transiently expressed in σ1B deficient cells and the cells were fixed, permeabilized and incubated with primary antibodies against IL2R and then decorated with secondary antibodies conjugated with Alexa488.

3.1.4   Analysis of sortilin in adipocytes isolated from σ1B 'knock-out' mouse

Sortilin is highly expressed in adipocytes and is a major constituent of Glut4 vesicles, which are an intracellular pool of Glut4 glucose transporters released to the plasma membrane upon insulin stimulation. Adipose tissues express σ1A and σ1B1/B3 but no σ1B2 or σ1C (Riel, 2004). Therefore we analyzed sortilin expression levels in adipocytes isolated from control and σ1B-deficient mice by western blot (Fig. 3.13)

Two animals of each genotype were tested. The epididymal fat pads were isolated from the wild-type (wt) and σ1B 'knock-out' mice and were digested with crude collagenase to disrupt the tissues. The adipocytes, which float in the top of the supernatant, were isolated from other tissues by low speed centrifugation. The isolated adipocytes were washed in homogenization buffer and homogenized using a teflon pestle homogenizer. This whole cell lysate was centrifuged to get rid of the nuclei and the post-nuclear supernatant was used for subsequent analysis. 100 σg of total protein from each sample were separated by 10% SDS-PAGE, blotted onto PVDF membrane and decorated with antibody against sortilin (Fig. 3.13 A). The signals of sortilin were quantified by 2D densitometry and normalized to that of Hsc70. The resulting values corresponding to each genotype were averaged and the ratio of difference in expression levels of sortilin in σ1B-deficient tissues compared to wt is presented in the plot (Fig. 3.13 B).

Both σ1B-deficient tissues showed a four fold increase in sortilin expression levels, after normalization of the signals against Hsc70 signals serving as control. These data indicate that the sortilin- AP-1 interactions are indeed important for sortilin trafficking in adipocytes. An increase in the amount of sortilin could be caused by a block in export out of one compartment, which would also block sortilin transport to lysosomes. However it could also be caused by an enhanced transcription/translation rate, induced by trapping of sortilin in one compartment or by enhanced degradation due to missorting to lysosomes. Further experiments with primary cell cultures will enable us to answer these questions.
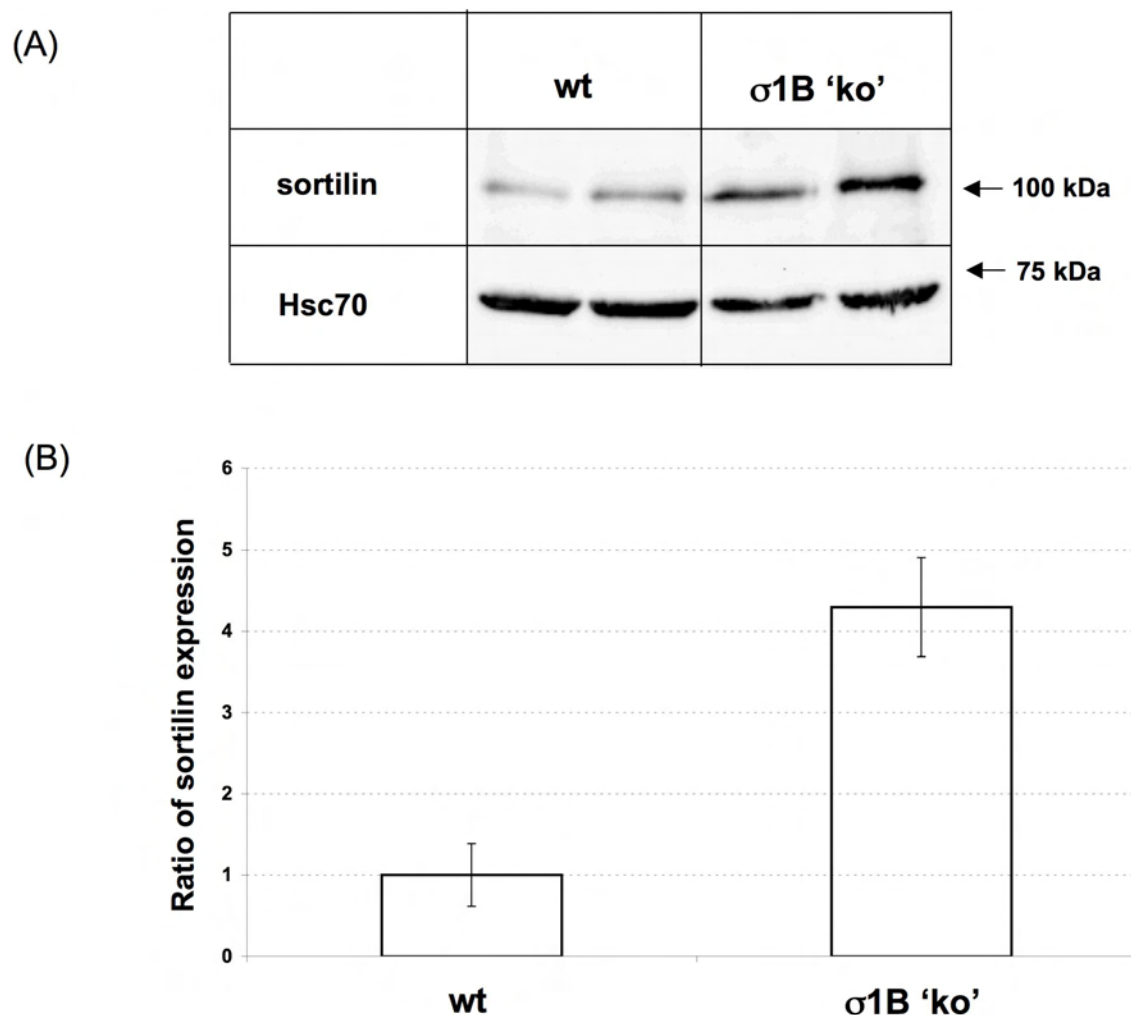
Figure 3.13: Analysis of sortilin in adipocytes isolated from σ1B 'knock-out' mouse. (A) The whole cell lysate of adipocytes isolated from two wild-type (wt) and σ1B 'knock-out' mice were separated by 10% SDS-PAGE, blotted onto PVDF membrane and decorated with antibody against sortilin. Hsc70 served as a loading control. The relative position of the molecular weight marker is indicated. (B) The signals of sortilin were quantified by 2D densitometry and normalized to that of Hsc70 and the ratio of difference in expression levels of sortilin in σ1B-deficient tissues compared to wt is represented. The error bars indicate the maximum deviation of values between samples of each genotype.

3.2   Specificity of $\gamma 1/\sigma 1$ adaptin interactions

Protein sorting by the heterotetrameric adaptor-protein complexes is mediated by the specificity of sorting motif recognition by these complexes as well as by their compartment specific membrane binding, which involves binding to specific phosphotidyl-inositol phosphates. In addition, a large number of proteins bind to the 'ear'-domains of $\gamma 1$ and α-adaptin of AP-2. The function of these proteins is not understood, however the binding of some of these interferes with AP-membrane binding and thus protein sorting. An additional intra-molecular interaction of an 'ear'-domain was observed with the δ-adaptin of the AP-3 complex. The δ-adaptin 'ear'-domain binds to the $\sigma 3$-adaptin, interfering with membrane-binding of AP-3, presumably by sterically blocking ARF-1 binding to the δ-adaptin core domain (Lefrancois *et al.*, 2004).

The $\sigma 1B3$-adaptin also contains a $\gamma 1$-adaptin 'ear' binding motif of the sequence 146EEWGGL151 (see Fig. 3.14 A). We therefore tested for $\gamma 1$-'ear' binding to $\sigma 1$-adaptins in the Y2H system. $\gamma 1$-'ear' binding to rabaptin-5α served as positive control (Fig.3.14). $\gamma 1$-'ear' was constructed as a fusion of Gal4 activation domain (prey). Only the C-terminal tail fragments of $\sigma 1$-adaptins (aa 70-156), were chosen for the study, because the homology between the $\sigma 1$-adaptin isoforms was the least in this region. Also, the highly identical N-terminal part is engaged in complex formation. The C-terminal tail fragments of $\sigma 1$-adaptins and rabaptin-5α were constructed as a fusion of Gal4 DNA binding domain (bait). Both the bait and prey constructs were co-transformed into the yeast strain and allowed to grow in reporter gene selection plates as shown (Fig. 3.14 B). The results were recorded after allowing to grow for 3 to 5 days.

Surprisingly, only $\sigma 1A$ bound to $\gamma 1$-'ear', but very weakly and via a different yet unidentified motif. But, $\sigma 1B3$ did not show any interaction. Therefore we speculated, that the neighbouring residues of the motif in $\sigma 1B3$-adaptin prevented the interaction. Indeed, deleting the preceding acidic residue E146 enabled $\gamma 1$-'ear' and $\sigma 1B3$ binding. Also, the mutation L151F increased the affinity of the motif so strong, that the negative effect of E146 was suppressed. This could indicate that the negative selection altered the motif to prevent interaction with the $\gamma 1$-'ear'-domain.

These data open the possibility that AP-1/$\sigma 1A$ and AP-1/$\sigma 1B$ membrane binding or transport vesicle formation are regulated in different ways enabling specific sorting functions of these AP-1 sub-complexes.

Since no cell line is available, which expresses just one $\sigma 1$-adaptin, this result could not be verified *in vivo*. However, cells from tissue of the $\sigma 1B$ 'knock-out' mouse should allow us to perform these experiments.

Figure 3.14: Analysis of interaction between $\gamma 1$-'ear'-hinge domain and C-terminal tail of $\sigma 1$-adaptins. A) $\gamma 1$-'ear' binding motifs present in respective proteins. Putative $\gamma 1$-'ear' binding motif present in $\sigma 1$B-3 and the mutants constructed for this study are depicted in bold. (B) Y2H analysis of interaction between $\gamma 1$-'ear'-hinge (as fusion of Gal4 DNA binding domain) and C-terminal tail of $\sigma 1$ isoforms and of $\sigma 1$B-3 mutants (as fusion of Gal4 activation domain). Rabaptin5α served as a positive control. The interaction was assessed based on the growth of yeast in reporter gene selection plates as shown.

3.3 A novel role for the N-terminal domain of μ1A in regulation of AP-1 function

3.3.1 Insights from previous studies on μ2/μ1-chimeric AP-1 complex

Previous study from our group provided evidence that the N-terminal seventy aminoacids of μ1A has a role in maintaining the fidelity of the sorting function of AP-1 complex ((Medigeshi Ramarao, 2003), Medegeshi Guruprasad and P. Schu, unpublished). In this study, domains of μ1A were replaced by those of μ2 to identify functions of μ1A domains.
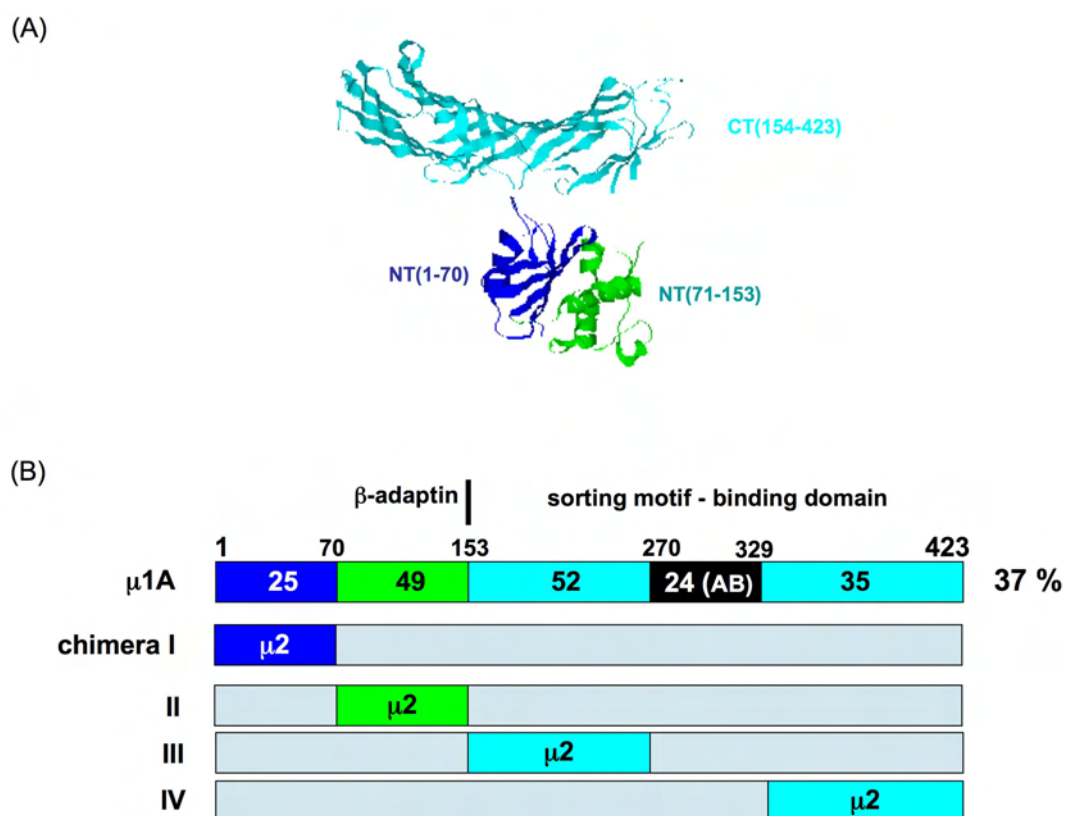
Figure 3.15: Design of μ2/μ1 chimeras. (A) Structural model of μ-adaptins colored for different domains used for designing chimeras. (B) Schematic representation of homology between μ1A and μ2-adaptins and strategy of chimera design. Numbers above the bar indicate the aminoacid number; within the bar indicate percent homology between domains as represented by colors in (A); overall homology 37%. AB indicates antibody binding region in μ1A, against which the antiserum for μ1A is directed. Chimera (I,II,III,IV) represent the different μ1A chimeras that were constructed and the colors indicate the position of replacement with corresponding μ2 domains represented in (A).

When expressed in μ1A-deficient cells, only chimera I was able to incorporate into a chimeric heterotetrameric adaptor complex, designated AP-1*, with functional membrane binding properties as evidenced by the restoration of the steady-state localization of γ1 adaptin, clathrin and MPRs to the peri-nuclear area. This was surprising, because in this μ2/μ1A chimera, the N-terminal 70 amino acid residues of μ1A were replaced with those of μ2, the region that showed the least sequence homology (Fig. 3.15). We compared the structure of μ1A and μ2 N-terminal

Figure 3.16: Comparison of N-terminal seventy amino acid domains of μ1A and μ2-adaptins. (A) Structural similarity of μ1A- and μ2- N-terminal seventy amino acid domains. (B) Primary sequence comparison of the N-terminal seventy amino acids of μ2 and μ1A-adaptins. Identical residues are indicated in bold.

domains, containing the first seventy amino acids, based on the recently solved X-ray crystallographic structures of AP-1 and AP-2 ((Heldwein *et al.*, 2004) and (Collins *et al.*, 2002) respectively). It revealed that, although the primary sequence had the least homology, the tertiary structure is highly conserved. This high degree of structural conservation is responsible for the wt level expression of AP-1* Fig. 3.16).

However, when MPR dependent cathepsin D sorting was followed, AP-1* expressing cells showed an intermediate mis-sorting phenotype compared to control and μ1A-deficient cells. In the presence of 5 mM mannose 6-phosphate, 40% of the Golgi precursor form of cathepsin D was mis-sorted into secretions in AP-1* expressing cells, compared to 61% in μ1A-deficient and 10-15% in control cells, demonstrating an impaired sorting function of AP-1* leading to only a partial complementation of AP-1-deficiency. Time dependent redistribution of AP-1

and AP-1* between membrane and the cytoplasm were followed by addition of Brefeldin A, a drug that interferes with ARF-1 mediated AP-1 membrane recruitment and thereby leads to the redistribution of membrane-bound AP-1 to cytoplasm. These experiments revealed that AP-1* redistribution was slowed-down compared to AP-1 indicating that its membrane-cytoplasm recycling dynamics were disturbed. Based on these preliminary results it was proposed that, the N-terminal seventy aminoacids of μ1A play a role in the regulation of cytoplasm-membrane recycling of AP-1, presumably by binding to and recruiting yet unknown protein(s) and thus regulate AP-1 sorting function.

In the present study, using AP-1* expressing cells as a model system, we attempted to further characterize and define the role of N-terminal seventy amino acids of μ1A-adaptin in the regulation of AP-1 sorting function.

3.3.2 Intracellular membrane morphology in AP-1* expressing cells

Since AP-1* expressing cells showed abnormality in lysosomal delivery of cathepsin D, we were interested in looking for any alterations in membrane morphology in these cells compared to control (μ1A-/-::μ1A) and AP-1-deficient (μ1A-/-) cells by electron microscopy. As shown in (Fig. 3.17 B), AP-1-deficient cells exhibited large membranous structures in the cytoplasm, compared to control cells (Fig. 3.17 A). Interestingly, AP-1* expressing cells also contained these large structures as seen in AP-1-deficient cells, (Fig.3.17 C) indicating that AP-1* expression in μ1A-deficient cells could not rescue the phenotype completely, consistent with the intermediate phenotype observed in cathepsin D sorting (Medigeshi Ramarao, 2003).

When probed for clathrin-heavy-chain and γ1-adaptin by immunogold-labelling, these structures exhibited a weak labelling (Fig. 3.17 D,E). To reveal the identity of these large membranous structures, the cells were allowed to endocytose BSA-gold for 10 and 30 minutes and were also labelled for LAMP-1, a marker for late endosomes/lysosomes. As shown in fig. 3.16 F, after 10 minutes, those enlarged organelles were loaded with BSA-gold indicating that they are connected to the endocytic pathway. A low level of LAMP-1 labelling in these organelles, consistent with kinetic characterization (Griffiths *et al.*, 1989), indicate these organelles as early endosomes. After 30 minutes, endocytosed BSA-gold were also found in late endosomes, characterized by presence of internal vesicles and a high density of LAMP-1 labelling (Fig. 3.17 G), demonstrating vesicle transport between these organelles.
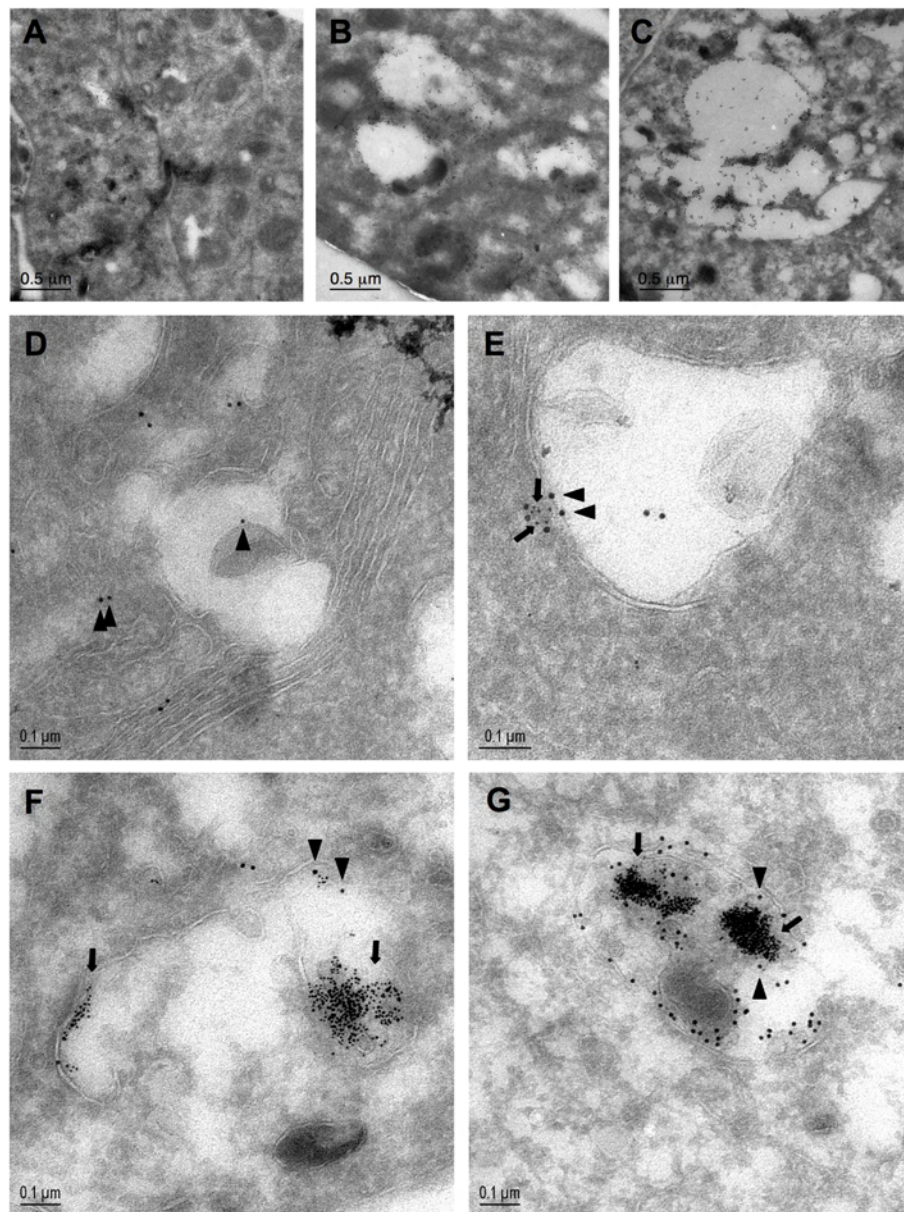
Figure 3.17: Electron microscopy of AP-1, AP-1-deficient (μ1A-/-) and AP-1* expressing cells. Overview of membrane morphology in (A) control cells, (B) AP-1-deficient cells and (C) AP-1* expressing cells. Large organelles in AP-1* expressing cells (D, E). Arrow tips point to clathrin labelling (10 nm gold) and arrows point to γ1-adaptin labelling (5 nm gold). Organelles labelled in AP-1* cells after 10 min (F) and 30 min (G), BSA-gold endocytosis. In (F) and (G), arrow tips point to LAMP-1 labelling (10 nm gold) and arrows to BSA-gold (5 nm gold).

3.3.3   Analysis of AP-1* membrane recycling at the TGN

It has been shown that membrane bound clathrin and adaptors are in dynamic equi-
librium with cytoplasmic pool of free clathrin and adaptors, through continuous and
rapid exchange between the membrane bound and soluble state and interestingly,
that adaptors recycling also occurs independent of vesicle budding (Wu *et al.*, 2001).
In a subsequent study, $\gamma 1$ labelled with EGFP was used to study the recycling kinetics
of AP-1 at the TGN, indicating that the presence of EGFP does not affect the function
of $\gamma 1$-adaptin (Wu *et al.*, 2003). Since, we had already observed that in the presence
of BFA, the redistribution of AP-1* was slower than AP-1 (Medigeshi Ramarao,
2003), we analyzed the membrane recycling dynamics of AP-1 and AP-1* in cells
transiently expressing EGFP-$\gamma 1$, using fluorescence recovery after photobleaching
(FRAP). This method allows us to bleach a region of interest (ROI) and measure
the fluorescence recovery in that ROI, which is a direct measure of the exchange
dynamics of bleached membrane-bound AP-1 with unbleached cytoplasmic ones.
As shown in Fig. 3.18, the recovery of fluorescence after photobleaching for 10
s was measured in the central TGN region at room temperature either in normal
buffer conditions or after treating the cells with 0.2 M sucrose for 30 minutes. The
fluorescence recovery half-time ($t_{1/2}$) in seconds (s), was calculated from a plot of
fluorescence values against time (in s) as shown in Fig. 3.19.

The kinetics of EGFP-$\gamma 1$-adaptin FRAP is depicted in the Fig. 3.19 which
is an average of indicated total number(n) of experiments under normal buffer
conditions. AP-1* showed an almost 50% reduction in recycling kinetics compared
to AP-1, with a $t_{1/2}$ of 17$\pm$2 s and 11$\pm$2 s, respectively. However, both AP-1* and
AP-1 exhibited similar average time-course of recovery (A_{recov}) values; 0.93$\pm$0.05
for AP-1 and 0.83$\pm$0.07 for AP-1*, ie., $\sim$ 85-90% of recovery at the measured
maximum time point. This indicates that membrane-bound AP-1* exchanges with
the cytoplasmic pool but with a reduced rate.

It has been reported that hypertonic sucrose induces the formation of empty
clathrin cage baskets and the exchange of clathrin is completely blocked in the
presence of hypertonic sucrose or upon K^+ depletion, whereas AP-1 and GGA still
exchange, but with reduced rates (Wu *et al.*, 2003). We were interested to see
the effect of clathrin exchange on AP-1*, as it can be argued that the observed
reduction in AP-1* recycling could be an indirect consequence of defective clathrin
uncoating process. We performed EGFP-$\gamma 1$ FRAP measurements in AP-1* and AP-1
expressing cells, wherein the exchange of clathrin at coated pits were blocked by
prior incubation of cells in hypertonic sucrose (0.2 M) for 30 minutes (Fig. 3.18 C).

As shown in fig. 3.19 (B), even after blocking clathrin exchange and thereby
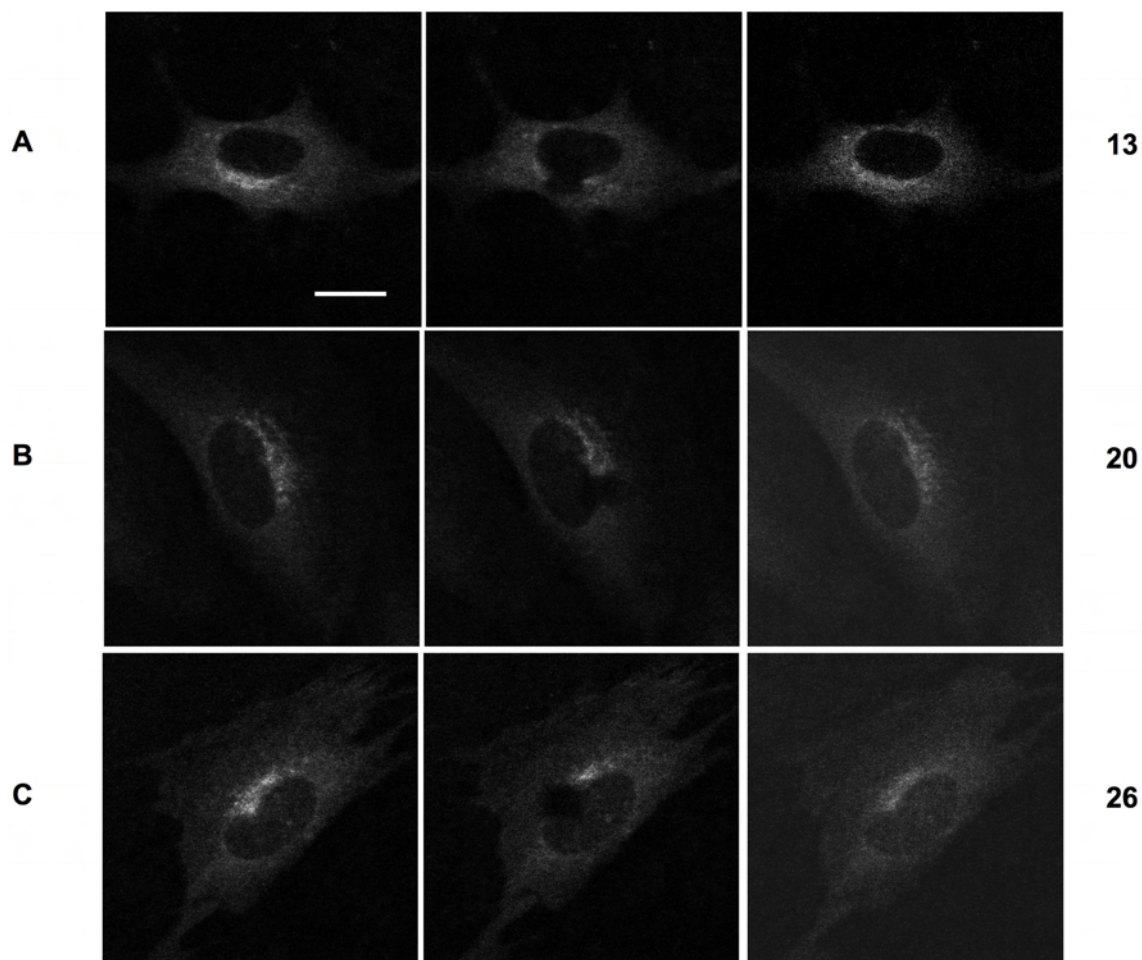
Figure 3.18: Fluorescence recovery after photobleaching in AP-1 and AP-1* expressing cells . EGFP-γ1 expressing control cells (A) and AP-1* cells (B) were subjected to photobleaching at the central TGN area, for 10 s and the fluorescence recovery was monitored under normal buffer conditions at 37° C. Panel C shows FRAP analysis in AP-1* cells treated with 0.2 M sucrose for 30 min. Numbers correspond to the observed fluorescence recovery half-time ($t_{1/2}$) in seconds.

vesicle budding, recovery of fluorescence for AP-1 was observed but at a slower rate with a $t_{1/2}$ of 20$\pm$6 s, in agreement with the reported study (Wu *et al.*, 2003). Also for AP-1*, we observed a reduction in the fluorescence recovery with a $t_{1/2}$ of 32$\pm$6 s in a pattern as observed under normal conditions. Moreover, AP-1 exhibited similar time-course of recovery, $\sim$ 85% as observed under normal conditions (fig. 3.19 B). But, AP-1* exhibited a remarkable reduction in the average time-course of recovery, $\sim$ 60%, when clathrin exchange is blocked, indicating that when vesicle budding is blocked, the fraction of AP-1* binds to the membrane firmly, presumably at non-productive sites and exchanges less with the cytoplasmic pool. These results indicate, that the observed reduced recycling of AP-1*, is a direct consequence of
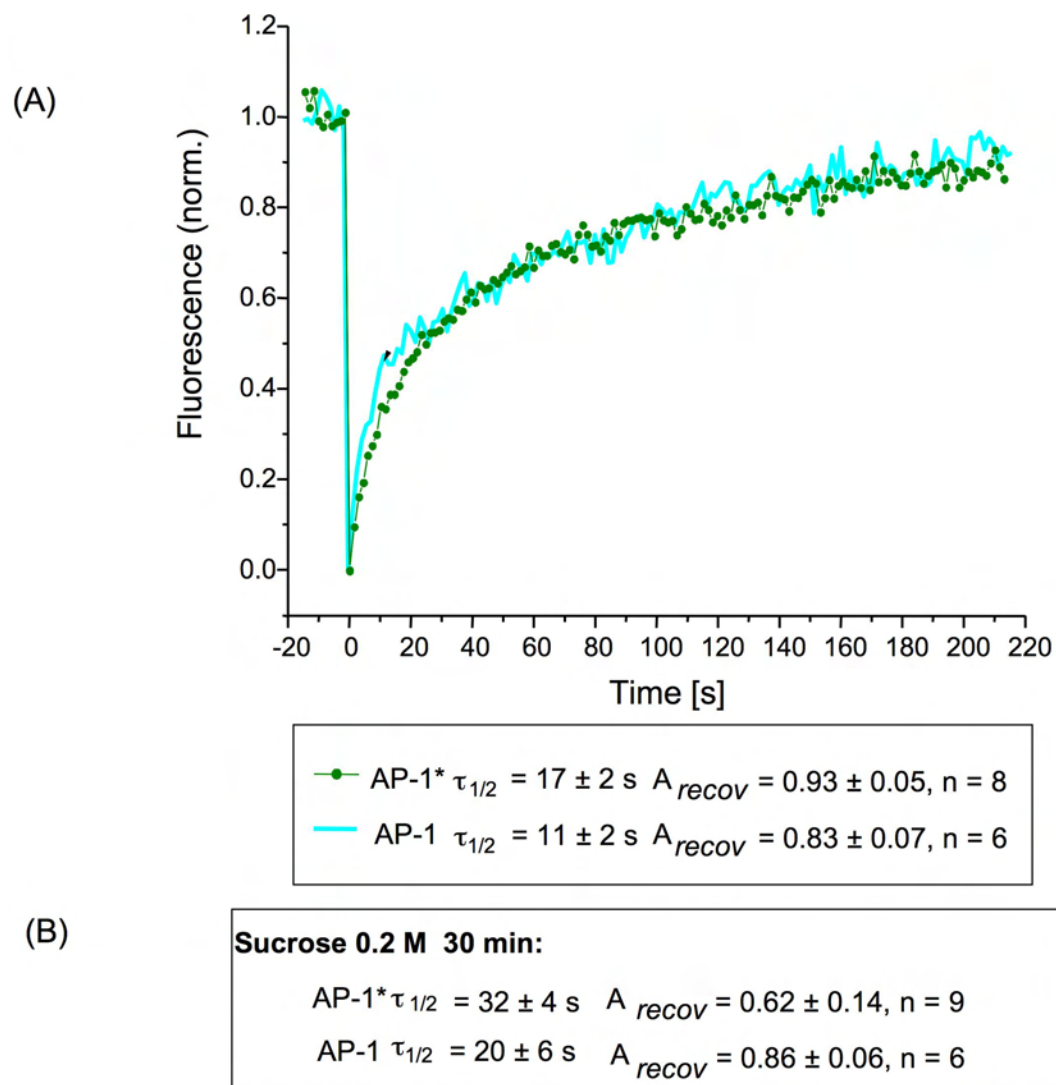
Figure 3.19: Kinetics of fluorescence recovery after photobleaching of AP-1 and AP-1*. (A) The plot depicts the kinetcs of fluorescence recovery of EGFP-AP-1 and EGFP-AP-1* measured at indicated time points (seconds) after photobleaching for 10 s under normal buffer conditions and at 37° C in control and AP-1* expressing cells. A_{recov} indicates the average time-course of complete recovery. (B) Statistics of fluorescence recovery after photobleaching for EGFP-AP-1 and EGFP-AP-1* measured after hypertonic sucrose treatment. n corresponds to number of individual experiments.

altered dynamics in membrane binding and exchange with free cytoplasmic AP-1*.

3.3.4 Analysis of known determinants that regulate AP-1/AP-1* membrane binding

The data from previous section, clearly demonstrate that the N-terminal seventy amino acids of μ1A play a role in AP-1 membrane binding dynamics. As a next step, we were interested to probe on the mechanism by which the N-terminus of μ1A operates to execute its regulatory function.

The crystal structure of AP-1 reveals that the N-terminal seventy amino acid domain of μ1A (colored blue in Fig. 3.20) are not in contact with the membrane, excluding direct μ-lipid interactions. However, it is accessible from the cytoplasmic face of the heterotetrameric adaptor complex (Fig. 3.20).

At the membrane face of the complex, the C-terminal sorting motif binding domain of μ1A-adaptin shields the μ1A N-terminus. However, in the phosphorylation-induced activated state, the sorting-motif binding domain has to flip out of the core complex in order to be able to interact with the cytoplasmic tails of transmembrane proteins, which again exposes the N-terminal domain.
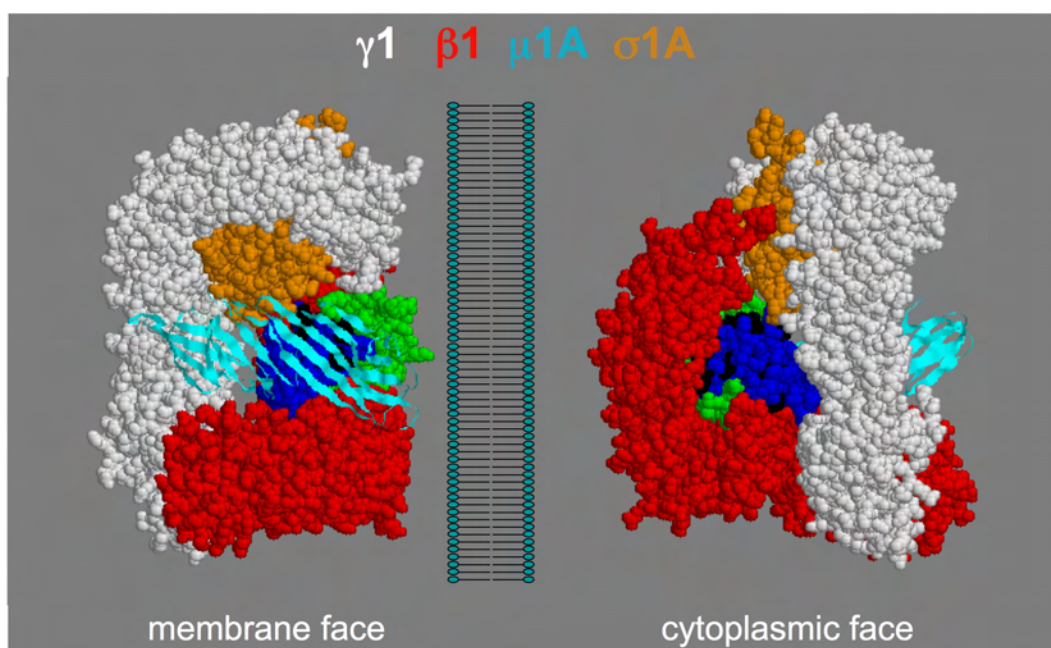

Figure 3.20: Position of N-terminal seventy amino acids of μ1A in AP-1 complex. The subunits are represented by their depicted color. The N-terminal seventy amino acids of μ1A is shown in blue; C-terminal domain of μ1A in cyan.

Several studies over the past years have identified cytosolic and membrane

bound factors to play a role in regulating the recruitment of AP-1 onto membranes. The N-terminal seventy amino acids of μ1A could recruit proteins directly or stabilize already recruited proteins that are known to be involved in AP-1 membrane binding. It is also possible that, as yet unknown cytoplasmic accessory and regulatory proteins involved in AP-1 mediated protein transport can bind to the μ1A N-terminus and regulate AP-1 membrane binding.

3.3.4.1   Influence of phosphorylation kinetics on AP-1* membrane binding

To gain insight on the reduced membrane-cytoplasm recycling of AP-1*, as observed in FRAP experiments, we were interested to look for the phosphorylation state of AP-1*, as it has been shown that the membrane recruitment of AP-1 is regulated by phosphorylation and de-phosphorylation cycles (Ghosh and Kornfeld, 2003a); the β1 subunit is phosphorylated in the cytoplasm, but will be dephosphorylated if AP-1 is bound to membrane, whereas μ1A is in the dephosphorylated state in the cytoplasm, but phosphorylated in the membrane bound state. Also it is known that phosphorylation of μ1A subunit induces high affinity binding to the cargo sorting motif facilitated by a conformational change in μ1A to an open conformation, as observed by X-ray crytallographic studies and sorting motif affinity analyses for AP-2 (Collins *et al.*, 2002). In the phosphorylation-induced open conformation, the hinge region of μ1A, that connects the N- and C-terminal domains, is accessible for trypsin digestion *in vitro*. Therefore susceptibility to trypsin digestion is an indirect measure of the phosphorylation state of μ1A and we took advantage of this property to analyze AP-1*.

Adaptor molecules were stripped off the membrane fractions prepared from control and AP-1* expressing cells and subjected to partial trypsin digestion by incubation at 37° C for 15 min, with increasing concentrations of trypsin. After inhibition of trypsinization, the samples were boiled in 1X Laemlli buffer and loaded on a 10% SDS-PAGE and decorated with rabbit anti-μ1-adapin antibody, which recognizes both μ1A and Chimera I-adaptins. The signals were quantified and the percentage of undigested μ1-adaptins were plotted against trypsin concentration.

As shown in Fig. 3.21, μ1A exhibits a dramatic dose dependent tryptic degradation pattern when compared to Chimera I, indicating that Chimera I is less sensitive to tryptic digestion than μ1A. At the highest concentration of trypsin used (1.5 μg/ml), $\sim$ 60% of Chimera I remains undigested compared to $\sim$ 30-40% of μ1A, an approximately two-fold decrease in degradation, indicating that a larger fraction of Chimera I is inaccessible for trypsin. This means that the membrane fraction of Chimera I is in an under-phosphorylated state. Two possibilities can be derived
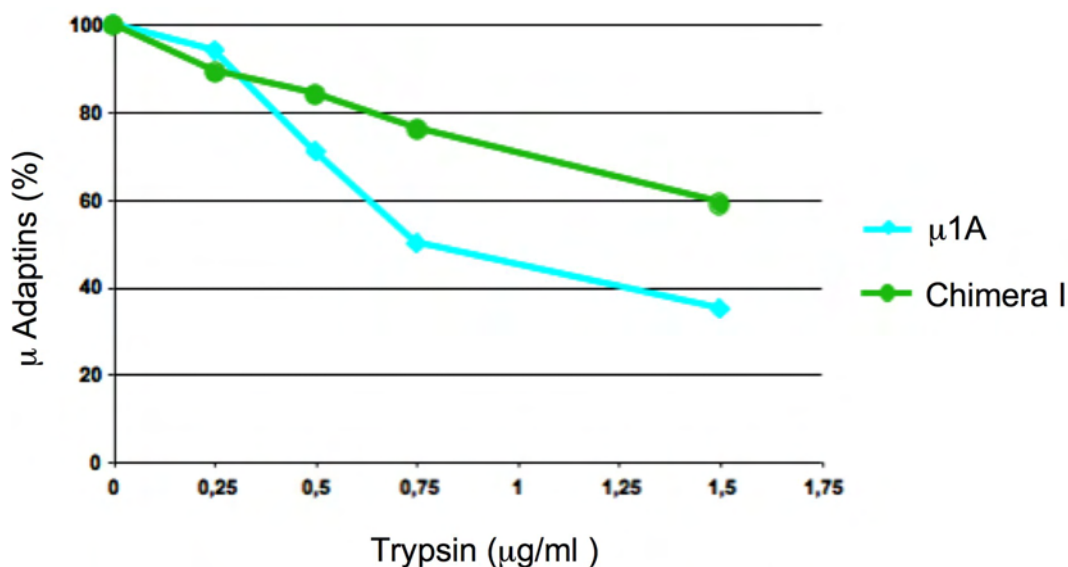
Figure 3.21: Dose dependent tryptic digestion of μ1A and Chimera I -adaptins. AP-1 and AP-1* prepared by stripping the membrane fraction of control and AP-1* expressing cells, were subjected to partial trypsin digestion and analyzed by SDS-PAGE for the levels of undigested μ1A and Chimera I -adaptins using rabbit anti-μ1-adaptin antibody. The signals were quantified and plotted as a function of percent undigested adaptin against increasing concentrations of trypsin. The data presented is a representative of four independent experiments (n=4).

for the state of under-phosphorylation; either due to increased de-phosphorylation or reduced phosphorylation combined with increased phosphorylation-independent membrane (or cargo) binding.

3.3.4.2   Y2H analysis of interaction between N-terminal seventy amino acids of μ1A and candidate proteins

By using Y2H method, we analyzed the interaction of N-terminal seventy aminoacids of μ1A with candidate proteins viz., BIG2, cyclin G associated kinase (GAK)/ auxilin 2, the B-subunit of Protein phosphatase 2A (PP2A) and γ-BAR (γ1-adaptin Brefeldin A Resistance) which were shown to be involved in regulating the membrane binding of AP-1 (Fig. 3.22). BIG2 was identified as a guanine-nucleotide exchange factor(GEF) for ARF-1 operating at the TGN, which when overexpressed, blocked the Brefeldin A-induced redistribution of AP-1 from membranes, indicating that it is implicated in AP-1 membrane binding (Shinotsuka *et al.*, 2002). The mechanism of BIG2 recruitment onto membranes is known to be independent of AP-1 or ARF-1.

γ-BAR is a recently identified peripheral membrane protein that was shown to interact directly with γ-appendage domain of AP-1 and its overexpression was
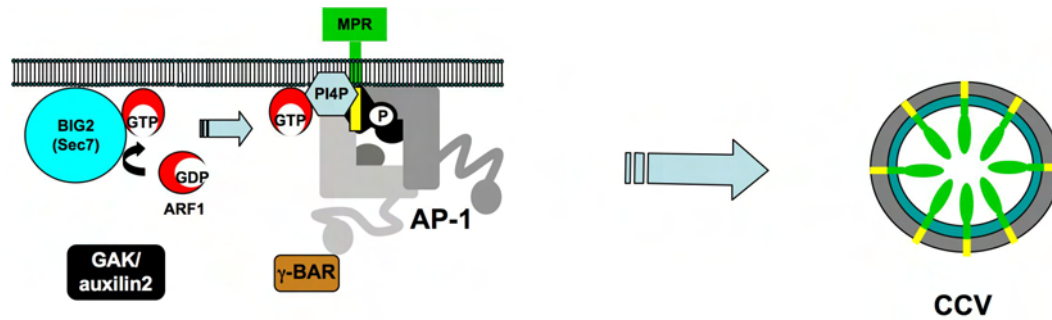
Figure 3.22: A model depicting the role of candidate proteins in AP-1 membrane recruitment and productive CCV formation.

shown to inhibit Brefeldin A-induced redistribution of AP-1 while its 'knock-down' directly reduced the membrane association of AP-1 (Neubrand *et al.*, 2005). The precise mechanism of action of γ-BAR is not known. Since, our previous results showed that AP-1* exhibited a slow redistribution from the membrane to the cytoplasm upon Brefeldin A treatment, we chose BIG2 and γ-BAR as potential candidates to test for interaction with N-terminal seventy aminoacids of μ1A, as both the proteins are known to be directly involved in the recruitment of AP-1 onto the membrane.

GAK was identified as a kinase, that is involved in activating hsc70-mediated clathrin uncoating and it was shown to interact with the γ- appendage domain of AP-1 complex (Umeda *et al.*, 2000). Also, it was shown to be one of the major protein kinases associated with CCVs and the one that predominantly mediates CCV-associated kinase activity (Korolchuk and Banting, 2002).

PP2Aβ was shown to play a role in the dephosphorylation of μ1 and β1 subunits and its activity was shown to regulate the membrane association and dissociation cycles of AP-1 (Ghosh and Kornfeld, 2003a). PP2A is a complex of three subunits-A, B and C. Subunit A, acts as a scaffold for complex formation and subunit C is the catalytic subunit. We chose subunit B for our studies, because it is the regulatory subunit that provides substrate specificity for the phosphatase. We were interested in GAK and PP2A-B subunit, as to ascertain for their role in the altered phosphorylation state of AP-1*.

The cDNAs encoding various domains of BIG2 (hBIG2), GAK and γ-BAR and the full length PP2A-B subunit were cloned into the prey vector(pACT2) and the N-terminal seventy amino acid domain of μ1A was cloned into the bait vector (pGBT9) and co-transformed into yeast strain AH109. The co-transformants were allowed to grow at 30° C in medium lacking histidine and adenine and results were recorded after 3 to 5 days. As shown in Fig. 3.23, none of the co-transformants showed
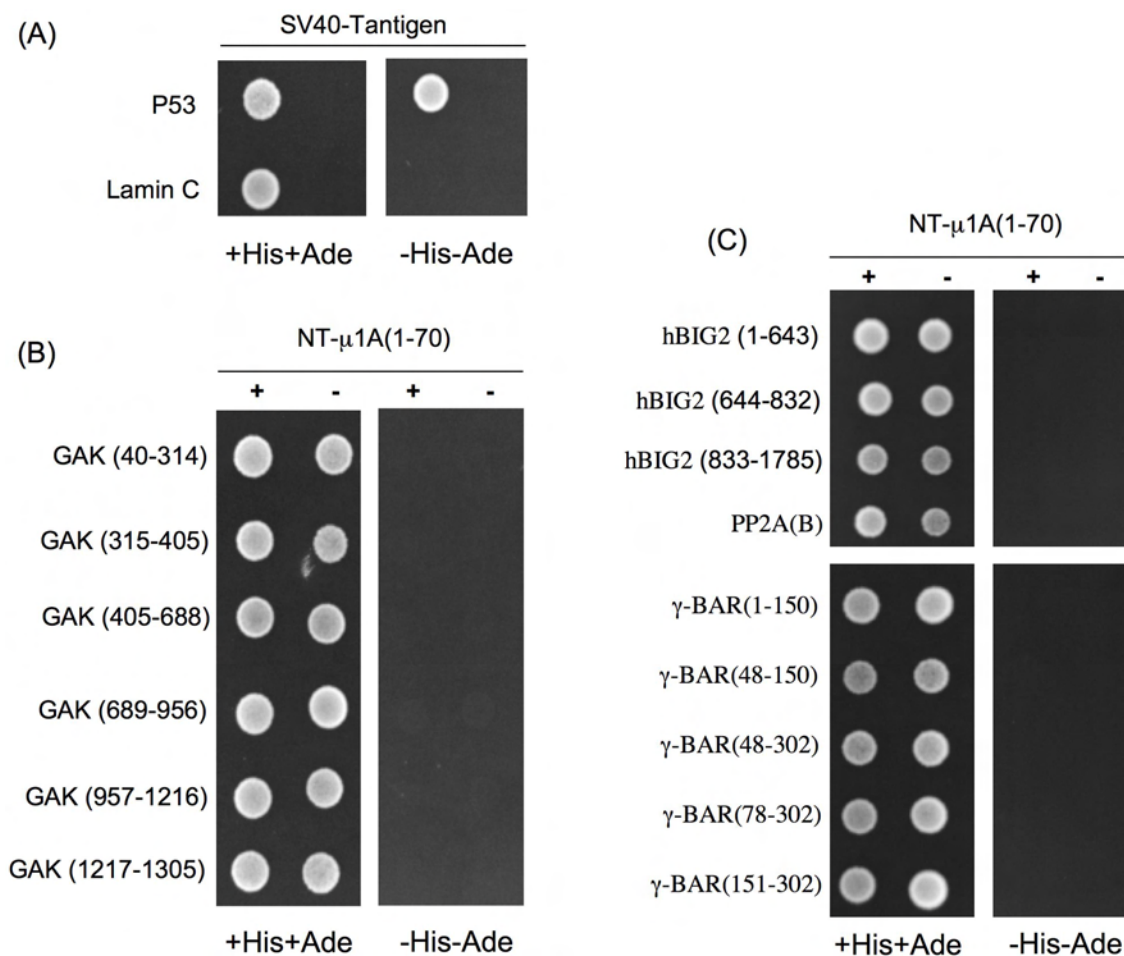
Figure 3.23: Y2H analysis of N-terminal μ1A with known candidate proteins. Different domains of BIG2, GAK, γ-BAR and full length PP2A-B subunit expressed from prey vector and N-terminal seventy aminoacids of μ1A (NT-μ1A(1-70)) expressed from bait vector were analyzed for interaction. Growth of co-transformants in selection medium lacking histidine and adenine (-his,-ade) indicates an interaction as depicted in (A) which served as a positive control. (B) Interaction assay with GAK domains and interaction assay with hBIG2, PP2A-B subunit and γ-BAR is shown in (C).

growth in the reporter selection plates. This indicates that the N-terminal seventy amino acids of μ1A do not interact with these proteins.

3.3.5 Identification of proteins binding to the N-terminal seventy amino acids of μ1A

In addition to testing candidate proteins, we performed a library scale Y2H screening using N-terminal seventy aminoacids of μ1A as the bait and an embryonic cDNA library prepared from 11.3 days old mouse embryo to identify new proteins involved in AP-1 regulation. A total of $\sim 10^6$ clones were screened and the initial
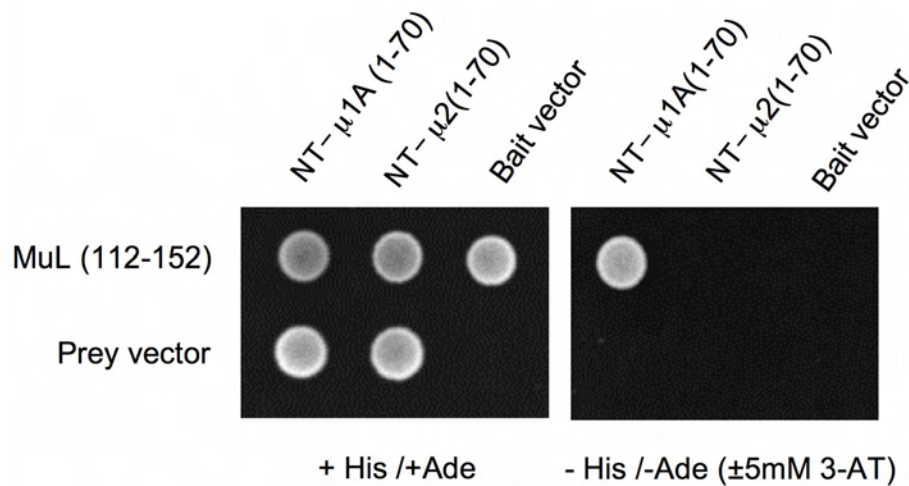
Figure 3.24: Comparison of MuL(112-195) interaction with N-terminus μ1A and μ2.
N-terminal seventy amino acids of μ1A and μ2; NT-μ1A(1-70) and NT-μ2(1-70) respectively, were used as baits to analyze their interaction with MuL(112-195). The growth of the co-transformants in medium lacking histidine and adenine(-His/-Ade) either in the presence or absence of 5 mM 3-AT were monitored for 3-5 days.

screen identified 44 clones positive for all four reporter genes of the AH109 tester strain. cDNA isolated from all the putative positive clones were sequenced, which resulted in 16 unique clones. One clone containing an insert of 275 bp was identified 18 times and exhibited a strong interaction. Upon retesting these 16 clones, for confirmation of interaction by re-transformation, only the clone that exhibited strong interaction in the initial screen was truly positive. A BLAST search of this cDNA sequence against the mouse genome identified an unnamed and uncharacterized protein of 725 amino acids in length. The protein was designated MuL for μ-Ligand.

To test for the specificity of the identified interaction between MuL(112-195) and N-terminal seventy amino acids of μ1A (NT-μ1A(1-70)), we performed a Y2H interaction assay between MuL(112-195) and N-terminal seventy amino acids of μ2-adaptin (NT-μ2(1-70)). As shown in Fig. 3.24, NT-μ1A(1-70) interacted with MuL(112-195), but NT-μ2(1-70) did not. This indicates that MuL(112-195) interacts specifically with NT- μ1A(1-70) and the interaction is very strong as indicated by the growth of yeast in selection media supplemented with 5 mM 3-AT, an inhibitor for the expression of the product of one of the reporter genes, *HIS3*. Absence of growth with respective empty bait and prey vectors excluded the possibility of an auto-activation of reporter genes and thereby validating that the observed interaction is true (see Fig. 3.24).

As MuL exhibits highly specific and strong interaction with N-terminal seventy
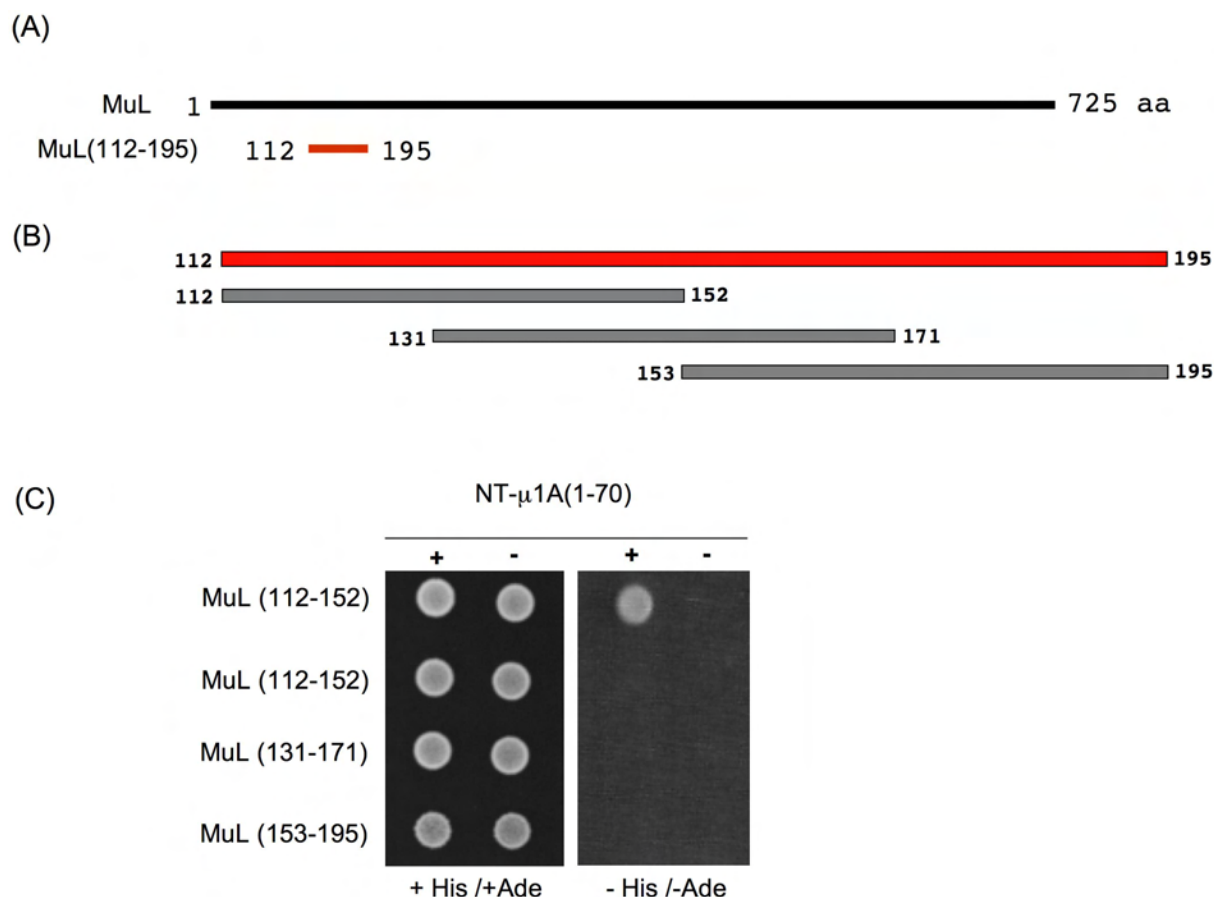
(A)

(B)

(C)

Figure 3.25: Interaction of N-terminal seventy aminoacids of μ1A with MuL(112-195) fragments. (A) Schematic representation of the fished MuL(112-195) with respect to the full length protein. (B) Schematic representation of the overlapping fragments of MuL(112-195), designed to map the region of interaction with N-terminal seventy aminoacids of μ1A (NT-μ1A(1-70)). (C) Y2H analysis of interaction between MuL fragments and (NT-μ1A(1-70). The cDNAs of MuL(112-195)or its fragments with overlapping regions as shown in (B) were cloned into prey vector and analyzed for interaction with (NT-μ1A(1-70). The growth of the co-transformants in medium lacking histidine and adenine(-His/-Ade) were monitored for 3-5 days.

amino acids of μ1A, we attempted to map the region that confers specificity. For this purpose, overlapping fragments of MuL(112-195) were checked for interaction with N-terminal seventy aminoacids of μ1A. As shown in Fig. 3.25 (C), interaction was observed only with MuL whereas none of the MuL(112-195) fragments exhibited interaction, indicating that a putative interacting motif formed by residues from all three fragments mediates the binding.

3.3.5.1 Analysis of the steady state distribution of AP-1/AP-1* in MuL-HA expressing cells

To validate the physiological relevance of the highly specific interaction between MuL(112-195) and N-terminal seventy aminoacids of μ1A, observed in our Y2H interaction studies, we analyzed the intracellular distribution of AP-1 and AP-1* in control and Chimera I (Chi-I) cells respectively, ectopically expressing MuL-HA. The complete cDNA of MuL was generated from mouse brain total RNA, by RT-PCR and was cloned into mammalian expression vector (pcDNA3) to be expressed with HA-tag at its C-terminus. The MuL-HA construct was transiently transfected in AP-1(control) and AP-1* expressing cells and analyzed by indirect immunofluorescence microscopy.

MuL-HA exhibited a cytoplasmic distribution in both control and Chi-I cells (Fig.3.26). When we analyzed for the steady-state distribution of AP-1 and AP-1* in cells that showed expression of MuL-HA, there was a remarkable reduction in the staining for γ1-adaptin at the peri-nuclear area compared to control cells (Fig. 3.26 A, B, C, D) indicating that the recruitment of AP-1 onto membranes is disturbed in MuL-HA over-expressing cells. As expected, AP-1* distribution was unaltered in the presence of MuL-HA expression (Fig. 3.26 E, F, G, H). The observation that MuL-HA disturbs the membrane binding of AP-1, but not that of AP-1*, substantiates the specificity of interaction observed in Y2H studies and also implicates that MuL plays a role in the membrane-cytoplasm recycling dynamics of AP-1.
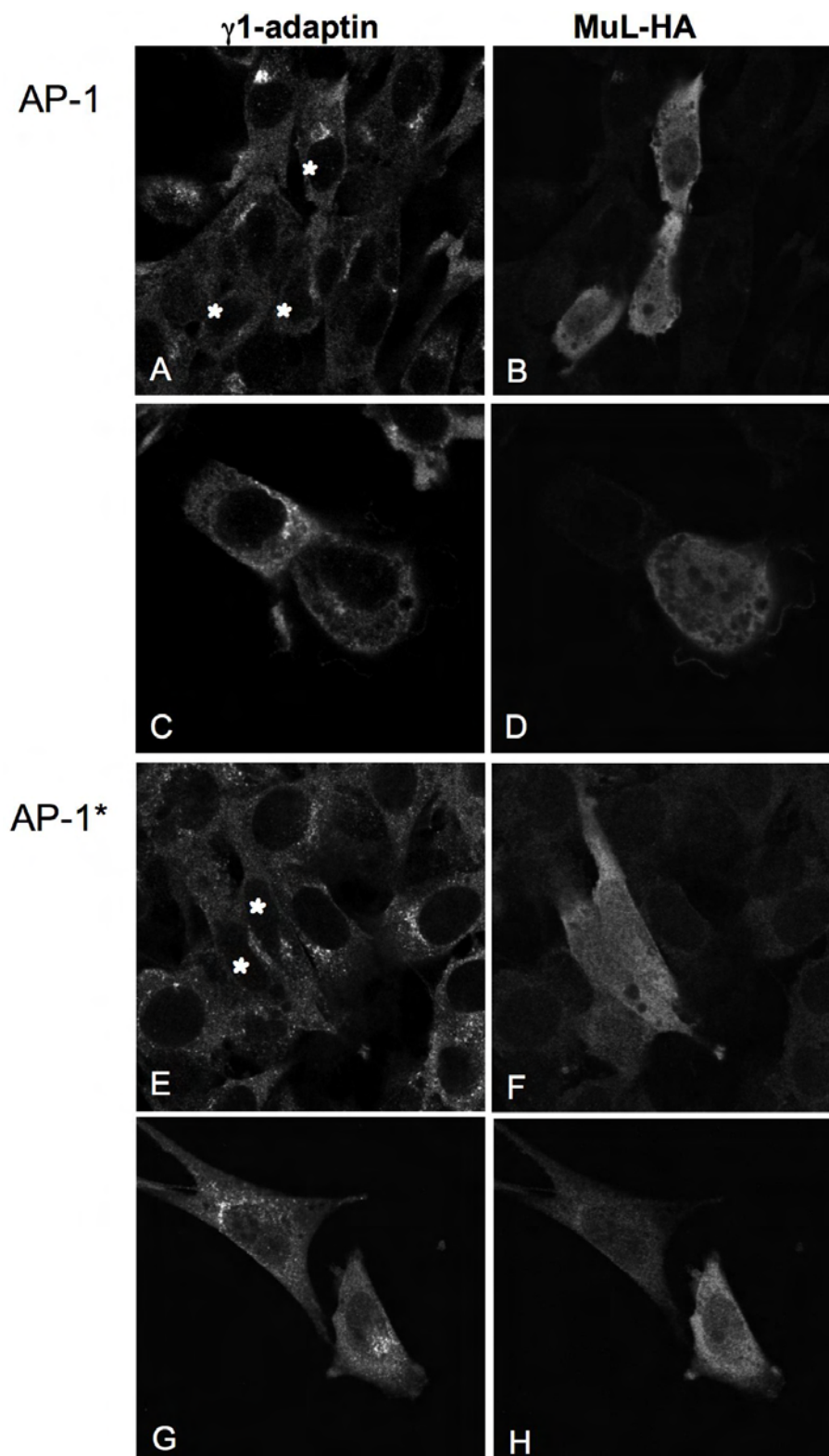
Figure 3.26: Steady-state distribution of AP-1/AP-1* in MuL-HA expressing cells. Control (AP-1) and Chimera I (AP-1*) mouse embryonic fibroblasts transiently transfected with MuL-HA were grown on coverslips and fixed with 3% PFA, 24 hours post-transfection. Permeabilized with 0.5% saponin and double immuno-stained with mouse anti-γ1-adaptin and rat anti-HA monoclonal antibodies which were then decorated with anti-mouse IgG-Alexa 488(green) and anti-rat IgG Cy3 (red). Note the loss of γ1-adaptin staining in MuL-HA expressing control cells indicated by astriek.

Chapter 4

Discussion

4.1 AP-1 in intracellular sorting of Sortilin

At the end of the biosynthetic pathway, a subset of newly synthesized proteins are sorted to their destinations by clathrin-coated vesicles (CCVs). The first step in this pathway, is the transport of membrane-bound cargo from the TGN, the main sorting station to the sorting substation, the early endosomes. So far, AP-1 and GGAs are known to be the main players acting in this process of CCV mediated transport from the TGN to endosomes. A pioneering study with AP-1-deficient mice (μ1A-adaptin 'knock-out') demonstrated, that AP-1 mediated also the retrograde transport of membrane-bound receptor MPR46 (Meyer *et al.*, 2000). The discovery of the role of monomeric receptors, the GGAs, in the anterograde transport of the MPRs, questioned the role of AP-1 in the anterograde pathway, although till now there is no evidence that GGAs are involved in the retrograde transport. Failure to identify the GGAs in CCV preparations and subsequent structural studies on GGAs, led to the proposal that the GGAs1 and 3 may act mainly in concentrating the membrane-bound cargo and sub-sequentially transfer the cargo to AP-1 in a GGA phosphorylation/de-phosphorylation cycle dependent fashion. However, GGA2 lacks such a phosphorylation cycle. The precise role of AP-1 and GGAs at the TGN remains elusive.

Recently, the GGAs were shown to be involved in the transport of a newly identified membrane-bound receptor, sortilin. Sortilin belongs to a growing family of Vps10p-domain containing, multi-ligand type I receptors involved in intracellular sorting of various ligands. It was shown that the cytoplasmic tail of sortilin contained bonafide intracellular sorting signals (Nielsen *et al.*, 2001). The primary sequence of the cytoplasmic domain of sortilin is closely related to the cytoplasmic domain of MPR300 (cation-independent mannose 6-phosphate receptor), with a

conserved tyrosine-based and a di-leucine based motif. The authors also reported that the sortilin cytoplasmic domain interacted with GGA2, a member of the GGA family of monomeric adaptors that are involved in the transport of cargo from the TGN to the endosome, concluding that the transport of sortilin from the TGN to endosomes is mediated by GGA2 (Nielsen *et al.*, 2001). But surprisingly, so far, all of the reported studies on sortilin transport, did not address the role of AP-1 in the transport of sortilin.

In the present study, we examined the role of AP-1 in the intracellular sorting of sortilin. Previous studies from our group, based on AP-1-deficient mice (μ1A-adaptin 'knock-out') has demonstrated the involvement of AP-1 in the transport of MPR300. Since sortilin exhibits similar sorting characteristics as of MPR300, we were interested to know the fate of sortilin in AP-1-deficient cells.

The mannose 6-phosphate receptors MPR46 and MPR300 are sorted into clathrin-coated vesicles by AP-1. Deficiency of AP-1 results in a redistribution of the receptors from the TGN, their main localization at steady-state, to early-endosomal compartments as observed in μ1A -/- fibroblasts (Meyer *et al.*, 2000). We analyzed the intracellular distribution of sortilin in AP-1-deficient MEFs by indirect-immunofluorescence microscopy (Fig. 3.1). As previously shown (Meyer *et al.*, 2000), in μ1A -/- cells, γ1-adaptin staining is lost or very weak at the TGN with more peripheral distribution of MPR300 compared to control cells, where both show overlapping staining at the TGN. Sortilin was shown to be predominantly localized at the TGN and vesicles with an extensive co-localization with MPR300 (Petersen *et al.*, 2001). In agreement with this, the distribution of sortilin and MPR300 (Fig. 3.1 G and H respectively) in control cells was mainly peri-nuclear and overlapped extensively (Fig. 3.1 I). But in μ1A -/- cells, there was a remarkable distribution of sortilin mainly to peripheral structures (Fig. 3.1 J) with dispersed staining, overlapping extensively with re-distributed MPR300 (Fig. 3.1 L). Since MPR300 is known to re-distribute to early endosomal structures in μ1A -/- cells (Meyer *et al.*, 2000), this co-localization implies that sortilin is also re-distributed to early-endosomes in a similar way as MPR300. Sortilin antibody endocytosis experiments demonstrated that sortilin is mis-localized to endosomes as it has been shown for both manose 6-phosphate receptors.

Although sortilin redistributed to MPR300 positive endosomes in μ1A -/- cells, its staining appeared even more widely dispersed. To ascertain whether sortilin is mis-sorted to late endosomes or lysosomes, we performed co-staining with LAMP-1, a marker for late endosomes and lysosomes. As shown in Fig.3.2 (D,E and F), sortilin is found in dispersed LAMP-1 negative structures, implying that sortilin is not mis-sorted to lysosomes. AP-3 is another member of the heterotetrameric adaptor

complexes, which has been shown to localize at the TGN and endosomes, but with a predominant localization at the early endosomes (Reusch *et al.*, 2002). To validate whether AP-3 is involved in the sorting events of sortilin, we analyzed the steady-state distribution of sortilin in AP3-/- cells, which are deficient for δ-3 adaptin. Sortilin stained predominantly in the peri-nuclear area as observed in control cells (Fig. 3.2 A) implying that its steady-state distribution is unaltered in the absence of AP-3.

Sortilin - AP-1 interactions

The observed difference in the steady-state localization of sortilin in μ1A-/- cells prompted us to check, whether the sortilin tail could mediate direct interaction with μ1A. The sortilin CD contains two sorting motifs: a tyrosine-based motif and an acidic di-leucine motif (Fig. 3.3) and both are able to mediate binding to AP-1 and AP-2 complexes as shown for MPR300 and many other proteins. We used the established Y2H method to check for possible interaction, as this system has proven to be successful in identifying even weak interactions. Two different constructs of sortilin cytoplasmic domain(CD) were used in this analysis; the full length CD (sortilin CD) and a truncated form lacking the tyrosine-based motif, but containing the di-leucine motif (sortilin CD(Δ1-30)). These two different sortilin CDs were checked for interaction with the C-terminal domain (150-450 aa) of μ1A (μ1A CT) that contains the Yxxϕ sorting motif binding site.

Our data indicate that sortilin CD interacts directly with μ1A CT albeit weakly. This interaction is most likely mediated by the tyrosine-based motif, as the sortilin CD lacking this motif failed to show even weak interaction (Fig. 3.4). MPR46 CD exhibited auto-activation and so its interaction could not be validated. However, MPR300 CD showed a strong interaction with μ1A CT. This apparent difference in the affinities could be explained in two ways. First, it has been shown that the MPR300 cytoplasmic tail contains four binding sites for AP-1 (Ghosh and Kornfeld, 2004). Using GST pull-down assay, the authors identified four binding motifs: a tyrosine -based motif (26YSKV29), an internal di-leucine based motif (39ETEWLM44), and two casein kinase 2 sites (84DSEDE88 and 154DDSDED159); YSKV motif mediated the strongest interaction with AP-1 and the two CK2 motifs bound AP-1 only when they were phosphorylated. Also, the authors had shown that the COOH-terminal di-leucine motifs were not required for interaction with AP-1. However other studies using surface plasmon resonance to test for AP-binding indicate that AP-1 as well as AP-2 are able to bind to the C-terminal di-leucine motif. Therefore, one can speculate that binding to more than one site, to both tyrosine-

based and internal di-leucine based motif of MPR300 cytoplasmic domain, leads to the increased affinity in our yeast two-hybrid assay.

Secondly, the nature of the tyrosine based (Yxxϕ; Y-tyrosine, x-any aminoacid, ϕ-residues with bulky side chain) sorting signal may be responsible for different affinities. There is substantial evidence that Yxxϕ motif is the minimal requirement to confine recognition by the μ-adaptins. However, the X residues and other residues flanking the motif also contribute to the strength of interaction and fine tuning of the specificity of the signals (Bonifacino and Traub, 2003). The Y residue is essential for function and in most cases cannot even be substituted by other aromatic amino acid residues, suggesting that the phenolic hydroxyl group of the tyrosine is a critical recognition element. The ϕ position can accommodate several residues with bulky hydrophobic side chains, although the exact identity of this residue can specify the properties of the signal. The X residues are highly variable, but tend to be hydrophilic. Such preferences are not clearly known for recognition by μ1A , but at least for μ2 it has been shown that mutations of the X-residues tend to decrease the strength of interaction. In the case of MPR300 and sortilin with YSKV and YSVL motifs respectively, the only obvious difference is the presence of valine(V) at Y+2 position in sortilin, a small residue with less hydrophilicity compared to lysine(K) in MPR300. Introduction of mutations to mimic either of the residues could provide an answer for this difference in affinities. In addition, the influence of flanking residues needs to be tested.

As a next step, we performed a GSTpull-down assay using GST-sortilin CD fusion proteins and cytosol preparations from control and μ1A -/- cells. GST-Sortilin CD efficiently pulled-down AP-1 from the control(ct) cytosol compared to GST-Sortilin CD(Δ1-30) that lacks the tyrosine-based motif (Fig. 3.6). This confirms that the tyrosine-based motif is sufficient for interaction between sortilin CD and μ1A, as observed by Y2H interaction study. Yet a weak signal for γ1 was observed in the pull-down fraction of GST-Sortilin CD(Δ1-30), which means that the interaction is not completely lost.

Surprisingly, similar results were observed, when cytosol from μ1A -/- cells was used for pull-down assays (Fig. 3.6). Apparently GST-Sortilin CD was able to pull-down γ1-adaptin, indicating that sortilin could bind to γ1, or most likely to a γ1-σ1 hemi-complex, independent of μ1A. It has been shown that a trimeric complex consisting of a γ1- σ1 hemi-complex and β1 adaptin still exists in μ1A-/- fibroblasts (Meyer *et al.*, 2000). However, this trimeric complex is non-functional in protein sorting because it does not bind to membranes *in vivo*, and *in vitro*. So, it is possible that sortilin CD interacts with the cytosolic γ1-σ1-β1 complex present in μ1A-/- cells. A recent study has shown that γ1-σ1A hemi-complex interacts with acidic

di-leucine motif present in the cytosolic tails of HIV-Nef and LIMP-II (Janvier *et al.*, 2003). Therefore, one can expect that the interaction between sortilin and the γ1-σ1 hemi-complex could be mediated by the acidic di-leucine motif present in sortilin CD, although only a weak signal for γ1 was observed in the pull-down fraction of GST-Sortilin CD(Δ1-30). One possible explanation to this discrepancy could be that the acidic di-leucine motif in GST- Sortilin CD(Δ1-30) may not be completely accessible for interaction due to steric hinderance or due to the requirement of a post-translational modification. In addition, that in μ1A-/- cells the remaining adaptins are not present in a 1:1:1 ratio. While γ1 is slightly reduced to 70% of wt levels, σ1 is reduced to 30%. Thus, reduced complex stability could contribute to the low pull-down efficiency.

We tested for interaction between sortilin and the hemi-complexes containing γ1 and various isoforms of σ1 including different splice variants for the σ1B gene, identified in a previous study of our lab (Riel, 2004). The splice variants exhibited tissue specific expression pattern. σ1B2 and σ1B3 are expressed mainly in the brain and skeletal muscle respectively. Both sortilin CD and sortilin CD(Δ1-30) interacted with the γ1-σ1 hemi-complex (Fig. 3.7 A). Surprisingly, this interaction was restricted only to the hemi-complex containing the σ1B isoform and its splice variants σ1B2 and σ1B3. But, σ1A and σ1C containing hemi-complexes showed extremely weak or no interaction. It has to be noted that in the study of Janvier *et al.*,2003, the acidic di-leucine motif of the type D/EXXXL(L/I) present in the cytosolic tails of HIV-Nef and LIMP-II interacted with γ1-σ1A hemi-complex, but interaction with hemi-complexes containing either σ1B or σ1C were not tested. This high affinity di-leucine based motif did not show any σ1- specificity, indicating low affinity di-leucine based signals are required to allow specific binding to a specific AP-1 complex *in vivo*.

Further, it was interesting to note different affinities of sortilin to the σ1B splice variants. The interaction between σ1B2 containing hemi-complex and sortilin CD(Δ1-30) was stronger than that of σ1B1 containing hemi-complex, as evident from the difference in growth rate of the yeast clones (Fig. 3.7 A). Of note, this specificity correlates with the tissue expression pattern of sortilin and of σ1B splice variants. Sortilin was shown to be mainly expressed in brain, skeletal muscle and adipocytes. In a seperate experiment, we checked for interaction between sortilin and γ1 or σ1 alone, but no interaction was observed. The interaction observed only with the hemi-complex implies that both the subunits form the binding site for interaction with sortilin.

After observing an interaction between sortilin and the γ1-σ1B hemi-complex by Y3H assay, we performed GST pulldown assays to see whether we can observe

the interaction *in vitro* in cells that are deficient for σ1B adaptin. The σ1B-deficient mouse embryonic fibroblasts were obtained from a σ1B 'knock-out' mouse generated in our lab (Riel, 2004). MEFs normally express σ1A, -B and -C. GST-Sortilin CD was able to pull-down AP-1 from the σ1B-/- cytosol, but no interaction with either GST-Sortilin CD(Δ1-30) or GST alone (Fig. 3.8), was detected. This was not surprising, because sortilin CD is able to bind to μ1A CT through the tyrosine-based motif (Fig. 3.4). Thus this motif appears to be responsible and thus sufficient for the pull-down of AP-1 by sortilin CD. In all pull-down experiments, the contribution of the di-leucine motif is barely detectable, indicating a low-affinity interaction. This observation substantiates the idea that sortilin CD interacts with AP-1 via both the tyrosine based and acidic di-leucine motifs.

The observed interaction between the sortilin di-leucine based motif and γ1-σ1B hemi-complex prompted us to check for the steady-state distribution of sortilin in σ1B-/- fibroblasts by indirect immunofluorescence microscopy. We were unable to see any change in the steady-state distribution of sortilin in σ1B-/- fibroblasts. The staining of sortilin was unaltered with predominant co-localization with MPR300 at the peri-nuclear region. This indicates that binding to μ1A-adaptin is sufficient to mediate TGN - endosome sorting in the mouse embryonic-fibroblasts. However traffic on additional routes could still be mediated by σ1B in the respective tissues. Examination of the steady-state distribution of sorting-motif mutants of sortilin further substantiates our finding that AP-1 is involved in the transport events of sortilin between the endosomes and the TGN. We followed steady-state distribution of IL2R-sortilin CD mutant chimeras in the control and σ1B-/- fibroblasts (Fig. 3.10 and Fig. 3.11). The IL2R-sortilin CD-Y14A mutant and also the -Y14A/L17A mutant are mis-sorted to peripheral structures, indicating that the tyrosine-residue is the most important for μ1A mediated transport, and that this binding mediates endosomes to TGN transport. IL2R-sortilin CD-ΔLL exhibited an absolute localization at the peri-nuclear compartment with little or no distribution in vesicular structures in contrast to sortilin-wt in control cells. This could indicate an impaired exit of IL2R-Sortilin CD-ΔLL receptor at the TGN, implicating the significance of di-leucine in transport of the receptor from the TGN. However, the mutant sortilin CD-Y14A/L17A+ΔLL exhibited a mixed pattern with prominent localization at the plasma membrane and also with considerable peri-nuclear and vesicular staining. This indicates that the ΔLL mutant is able to leave the TGN, presumably by constitutive exocytosis. Both motifs however appear to be required for endocytosis, mediated by the homologous AP-2. All other sortilin mutants: sortilin CD-S47D, -S47A, -G42A/Y43A, -D45A/D46A and -D48A/E49A/D50A showed a predominant localization at the peri-nuclear compartment, a pattern as exhibited by sortilin-wt

in control cells, indicating that they are dispensible for the intracellular sorting of sortilin.

4.1.1 Perspective

Our finding that the di-leucine based motif interacts specifically with γ1-σ1B hemi-complex leads to an intriguing possibility of the existence of a sub-population of AP-1, containing variants of σ1B-adaptins that mediate the sorting events involving sortilin, in specialized tissues. The similarity in the expression pattern of σ1B and its splice variants and of sortilin substantiates this idea. In a recent study, it was shown that sortilin is essential for the biogenesis of Glut4 storage vesicles in 3T3L1-adipocytes (Shi and Kandror, 2005). In the absence of sortilin, it has been shown that the Glut4 transporter is rapidly degraded. Moreover, it has been shown that AP-1 is associated with Glut4 vesicles (Gillingham *et al.*, 1999). However, AP-3 was also found to be associated to these vesicles. In addition, it was proposed that sortilin sorting by GGA2 mediates Glut4 sorting via sortilin-Glut4 dimerization. The data presented in this thesis, however, indicate that AP-1/σ1B complexes might play a role in sortilin sorting and thus Glut4 vesicle biogenesis. Currently experiments are performed to test this hypothesis using tissues cultured from the σ1B 'knock-out' mouse.

4.2 A role for the N-terminal domain of μ1A in regulation of AP-1 function

AP-1, a heterotetrameric clathrin adaptor complex, is mainly involved in the clathrin coated vesicle mediated transport of membrane receptors and their cargo between the TGN and the endosomes. In this study, we performed a comprehensive analysis of the N-terminal domain of μ1A and present data demonstrating that its N-terminal seventy amino acids play a role in the regulation of the sorting function of AP-1 complex.

4.2.1 Influence of the N-terminal domain of μ1A on AP-1 mediated protein sorting

Studies on μ2/μ1-chimeric AP-1 complex (AP-1*) provided the first evidence for a role of the N-terminal domain of μ1A-adaptin in protein sorting (Medigeshi Ramarao, 2003), Guruprasad Medegeshi and Schu.P, unpublished). The $\mu2^{1-70}/\mu1^{71-423}$ chimera (Chimera I, Fig.3.15) was incorporated into an AP-1* complex, which localized with clathrin and with the mannose-6-phosphate receptor at the perinuclear TGN. However AP-1* was able to restore mannose-6-phosphate receptor mediated cathepsin D sorting only partially. Also, redistribution of AP-1* into the cytoplasm induced by Brefeldin A was slower than that of AP-1. Cryo-electron microscopic analysis of AP-1* expressing cells, in the present study, displayed enlarged early endosomal organelles as observed in AP-1-deficient (μ1A-/-) cells indicating an imbalance in membrane trafficking (Fig.3.17 B and C).

In the μ1A 'knock-out' cells, peri-nuclear TGN staining of γ1-adaptin is lost and also clathrin staining is severely reduced. The mannose-6-phosphate receptors MPR46 and MPR300, which mediate sorting of lysosomal enzymes between the TGN and endosomes are redistributed from their preferential peri-nuclear TGN localization to early endosomes. This is due to a block in retrograde endosome to TGN transport (Meyer *et al.*, 2000, 2001). Although, AP-1* was able to restore the predominant TGN localization of mannose-6-phosphate receptors, TGN to endosome sorting of MPRs is impaired as indicated by the secretion of cathepsin D. That AP-1* cells still display enlarged endosomes also demonstrates impaired endosomal trafficking. These data demonstrate that the N-terminal seventy amino acids of μ1A-adaptin are important for AP-1 mediated sorting of membrane receptors and their cargo.

4.2.2   Role in AP-1 membrane binding dynamics

Having provided evidence that the N-terminal seventy amino acids of μ1A-adaptin could be involved in the regulation of AP-1 mediated vesicle transport, we studied the membrane recycling kinetics of AP-1*. It has been demonstrated that clathrin-coated pits are dynamic structures wherein the membrane bound clathrin and adaptors, dynamically exchange with their free counterparts in the cytoplasmic pool, also independent of eachother and that the adaptors exchange independent of vesicle budding. This has been demonstrated for AP-1 and AP-2 (Wu *et al.*, 2001, 2003). By FRAP analysis, we studied the nature of AP-1 and AP-1* cytoplasm - membrane recycling kinetics at the TGN, to gain insight into their varied response to Brefeldin A treatment. Our data show that the rate of exchange of AP-1* between the membrane bound fraction and the cytoplasmic pool is reduced. Although the membrane bound AP-1 and AP-1* were able to exchange with the cytoplasmic pool of adaptors as evidenced by the complete recovery of fluorescence at the photobleached area (see Fig. 3.18), AP-1* exhibited slow recycling kinetics, with almost a 50% reduction in its recycling rate compared to AP-1(Fig.3.19 A). When vesicle budding was blocked by treatment with hypertonic sucrose, AP-1* exchanged slowly with the cytoplasmic pool (Fig. 3.19 B) as did AP-1, but the difference in recovery remained at 50%. However the total recovery of AP-1* fluorescence was reduced to about $\sim$60%, whereas recovery of AP-1 was $\sim$90% also under these conditions. These data demonstrate that in the absence of vesicle budding process, a larger fraction of AP-1* binds to the membrane more firmly than AP-1, presumably at non-productive sites leading to reduced recycling.

The membrane recruitment of AP-1 is regulated by cycles of phosphorylation and de-phosphorylation of the β1-and μ1-adaptins (Ghosh and Kornfeld, 2003a). It was shown that the β1-adaptin is phosphorylated in the cytoplasm, but will be de-phosphorylated, when AP-1 is bound to the membrane, whereas μ1A is in the de-phosphorylated state in the cytoplasm, but phosphorylated in the membrane bound state. A model has been developed based on two observations. Firstly, upon μ-phosphorylation, AP-cargo binding is enhanced and secondly, in the AP-complex, the cargo-sorting motif binding site of μ-adaptin is covered by β-adaptin. Therefore, it was proposed that the phosphorylation of μ induces high affinity binding to the cargo sorting motif, by facilitating or stabilizing a conformational change in μ, that exposes its sorting motif binding site. This model applies to both AP-2 and AP-1. One can expect that, an impairment in this phosphorylation/de-phosphorylation cycle could lead to altered membrane binding properties of AP-1. Since our FRAP data revealed an impairment in the membrane-cytoplasm recycling of AP-1*, we

were interested to look for the phosphorylation state of AP-1*.

In the phosphorylation-induced open conformation, μ1A is accessible for trypsin digestion *in vitro*. Therefore susceptibility to trypsin digestion is an indirect measure of the phosphorylation state of μ1A and we took advantage of this property to compare the phosphorylation state of AP-1* and AP-1. μ1A of membrane-bound AP-1 exhibited a dramatic dose-dependent tryptic degradation, but Chimera I of membrane-bound AP-1* was less sensitive and indicated that the unphosphroylated membrane-bound fraction of AP-1* is larger than that of AP-1 (Fig. 3.21). Two possibilities can be derived for the state of under-phosphorylation; either due to increased de-phosphorylation or reduced phosphorylation combined with increased phosphorylation-independent membrane/cargo binding. Of note, it has been shown that the phosphorylation event of μ1A is associated with clathrin coated vesicle formation and budding and its de-phosphorylation with release from membrane (Ghosh and Kornfeld, 2003a). The under-phosphorylation state, taken together with our observation from FRAP analysis, makes it likely that there is an increased phosphorylation-independent membrane binding of AP-1* at non-productive sites. As a consequence of this binding to non-productive sites, the fraction of the cytoplasmic pool available for productive transport vesicle formation, becomes smaller and thus limiting for transport vesicle formation.

4.2.3   A novel protein as a potential regulator of AP-1 membrane binding

Little is known about the mechanisms that regulate the recruitment of AP-1 onto membranes and the proteins involved in its regulation. The N-terminal seventy amino acids of μ1A-adaptin can mediate its regulatory role by either directly recruiting the regulatory proteins or by stabilizing already recruited proteins. Given the fact that the N-terminal seventy amino acids of μ1A-adaptin are accessible from the cytoplasmic face of the heterotetrameric adaptor complex (Fig. 3.20), it is possible that cytoplasmic accessory and regulatory proteins involved in AP-1 mediated protein transport can bind to the μ1A N-terminus and regulate AP-1 membrane binding.

The proteins that are shown to be involved in the membrane recruitment of AP-1, obviously define the potential candidates for interaction. Membrane bound ARF-1 recruits AP-1 onto membranes at the site of vesicle formation at the TGN and the events leading to receptor sorting and transport vesicle formation. BIG2 was identified as a guanine-nucleotide exchange factor (GEF) for ARF-1 operating at the TGN, which when overexpressed, blocked the Brefeldin A-induced redistribution of

AP-1 from membranes, indicating that it is implicated in AP-1 membrane binding (Shinotsuka *et al.*, 2002). Since we know from our Brefeldin A treatment studies that AP-1* was still found bound to the membranes, BIG2 could be an ideal candidate to test for interaction. But our yeast two-hybrid studies indicate that none of the domains tested interacts with the N-terminal seventy aminoacids of μ1A. Similarly, the other potential candidates tested, cyclin G associated kinase (GAK)/ auxilin 2, the B-subunit of Protein phosphatase 2A (PP2A) and γ-BAR (γ1-adaptin Brefeldin A Resistance), did not show an interaction (see Fig. 3.23). This indicates that a mechanism that does not involve these proteins might operate in the N-terminal μ1A mediated regulation of AP-1 membrane binding.
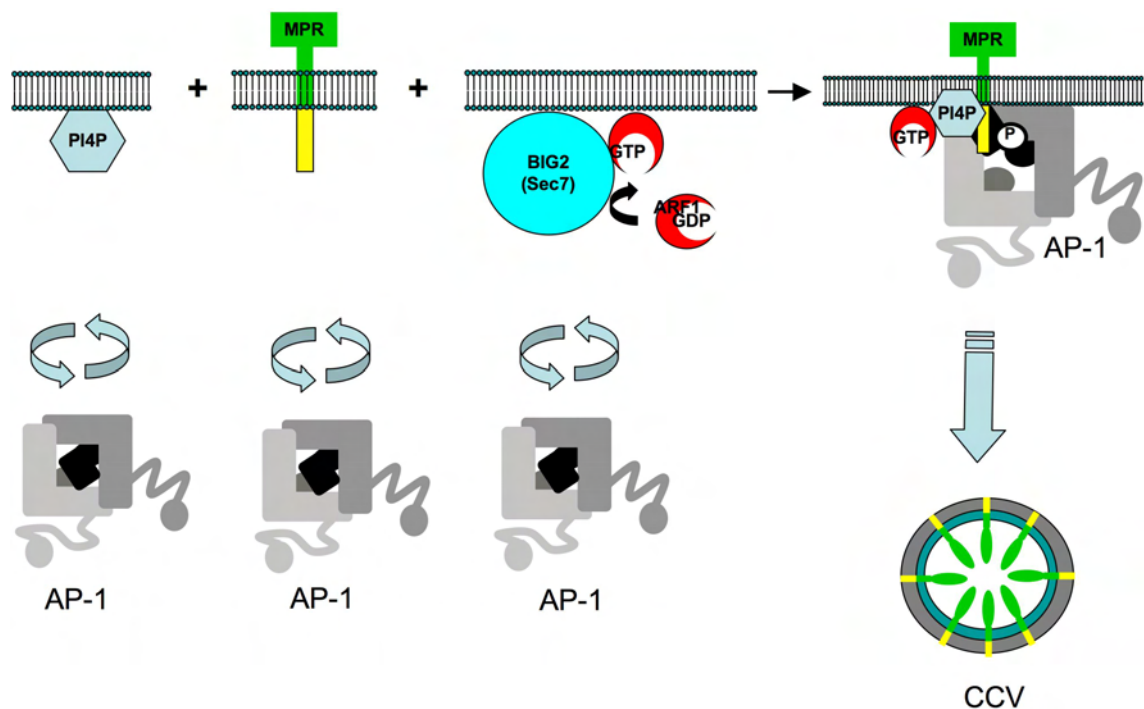

Figure 4.1: A model depicting the possible role of MuL in regulation of AP-1 membrane binding.

To identify new proteins that could potentially bind, we performed a Y2H library screening using N-terminal seventy aminoacids of μ1A as the bait and a mouse embryonic cDNA library. We identified a fragment of an unknown and an uncharacterized protein that showed a strong interaction. This interaction was also highly specific, because it did not interact with the corresponding domain of μ2 (Fig. 3.24). When we analyzed for the steady-state distribution of AP-1 and AP-1* in cells that showed transient expression of MuL-HA, there was a remarkable reduction in the staining for γ1-adaptin at the peri-nuclear area compared to control cells, indicating that the recruitment of AP-1 onto membranes is disturbed in MuL-HA

over-expressing cells. As expected, AP-1* distribution was unaltered in the presence of MuL-HA expression. The observation that MuL-HA disturbs the membrane binding of AP-1, but not that of AP-1*, substantiates the specificity of interaction observed in Y2H studies and also implicates that MuL plays a role in the membrane-cytoplasm recycling dynamics of AP-1.

So, how could MuL mediate its regulatory role? Based on our results, we propose a model by which MuL executes its role in AP-1 membrane binding (Fig.4.1). AP-1 high affinity membrane binding requires cargo, activated ARF-1 and PI4P and all the three factors are required for vesicle formation. However, AP-1 binding by just one of these factors is sufficient to permit AP-1 membrane recruitment *in vitro*. MuL-overexpression phenotype indicates that AP-1 membrane binding mediated by just one of the factors also occurs *in vivo*, reducing the cytoplasmic, mobile AP-1 pool available for binding at sites of vesicle formation and that MuL action ensures rapid release of AP-1 from membrane sites where vesicle budding cannot take place. MuL might perform this function alone or it could act as an adaptor protein.

Summary

The data presented in this thesis project provide the first data for the function of $\sigma 1$-adaptin isoforms and thus a function of tissue specifically expressed AP-1 complexes. Most tissues express two of the three $\sigma 1$A, $\sigma 1$B and $\sigma 1$C adaptins and in addition, in some tissues, the $\sigma 1$B-adaptin is present in isoforms generated by alternative RNA splicing. It is shown that the two previously characterized sorting motifs in the sortilin receptor are recognized by two different adaptins; the tyrosine-based motif is recognized by the ubiquitously expressed $\mu 1$A-adaptin, whereas the di-leucine based motif is specifically recognized by a $\gamma 1$-$\sigma 1$B hemi-complex. Sortilin is a recently identified multi-ligand receptor belonging to the Vps10p-domain receptor family, involved in the sorting of various unrelated ligands to the lysosomes. Similar to MPRs, it cycles between the TGN and the early and late endosomes mediated by clathrin-coated vesicles and its steady-state localization is confined to the TGN. The monomeric adaptor GGAs were shown to be responsible for mediating the TGN to endosome transport of sortilin by binding the di-leucine based sorting motif. Our study demonstrates that, AP-1 is also necessary for intracellular sorting of sortilin. The steady-state localization of sortilin in AP-1-deficient ($\mu 1$A-/-) cells, is altered with a redistribution to early-endosomes in a similar way as MPRs. This indicates that AP-1 is required for the retrograde transport of sortilin from the early-endosomes back to the TGN. Although the steady-state distribution of sortilin, was unaltered in $\sigma 1$B-deficient ($\sigma 1$B 'knock-out') fibroblasts, the significance of this interaction should be studied further in other tissues, owing to the striking similarity in the tissue-specific expression pattern of sortilin and $\sigma 1$B splice variants, $\sigma 1$B2 and $\sigma 1$B3. These include muscle, brain and adipose tissues. Since a $\sigma 1$B 'knock-out' mouse had been generated in our group, which is viable, tissue specific functions can now be analyzed in the molecular level.

In a second project, the regulation of AP-1 complex membrane-recycling was studied. The AP-1* complex containing the $\mu 2^{1-70}/\mu 1^{71-423}$chimera was able to bind membrane, but was not able to fully restore the phenotype of $\mu 1$A-deficiency. AP-1* expressing cells displayed enlarged endosomes as seen in AP-1-deficient ($\mu 1$A-/-) cells, which demonstrates an imbalance in membrane trafficking and thereby, the

significance of μ1A$^{1-70}$ in maintaining the fidelity of AP-1 function. AP-1* exhibited slow cytoplasm-membrane recycling kinetics compared to AP-1. Moreover, the data indicate that AP-1* binds to the membrane more firmly than AP-1 and at non-productive sites. μ1A of membrane-bound AP-1 exhibited a dramatic dose-dependent tryptic degradation, a consequence of phosphorylation-induced change in conformation and accessibility to trypsin digestion. But μ2$^{1-70}$/μ1$^{71-423}$ chimera of membrane-bound AP-1* was less sensitive, indicating that the unphosphroylated membrane-bound fraction of AP-1* is larger than that of AP-1. As a consequence of this binding to non-productive sites, the fraction of the cytoplasmic pool available for productive transport vesicle formation, becomes smaller and thus limiting for transport vesicle formation. Since, the N-terminal seventy amino acids of μ1A-adaptin are accessible from the cytoplasmic face of the heterotetrameric adaptor complex, we speculated that it can execute its regulatory role by interacting with other regulatory proteins. Our yeast two-hybrid analysis indicated that candidate known regulatory proteins do not interact with μ1A$^{1-70}$. But, by yeast two-hybrid library screening, we identified an uncharacterized protein binding with high specificity and affinity to μ1A$^{1-70}$ and designated it as MuL (μ1A-Ligand). Preliminary *in vivo* analysis indicate that over-expression of MuL reduces the membrane recruitment of AP-1, but not that of AP-1*. A detailed functional analysis of AP-1 membrane binding in MuL 'knock-down' system and additional AP-1-MuL interaction studies should yield an understanding of its mechanism of action.

Bibliography

Ball, C. L., Hunt, S. P., and Robinson, M. S. (1995). Expression and localization of α-adaptin isoforms. J Cell Sci *108*(8), 2865–2875. 9

Barlowe, C., Orci, L., Yeung, T., Hosobuchi, M., Hamamoto, S., Salama, N., Rexach, M. F., Ravazzola, M., Amherdt, M., and Schekman, R. (1994). COPII: a membrane coat formed by sec proteins that drive vesicle budding from the endoplasmic reticulum. Cell *77*, 895–907. 2

Bonifacino, J. S. (2004). The GGA proteins: adaptors on the move. Nat Rev Mol Cell Biol *5*, 23–32. 10

Bonifacino, J. S. and Glick, B. S. (2004). The mechanisms of vesicle budding and fusion. Cell *116*, 153–166. 2, 15

Bonifacino, J. S. and Traub, L. M. (2003). Signals for sorting of transmembrane proteins to endosomes and lysosomes. Annu Rev Biochem *72*, 395–447. 17, 56, 92

Borgne, R. L. and Hoflack, B. (1997). Mannose 6-phosphate receptors regulate the formation of clathrin-coated vesicles at the tgn. J Cell Biol *137*, 335–345. 19

Chidambaram, S., Müllers, N., Wiederhold, K., Haucke, V., and von Mollard, G. F. (2004). Specific interaction between SNAREs and epsin N-terminal homology (ENTH) domains of epsin-related proteins in *trans*-golgi network to endosome transport. J Biol Chem *279*(6), 4175–4179. 13

Claing, A., Laporte, S. A., Caron, M. G., and Lefkowitz, R. J. (2002). Endocytosis of G protein-coupled receptors: roles of G protein-coupled receptor kinases and beta-arrestin proteins. Prog Neurobiol . 9

Claussen, M., Buergisser, D., Schuller, A. G. P., Matzner, U., and Braulke, T. (1995). Regulation of insulin-like growth factor (IGF)-binding protein-6 and mannose 6-phosphate/IGF-II receptor expressing in IGF-II-overexpressing NIH 3T3 cells. Mol Endocrinol *9*, 902–912. 28

Collins, B. M., McCoy, A. J., Kent, H. M., Evans, P. R., and Owen, D. J. (2002). Molecular architecture and functional model of the endocytic AP2 complex. Cell *109*(4), 523–535. 7, 73, 80

Cremona, O., Di Paolo, G., Wenk, M. R., Luthi, A., Kim, W. T., Takei, K., Daniell, L., Nemoto, Y., Shears, S. B., Flavell, R. A., McCormick, D. A., and De Camilli, P. (1999). Essential role of phosphoinositide metabolism in synaptic vesicle recycling. Cell *99*(2), 179–88. 16

Crump, C. M., Xiang, Y., Thomas, L., Gu, F., Austin, C., Tooze, S. A., and Thomas, G. (2001). PACS-1 binding to adaptors is required for acidic cluster motif-mediated protein traffic. EMBO J *20*, 2192–2201. 18

Dell'Angelica, E. C., Klumperman, J., Stoorvogel, W., and Bonifacino, J. S. (1998). Association of the AP-3 adaptor complex with clathrin. Science *280*, 431–434. 6

Dell'Angelica, E. C., Ohno, H., Ooi, C. E., Rabinovich, E., Roche, K. W., and Bonifacino, J. S. (1997). AP-3: an adaptor-like protein complex with ubiquitous expression. EMBO J *16*(5), 917–928. 5

Deneka, M., Neeft, M., Popa, I., van Oort, M., Sprong, H., Oorschot, V., Klumperman, J., Schu, P., and van der Sluijs, P. (2003). Rabaptin-5 α/rabaptin-4 serves as a linker between rab4 and γ1-adaptin in membrane recycling from endosomes. EMBO J *22*(11), 2645–2657. 14

Dho, S. E., French, M. B., Woods, S. A., and McGlade, C. J. (1999). Characterization of four mammalian numb protein isoforms. identification of cytoplasmic and membrane-associated variants of the phosphotyrosine binding domain. J Biol Chem *274*(46), 33097–33104. 9

Doray, B., Ghosh, P., Griffith, J., Geuze, H. J., and Kornfeld, S. (2002). Cooperation of GGAs and AP-1 in packaging MPRs at the *trans*-golgi network. Science *297*, 1700–1703. 11, 20

Duncan, M. C., Costaguta, G., and Payne, G. S. (2003). Yeast epsin-related proteins required for Golgi-endosome traffic define a γ-adaptin ear-binding motif. Nat Cell Biol *5*, 77–81. 13

Edeling, M. A., Smith, C., and Owen, D. (2006). Life of a clathrin coat: insights from clathrin and ap structures. Nat Rev Mol Cell Biol *7*(1), 32–44. 4

Erdtmann, L., Janvier, K., Rapaso, G., Craig, H. M., Benaroch, P., Berlioz Torrent, C., Guatelli, J. C., Benarous, R., and Benichou, S. (2000). Two independent regions of HIV-1 Nef are required for connection with the endocytic pathway through binding to the mu 1 chain of AP1 complex. Traffic *1*, 871–883. 19

Eskelinen, E.-L., Meyer, C., Ohno, H., von Figura, K., and Schu, P. (2002). The polarized epithelia-specific μ1B-adaptin complements μ1A-deficiency in fibroblasts. EMBO reports *3*(5), 471–477. 9

Faúndez, V., Horng, J.-T., and Kelly, R. B. (1998). A function for the AP3 coat complex in synaptic vesicle formation from endosomes. Cell *93*, 423–432. 9

Fölsch, H., Ohno, H., Bonifacino, J. S., and Mellman, I. (1999). A novel clathrin adaptor complex mediates basolateral targeting in polarized epithelial cells. Cell *99*, 189–198. 9

Ford, M. G., Pearse, B. M., Higgins, M. K., Vallis, Y., Owen, D. J., Gibson, A., Hopkins, C. R., Evans, P. R., and McMahon, H. T. (2001). Simultaneous binding of PtdIns(4,5)P2 and clathrin by AP180 in the nucleation of clathrin lattices on membranes. Science *291*(5506), 1051–1055. 9

Ford, M. G. J., Mills, I. G., Peter, B. J., Vallis, Y., Praefcke, G. J. K., Evans, P. R., and McMahon, H. T. (2002). Curvature of clathrin-coated pits driven by epsin. Nature *419*, 361–366. 13

Gaidarov, I. and Keen, J. H. (1999). Phosphoinositide-AP-2 interactions required for targeting to plasma membrane clathrin-coated pits. J Cell Biol *146*, 755–764. 9

Garcia, C. K., Wilund, K., Arca, M., Zuliani, G., Fellin, R., Maioli, M., Calandra, S., Bertolini, S., Cossu, F., Grishin, N., Barnes, R., Cohen, J. C., and Hobbs, H. H. (2001). Autosomal recessive hypercholesterolemia caused by mutations in a putative LDL receptor adaptor protein. Science *292*(5520), 1394–1398. 9

Ghosh, P., Griffith, J., Geuze, H. J., and Kornfeld, S. (2003). Mammalian GGAs act together to sort mannose 6-phosphate receptors. J Cell Biol *163*(4), 755–766. 11

Ghosh, P. and Kornfeld, S. (2003a). AP-1 binding to sorting signals and release from clathrin-coated vesicles is regulated by phosphorylation. J Cell Biol *160*(5), 699–708. 17, 80, 82, 97, 98

Ghosh, P. and Kornfeld, S. (2003b). Phosphorylation-induced conformational changes regulate GGAs 1 and 3 function at the *trans*-golgi network. J Biol Chem *278*, 14543–14549. 10, 11, 14, 21

Ghosh, P. and Kornfeld, S. (2004). The cytoplasmic tail of cation-independent mannose 6-phosphate receptor contains four binding sites for AP-1. Arch Biochem Biophys *426*(2). 91

Gillingham, A. K., Koumanov, F., Pryor, P. R., Reaves, B. J., and Holman, G. D. (1999). Association of ap1 adaptor complexes with GLUT4 vesicles. J Cell Sci *112*(Pt 24), 4793–4800. 95

Godi, A., Di Campli, A., Konstantakopoulos, A., Di Tullio, G., Alessi, D. R., Kular, G. S., Daniele, T., Marra, P., Lucocq, J. M., and De Matteis, M. A. (2004). FAPPs control Golgi-to-cell-surface membrane traffic by binding to ARF and PtdIns(4)P. Nat Cell Biol *6*(5). 3

Greene, B., Liu, S. H., Wilde, A., and Brodsky, F. M. (2000). Complete reconstitution of clathrin basket formation with recombinant protein fragments: adaptor control of clathrin self-assembly. Traffic *1*(1), 69–75. 14

Griffiths, G., Back, R., and Marsh, M. (1989). A quantitative analysis of the endocytic pathway in baby hamster kidney cells. J Cell Biol *109*, 2703–2720. 74

Hannan, L. A., Newmyer, S. L., and Schmid, S. L. (1998). ATP- and cytosol-dependent release of adaptor proteins from clathrin-coated vesicles: a dual role for Hsc70. Mol Biol Cell *9*, 2217–2229. 16

Heldwein, E. E., Macia, E., Wang, J., Yin, H. L., Kirchhausen, T., and Harrison, S. C. (2004). Crystal structure of the clathrin adaptor protein 1 core. Proc Natl Acad Sci U S A *101*(39), 14108–14113. 7, 73

Hille Rehfeld, A. (1995). Mannose 6-phosphate receptors in sorting and transport of lysosomal enzymes. Biochim Biophys Acta *1241*, 177–194. 19

Hinrichsen, L., Harborth, J., Andrees, L., Weber, K., and Ungewickell, E. J. (2003). Effect of clathrin heavy chain- and α-adaptin specific small interfering RNAs on endocytic accessory proteins and receptor trafficking in HeLa cells. J Biol Chem *278*(46), 45160–45170. 10

Hinrichsen, L., Meyerholz, A., Groos, S., and Ungewickell, E. J. (2006). Bending a membrane: how clathrin affects budding. Proc Natl Acad Sci U S A *103*(23), 8715–8720. 5

Hinshaw, J. E. and Schmid, S. L. (1995). Dynamin self-assembles into rings suggesting a mechanism for coated vesicle budding. Nature *374*(6518), 190–192. 15

Hirst, J., Lindsay, M., and Robinson, M. S. (2001). GGAs: roles of the different domains and comparison with AP-1 and clathrin. Mol Biol Cell *12*(11). 20

Hirst, J., Motley, A., Harasaki, K., Chew, S. Y. P., and Robinson, M. S. (2003). EpsinR: an ENTH domain-containing protein that interacts with AP-1. Mol Biol Cell *14*, 625–641. 13

Hirst, J. and Robinson, M. S. (1998). Clathrin and adaptors. Biochim Biophys Acta *1404*, 173–193. 5

Hofmann, M. W., Höning, S., Rodionov, D., Dobberstein, B., von Figura, K., and Bakke, O. (1999). The leucine-based sorting motifs in the cytoplasmic domain of the invariant chain are recognized by the clathrin adaptors AP1 and AP2 and their medium chains. J Biol Chem *274*(51), 36153–36158. 18

Höning, S., Sosa, M., Hille-Rehfeld, A., and von Figura, K. (1997). The 46-kDa mannose 6-phosphate receptor contains multiple binding sites for clathrin adaptors. J Biol Chem *272*(32), 19884–19890. 19

Hooper, M., Hardy, K., Handyside, A., Hunter, S., and Monk, M. (1987). HPRT-deficient Lesch-Nyhan mouse embryos derived from germline colonization by cultured cells. Nature *326*, 292–295. 26

Howell, B. W., Lanier, L. M., Frank, R., Gertler, F. B., and Cooper, J. A. (1999). The disabled 1 phosphotyrosine-binding domain binds to the internalization signals of transmembrane glycoproteins and to phospholipids. Mol Cell Biol *19*(7), 5179–5188. 9

Huang, F., Nesterov, A., Carter, R. E., and Sorkin, A. (2001). Trafficking of yellow-fluorescent-protein-tagged μ1 subunit of clathrin adaptor AP-1 complex in living cells. Traffic *2*, 345–357. 20

Huttner, W. B. and Schmidt, A. (2000). Lipids, lipid modification and lipid-protein interaction in membrane budding and fission–insights from the roles of endophilin A1 and synaptophysin in synaptic vesicle endocytosis. Curr Opin Neurobiol *10*(5), 543–551. 16

Itoh, T., Koshiba, S., Kigawa, T., Kikuchi, A., Yokoyama, S., and Takenawa, T. (2001). Role of the ENTH domain in phosphatidylinositol-4,5-bisphosphate binding and endocytosis. Science *291*, 1047–1051. 13

Jahn, R., Lang, T., and Südhof, T. C. (2003). Membrane fusion. Cell *112*, 519–533. 17

Janvier, K., Kato, Y., Boehm, M., Rose, J. R., Martina, J. A., Kim, B.-Y., Venkatesan, S., and Bonifacino, J. S. (2003). Recognition of dileucine-based sorting signals from HIV-1 Nef and LIMP-II by the AP-1 $\gamma - \sigma 1$ and AP-3 $\delta - \sigma 3$ hemicomplexes. J Cell Biol *163*(6), 1281–1290. 18, 60, 62, 93

Kent, H. M., McMahon, H. T., Evans, P. R., Benmerah, A., and Owen, D. J. (2002). γ-adaptin appendage domain: Structure and binding site for Eps15 and γ-synergin. Structure *10*, 1139–1148. 13

Kirchhausen, T. (2000). Clathrin. Annu Rev Biochem *69*, 699–727. 4

Kirchhausen, T. and Harrison, S. C. (1981). Protein organization in clathrin trimers. Cell *23*(3), 755–761. 5

Klumperman, J., Hille, A., Veenendaal, T., Oorschot, V., Stoorvogel, W., von Figura, K., and Geuze, H. J. (1993). Differences in the endosomal distributions of the two mannose 6-phosphate receptors. J Cell Biol *121*, 997–1010. 19, 28

Klumperman, J., Kuliawat, R., Griffith, J. M., Geuze, H. J., and Arvan, P. (1998). Mannose 6-phosphate receptors are sorted from immature secretory granules via adaptor protein AP-1, clathrin, and syntaxin 6-positive vesicles. J Cell Biol *141*(2), 359–371. 19

Korolchuk, V. I. and Banting, G. (2002). CK2 and GAK/auxilin2 are major protein kinases in clathrin-coated vesicles. Traffic *3*(6), 428–439. 82

Lefrancois, S., Janvier, K., Boehm, M., Ooi, C., and Bonifacino, J. S. (2004). An ear-core interaction regulates the recruitment of the AP-3 complex to membranes. Dev Cell *7*(4), 619–625. 70

Lemmon, S. K. (2001). Clathrin uncoating: Auxilin comes to life. Current Biology *11*, 49–52. 16

Lui, W. W. Y., Collins, B. M., Hirst, J., Motley, A., Millar, C., Schu, P., Owen, D. J., and Robinson, M. S. (2003). Binding partners for the COOH-terminal appendage domains of the GGAs and γ-adaptin. Mol Biol Cell *14*, 2385–2398. 11

Mallard, F., Antony, C., Tenza, D., Salamero, J., Goud, B., and Johannes, L. (1998). Direct pathway from early/recycling endosomes to the Golgi apparatus revealed through the study of Shiga toxin B-fragment transport. J Cell Biol *143*(4), 973–990. 19

Marchese, A., Chen, C., Kim, Y. M., and Benovic, J. L. (2003). The ins and outs of G protein-coupled receptor trafficking. Trends Biochem Sci *28*(7), 369–376. 9

Marks, M. S., Woodruff, L., Ohno, H., and Bonifacino, J. S. (1996). Protein targeting by tyrosine- and di-leucine-based signals: Evidence for distinct saturable components. J Cell Biol *135*(2), 341–354. 17, 18

Mattera, R., Arighi, C. N., Lodge, R., Zerial, M., and Bonifacino, J. S. (2003). Divalent interaction of the GGAs with the rabaptin-5-rabex-5 complex. EMBO J *22*, 78–88. 11

Mattera, R., Puertollano, R., Smith, W. J., and Bonifacino, J. S. (2004). The trihelical bundle subdomain of the GGA proteins interacts with multiple partners through overlapping but distinct sites. J Biol Chem *279*(30), 31409–31418. 14

Maurer, M. E. and Cooper, J. A. (2006). The adaptor protein Dab2 sorts LDL receptors into coated pits independently of AP-2 and ARH. J Cell Sci. *119*(Pt 20), 4235–4246. 10

Medigeshi Ramarao, G. (2003). PhD thesis Georg-August-University Goettingen. 72, 74, 76, 96

Meyer, C., Eskelinen, E.-L., Guruprasad, M. R., von Figura, K., and Schu, P. (2001). μ1A-deficiency induces a profound increase of MPR300/IGF-II receptor internalization rate. J Cell Sci *114*, 4469–4476. 96

Meyer, C., Zizioli, D., Lausmann, S., Eskelinen, E.-L., Hamann, J., Saftig, P., von Figura, K., and Schu, P. (2000). μ1A adaptin-deficient mice: lethality, loss of AP-1 binding and rerouting of mannose 6-phosphate receptors. EMBO J *19*, 2193–2203. 19, 26, 28, 52, 55, 59, 89, 90, 92, 96

Mills, I. G., Praefcke, G. J. K., Vallis, Y., Peter, B. J., Olesen, L. E., Gallop, J. L., Butler, P. J. G., Evans, P. R., and McMahon, H. T. (2003). EpsinR: an AP1/clathrin interacting protein involved in vesicle trafficking. J Cell Biol *160*(2), 213–222. 13

Mishra, S. K., Keyel, P. A., Hawryluk, M. J., Agostinelli, N. R., Watkins, S. C., and Traub, L. M. (2002a). Disabled-2 exhibits the properties of a cargo-selective endocytic clathrin adaptor. Embo J . 9

Mishra, S. K., Watkins, S. C., and Traub, L. M. (2002b). The autosomal recessive hypercholesterolemia (ARH) protein interfaces directly with the clathrin-coat machinery. Proc Natl Acad Sci U S A . 9

Molloy, S. S., Anderson, E. D., Jean, F., and Thomas, G. (1999). Bi-cycling the furin pathway: from TGN localization to pathogen activation and embryogenesis. Trends Cell Biol *9*, 28–35. 19

Morris, S. M., Arden, S. D., Roberts, R. C., Kendrick-Jones, J., Cooper, J. A., Luzio, J. P., and Buss, F. (2002). Myosin VI binds to and localises with Dab2, potentially linking receptor-mediated endocytosis and the actin cytoskeleton. Traffic *3*(5), 331–341. 9

Motley, A., Bright, N. A., Seaman, M. N., and Robinson, M. S. (2003). Clathrin-mediated endocytosis in AP-2-depleted cells. J Cell Biol *162*, 909–918. 10

Müller, W., Kuhn, R., and Rajewsky, K. (1991). Major histocompatibility complex class II hyperextension on B cells in interleukin 4-transgenic mice does not lead to B cell proliferation and hypergammaglobulinemia. Eur J Immunol *21*(4), 921–925. 26

Neubrand, V. E., Will, R. D., Mobius, W., Poustka, A., Wiemann, S., Schu, P., Dotti, C. G., Pepperkok, R., and Simpson, J. C. (2005). Gamma-bar, a novel AP-1-interacting protein involved in post-golgi trafficking. Embo J *24*(6), 1122–1133. 14, 82

Nielsen, M., Madsen, P., Christensen, E. I., Nykjaer, A., Gliemann, J., Kasper, D., Pohlmann, R., and Petersen, C. (2001). The sortilin cytoplasmic tail conveys Golgi-endosome transport and binds the VHS domain of the GGA2 sorting protein. Embo J *20*(9), 2180–2190. 51, 52, 65, 89, 90

Ohno, H., Aguilar, R. C., Yeh, D., Taura, D., Saito, T., and Bonifacino, J. S. (1998). The medium subunits of adaptor complexes recognize distinct but overlapping sets of tyrosine-based sorting signals. J Biol Chem *273*(40), 25915–25921. 17

Ohno, H., Tomemori, T., Nakatsu, F., Okazaki, Y., Aguilar, R. C., Fölsch, H., Mellman, I., Saito, T., Shirasawa, T., and Bonifacino, J. S. (1999). μ1B, a novel adaptor medium chain expressed in polarized epithelial cell. FEBS Lett *449*, 215–220. 9

Owen, D. J. and Evans, P. R. (1998). A structural explanation for the recognition of tyrosine-based endocytotic signals. Science *282*, 1327–1332. 17

Page, L. J., Sowerby, P. J., Lui, W. W. Y., and Robinson, M. S. (1999). γ-synergin: An EH domain-containing protein that interacts with γ-adaptin. J Cell Biol *146*(5), 993–1004. 13

Palade, G. (1975). Intracellular aspects of the process of protein synthesis. Science *189*, 347–58. 1

Pearse, B. and Robinson, M. S. (1984). Purification and properties of 100kd proteins from coated vesicles and their reconstitution with clathrin. EMBO J *4*, 2457–2460. 5

Peden, A. A., Oorschot, V., Hesser, B. A., Austin, C. D., Scheller, R. H., and Klumperman, J. (2004). Localization of the AP-3 adaptor complex defines a novel endosomal exit site for lysosomal membrane proteins. J Cell Biol *164*(7), 1065–1076. 6

Petersen, C., Nielsen, M., Nykjaer, A., Jacobsen, L., Tommerup, N., Rasmussen, H., Roigaard, H., Gliemann, J., Madsen, P., and Moestrup, S. K. (2001). Molecular identification of a novel candidate sorting receptor purified from human brain by receptor-associated protein affinity chromatography. J Biol Chem *272*(6), 3599–3605. 51, 90

Prasad, K., Heuser, J., Eisenberg, E., and Greene, L. (1994). Complex formation between clathrin and uncoating ATPase. J Biol Chem *269*, 6931–6939. 16

Puertollano, R., Aguilar, R. C., Gorshkova, I., Crouch, R. J., and Bonifacino, J. S. (2001). Sorting of mannose 6-phosphate receptors mediated by the GGAs. Science *292*, 1712–1716. 18, 20

Puertollano, R. and Bonifacino, J. S. (2004). Interactions of GGA3 with the ubiquitin sorting machinery. Nat Cell Biol *6*(3), 244–251. 11, 12

Raiborg, C., Bache, K. G., Mehlum, A., Stang, E., and Stenmark, H. (2001a). Hrs recruits clathrin to early endosomes. EMBO J *20*, 5008–5021. 12

Raiborg, C., Bremnes, B., Mehlum, A., Gillooly, D. J., D'Arrigo, A., Stang, E., and Stenmark, H. (2001b). FYVE and coiled-coil domains determine the specific localisation of Hrs to early endosomes. J Cell Sci *114*, 2255–2263. 12

Rapoport, I., Chen, Y. C., Cupers, P., Shoelson, S. E., and Kirchhausen, T. (1998). Dileucine-based sorting signals bind to the β chain of AP-1 at a site distinct and regulated differently from the tyrosine-based motif-binding site. EMBO J *17*(8), 2148–2155. 18

Reusch, U., Bernhard, O., Koszinowski, U., and Schu, P. (2002). AP-1A and AP-3A lysosomal sorting functions. Traffic *3*, 752–761. 91

Reusch, U., Muranyi, W., Lucin, P., Burgert, H. G., Hengel, H., and Koszinowski, U. H. (1999). A cytomegalovirus glycoprotein re-routes MHC class I complexes to lysosomes for degradation. EMBO J *18*, 1081–1091. 19

Riel, C. (2004). PhD thesis Georg-August-University Goettingen. 8, 26, 62, 68, 93, 94

Robinson, M. S. and Bonifacino, J. S. (2001). Adaptor-related proteins. Curr Opin Cell Biol *13*, 444–453. 4, 5

Rodionov, D. G. and Bakke, O. (1998). Medium chains of adaptor complexes AP-1 and AP-2 recognize leucine-based sorting signals from the invariant chains. J Biol Chem *273*, 6005–6008. 19

Rohrer, J., Schweizer, A., Russell, D., and Kornfeld, S. (1996). The targeting of lamp1 to lysosomes is dependent on the spacing of its cytoplasmic tail tyrosine sorting motif relative to the membrane. J Cell Biol *132*, 565–576. 17

Royle, S. J., Bright, N. A., and Lagnado, L. (2005). Clathrin is required for the function of the mitotic spindle. Nature *434*(7037), 1152–1157. 5

Sachse, M., Urbé, S., Oorschot, V., Strous, G. J., and Klumperman, J. (2002). Bilayered clathrin coats on endosomal vacuoles are involved in protein sorting toward lysosomes. Mol Biol Cell *13*, 1313–1328. 12

Santolini, E., Puri, C., Salcini, A. E., Gagliani, M. C., Pelicci, P., Tacchetti, C., and Di Fiore, P. P. (2000). Numb is an endocytic protein. J cell Biol. *151*(6), 1345–1352. 9

Schu, P. (2001). Vesicular protein transport. Pharmacogenomics J *1*, 262–271. 5

Shi, J. and Kandror, K. V. (2005). Sortilin is essential and sufficient for the formation of Glut4 storage vesicles in 3T3-L1 adipocytes. Dev Cell *9*(1), 99–108. 95

Shih, W., Gallusser, A., and Kirchhausen, T. (1995). A clathrin-binding site in the hinge of the beta 2 chain of mammalian AP-2 complexes. J Biol Chem *270*(52), 31083–31090. 14

Shinotsuka, C., Yoshida, Y., Kawamoto, K., Takatsu, H., and Nakayama, K. (2002). Overexpression of an ADP-ribosylation factor-guanine nucleotide exchange factor,

BIG2, uncouples Brefeldin A-induced adaptor protein-1 coat dissociation and membrane tubulation. J Biol Chem *277*(11), 9468–9473. 81, 99

Simmen, T., Höning, S., Icking, A., Tikkanen, R., and Hunziker, W. (2002). AP-4 binds basolateral signals and participates in basolateral sorting in epithelial MDCK cells. Nat Cell Biol *4*, 154–159. 6

Simpson, F., Peden, A. A., Christopoulou, L., and Robinson, M. S. (1997). Characterization of the adaptor-related protein complex,AP-3. J Cell Biol *137*(4), 835–845. 5

Slepnev, V. and De Camilli, P. (2000). Accessory factors in clathrin-dependent synaptic vesicle endocytosis. Nat Rev Neurosci *1*, 161–172. 13

Stenmark, H., Vitale, G., Ullrich, O., and Zerial, M. (1995). Rabaptin-5 is a direct effector of the small GTPase Rab5 in endocytic membrane fusion. Cell *83*(3), 423–433. 14

Takatsu, H., Futatsumori, M., K.Yoshino, Yoshida, Y., Shin, H.-W., and Nakayama, K. (2001). Similar subunit interactions contribute to assembly of clathrin adaptor complexes and COPI complex: Analysis using yeast three-hybrid system. Biochem Biophys Res Commun *284*, 1083–1089. 8

Takatsu, H., Sakurai, M., Shin, H. W., Murakami, K., and Nakayama, K. (1998). Identification and characterization of novel clathrin adaptor-related proteins. J Biol Chem *273*(38), 24693–24700. 8

Tooze, S. A., Martens, G. J., and Huttner, W. B. (2001). Secretory granule biogenesis: rafting to the SNARE. Trends Cell Biol *11*(3). 3

Umeda, A., Meyerholz, A., and Ungewickell, E. (2000). Identification of the universal cofactor (auxilin 2) in clathrin coat dissociation. Eur J Cell Biol *79*, 336–342. 82

Ungewickell, E., Ungewickell, H., Holstein, S. E., Lindner, R., Prasad, K., Barouch, W., Martin, B., Greene, L. E., and Eisenberg, E. (1995). Role of auxilin in uncoating clathrin-coated vesicles. Nature *378*, 632–635. 16

Waguri, S., Dewitte, F., Borgne, R. L., Rouillé, Y., Uchiyama, Y., Dubremetz, J.-F., and Hoflack, B. (2003). Visualization of TGN to endosome trafficking through fluorescently labeled MPR and AP-1 in living cells. Mol Biol Cell *14*, 142–155. 20

Wan, L., Molloy, S. S., Thomas, L., Liu, G., Xiang, Y., Rybak, S. L., and Thomas, G. (1998). PACS-1 defines a novel gene family of cytosolic sorting proteins required for *trans* Golgi network localization. Cell *94*, 205–216. 18

Wendland, B. (2002). Epsins: adaptors in endocytosis? Nat Rev Mol Cell Biol *3*(12), 971–977. 9

Wilde, A. and Brodsky, F. M. (1996). *In vivo* phosphorylation of adaptors regulates their interaction with clathrin. J Cell Biol *135*. 14

Wu, X., Zhao, X., Baylor, L., Kaushal, S., Eisenberg, E., and Greene, L. E. (2001). Clathrin exchange during clathrin-mediated endocytosis. J Cell Biol *155*(2), 291–300. 76, 97

Wu, X., Zhao, X., Puertollano, R., Bonifacino, J. S., Eisenberg, E., and Greene, L. E. (2003). Adaptor and clathrin exchange at the plasma membrane and trans-Golgi network. Mol Biol Cell *14*(2), 516–528. 5, 76, 77, 97

Yasukawa, T., Kanei-Ishii, C., Maekawa, T., Fujimoto, J., Yamamoto, T., and Ishii, S. (1995). Increase of solubility of foreign proteins in *escherichia coli* by coproduction of bacterial thioredoxin. J Biol Chem *270*(43), 25328–25331. 25

Zhang, B., Koh, Y. H., Beckstead, R. B., Budnik, V., Ganetzky, B., and Bellen, H. J. (1998). Synaptic vesicle size and number are regulated by a clathrin adaptor protein required for endocytosis. Neuron *21*(6), 1465–1475. 10

Zhu, Y., Doray, B., Poussu, A., Lehto, V. P., and Kornfeld, S. (2001). Binding of GGA2 to the lysosomal enzyme sorting motif of the mannose 6-phosphate receptor. Science *292*, 1716–1718. 18

Acknowledgements

At the outset, I would like to thank Prof. Dr. Kurt von Figura, for giving me an opportunity to work in this institute and for being a source of inspiration.
I thank Prof. Dr. Fritz, for agreeing to be my co-referee.

I thank Prof. Dr. Peter Schu for his support, guidance and for being a good mentor. During these three years, I had learnt the art of critical scientific thinking and well thought experimental planning. Thanks again for your patience and guidance in the completion of this thesis.

With great pleasure, I would like to thank my colleagues who extended their help with all their kindness and patience and for creating a lively working atmosphere in the lab. Thank you Olaf and Jutta for all your help with the experiments. Olaf, thanks for all the good discussions we had during our coffee breaks. I thank Dr. Constanze Riel, for her help during the early stages of my work. Thank you Rekha for being a good friend.

I would like to thank both Tanja Benkert and Jennifer Baltes for being so kind to be always there during hardships not only at work, but outside the lab too. Thank you Jenny and Tanja for being critical towards my mistakes, which I appreciate, for it has improved my working style.

I thank Prof. Dr. Torben Luebcke and his group members Katrin, Ellen, Florian and Markus for their help and discussions. I thank Prof. Dr. Michael Thumm and his group for their help with my yeast experiments. I would like to thank Prof. Dr. Thomas Dierks and Dr. Bernhard Schmidt for their help.

Special thanks to Dr. Malaiyalam, and Santhosh lakshmi for all the scientific discussions we had, which for sure helped me to work better. Thank you Mals and santosh for your all your help. Thank you Prem for being such a caring friend. I would like to thank Sridhar Sriramulu and Mals for their timely help with their

115

expertise in LaTex, which helped me to successfully finish writing the thesis.

I would like to thank my friends Krishna, Ajay, Sunil, Rajesh and Chakravarthi for all their help and being nice friends.

This work would not be possible without the moral support and care of my parents and my sister. I extend my gratitude to them and other relatives.

Curriculum Vitae

Name: Radhakrishnan Karthikeyan.

Date of Birth: 16.11.1976.

Father's Name: Mr. Radhakrishnan Viswanathan.

Mother's Name: Mrs. Saraswathi Radhakrishnan .

Place of Birth: Krishnagiri, India.

1992 - 1994: High School, Krishnagiri.

1994 - 1997: Bachelor of Science in Biochemistry, Islamiah college, Vaniyambadi, India

1997 - 1999: Master of Science in Biochemistry, University of Madras, India.

July 1999 - Aug 2000: Worked as Junior Research Fellow with Prof. P.V. Sundaram, PROMED, Chennai, India.

Sep 2000 - Aug 2002: Worked as Junior Research Fellow in Institute of Chemistry, Academia Sinica, Taipei, Taiwan .

Apr 2003 - Present Doctorate student under Prof. Dr. Peter Schu, Biochemistry II, University of Goettingen.